

On the Oscillation Length Resonance in the Transitions of Solar and Atmospheric Neutrinos Crossing the Earth Core

M. Chizhov ^{a)}, M. Maris ^{b)} and S.T. Petcov ^{c,d)*}

a) Department of Physics, University of Sofia, 1164 Sofia, Bulgaria

b) Osservatorio Astronomico di Trieste, I-34113 Trieste, Italy

c) Scuola Internazionale Superiore di Studi Avanzati, I-34013 Trieste, Italy

d) Istituto Nazionale di Fizica Nucleare, Sezione di Trieste, I-34013 Trieste, Italy

Abstract

Assuming two-neutrino mixing takes place in vacuum, we study in detail the conditions under which the $\nu_2 \rightarrow \nu_e$ and $\nu_\mu \rightarrow \nu_e$ ($\nu_e \rightarrow \nu_{\mu(\tau)}$) transitions in the Earth are strongly enhanced by the neutrino oscillation length resonance when the neutrinos cross the Earth core. We show, in particular, that the neutrino oscillation length resonance is operative also in the $\bar{\nu}_\mu \rightarrow \bar{\nu}_s$ (or $\nu_\mu \rightarrow \nu_s$) transitions at small mixing angles. The properties of the $\nu_2 \rightarrow \nu_e$ and $\nu_\mu \rightarrow \nu_e$ ($\nu_e \rightarrow \nu_{\mu(\tau)}$) transition probabilities in the corresponding resonance regions are examined. Some implications of our results for the transitions of solar and atmospheric neutrinos traversing the Earth core, relevant for the interpretation of the results of the solar and atmospheric neutrino experiments, are also discussed.

*Also at: Institute of Nuclear Research and Nuclear Energy, Bulgarian Academy of Sciences, 1784 Sofia, Bulgaria.

1. Introduction

The $\nu_2 \rightarrow \nu_e$ and $\nu_\mu \rightarrow \nu_e$ ($\nu_e \rightarrow \nu_{\mu(\tau)}$) transitions/oscillations of solar and atmospheric neutrinos in the Earth, caused by neutrino mixing (with nonzero mass neutrinos) in vacuum¹, can be strongly amplified by a new type of resonance which differs from the MSW one and takes place when the neutrinos traverse the Earth core on the way to the detector [1]. At small mixing angles ($\sin^2 2\theta \lesssim 0.05$), the maxima due to this resonance in the corresponding transition probabilities, $P(\nu_2 \rightarrow \nu_e) \equiv P_{e2}$ and $P(\nu_\mu \rightarrow \nu_e)$ ($P(\nu_e \rightarrow \nu_{\mu(\tau)})$), are absolute maxima and dominate in P_{e2} and $P(\nu_\mu \rightarrow \nu_e)$: the values of the probabilities at these maxima in the simplest case of two-neutrino mixing are considerably larger - by a factor of $\sim (2.5 - 4.0)$ ($\sim (3.0 - 7.0)$), than the values of P_{e2} and $P(\nu_\mu \rightarrow \nu_e) = P(\nu_e \rightarrow \nu_{\mu(\tau)})$ at the local maxima associated with the MSW effect taking place in the Earth core (mantle). The enhancement is less dramatic at large mixing angles. Even at small mixing angles the resonance is relatively wide in the neutrino energy (or resonance density) - it is somewhat wider than the MSW resonance. It also exhibits strong energy dependence.

The conditions for existence of the indicated resonance in the probabilities P_{e2} and $P(\nu_\mu \rightarrow \nu_e)$ ($P(\nu_e \rightarrow \nu_{\mu(\tau)})$) include specific constraints on the neutrino oscillation length in the Earth mantle and in the Earth core [1]. When satisfied, these conditions ensure that the relevant oscillating factors in the $\nu_2 \rightarrow \nu_e$ and $\nu_\mu \rightarrow \nu_e$ ($\nu_e \rightarrow \nu_{\mu(\tau)}$) transition probabilities are maximal and that this produces a resonance maximum in P_{e2} and $P(\nu_\mu \rightarrow \nu_e)$ ($P(\nu_e \rightarrow \nu_{\mu(\tau)})$). Accordingly, the term “neutrino oscillation length resonance” or simply “oscillation length resonance” was used in [1] to denote the resonance of interest². In contrast, the MSW effect is, as is well-known, a resonance in the neutrino mixing. There exists a beautiful analogy between the neutrino oscillation length resonance and the electron spin-flip resonance taking place in a specific configuration of two magnetic fields (see [1] for a somewhat more detailed discussion)³. The neutrino oscillation length resonance is also in many respects similar to the resonance transforming a circularly polarized LH photon into a RH photon when the photon traverses three layers of optically active medium such that the optical activity and the length of the path of the photon in the first and the third layers are identical but differ from those in the second layer.

The implications of the oscillation length resonance enhancement of the probability P_{e2} for the tests of the MSW $\nu_e \rightarrow \nu_{\mu(\tau)}$ and $\nu_e \rightarrow \nu_s$ transition solutions of the solar neutrino problem are discussed in ref. [1] and in much greater detail in refs. [2,3] (see also [4]). It is quite remarkable that for values of $\Delta m^2 \cong (4.0 - 8.0) \times 10^{-6} \text{ eV}^2$ from the small mixing angle (SMA) MSW solution region and the geographical latitudes at which the Super-Kamiokande, SNO and ICARUS detectors are located, the enhancement takes place in the $\nu_e \rightarrow \nu_{\mu(\tau)}$ case for values of the ^8B neutrino energy lying in the interval $\sim (5 - 12) \text{ MeV}$ to which these

¹The $\nu_2 \rightarrow \nu_e$ transition probability accounts, as is well-known, for the Earth effect in the solar neutrino survival probability in the case of the MSW two-neutrino $\nu_e \rightarrow \nu_{\mu(\tau)}$ and $\nu_e \rightarrow \nu_s$ transition solutions of the solar neutrino problem, ν_s being a sterile neutrino.

²The oscillation length resonance can produce deep absolute minima in the probability P_{e2} as well (see further).

³This analogy was brought to the attention of the author of [1] by L. Wolfenstein.

detectors are sensitive. The resonance maximum in P_{e2} at $\sin^2 2\theta = 0.01$ for the trajectory with a Nadir angle $h = 23^\circ$, for instance, is located at a resonance density $\rho_{man}^{res} \sim 8.0 \text{ g/cm}^3$, which corresponds to $E \cong 5.3 \text{ (10.5) MeV}$ if $\Delta m^2 = 4.0 \text{ (8.0)} \times 10^{-6} \text{ eV}^2$. Accordingly, at small mixing angles this enhancement is predicted to produce [2] a much bigger - by a factor of ~ 6 , day-night (D-N) asymmetry in the Super-Kamiokande sample of solar neutrino events, whose night fraction is due to the *core-crossing* solar neutrinos, in comparison with the asymmetry determined by using the *whole night* Super-Kamiokande event sample ⁴. On the basis of these results it was concluded in [2] that it may be possible to test a rather large part of the MSW $\nu_e \rightarrow \nu_{\mu(\tau)}$ small mixing angle (SMA) solution region in the $\Delta m^2 - \sin^2 2\theta$ plane by performing selective, i.e., *core* D-N asymmetry measurements. The Super-Kamiokande collaboration has already successfully applied this approach to the analysis of their solar neutrino data in terms of the MSW effect [6,7]: the limit the collaboration has obtained on the D-N asymmetry utilizing only the *core* event sample permitted to exclude a part of the SMA solution region allowed by the mean event rate data from all solar neutrino experiments (Homestake, GALLEX, SAGE, Kamiokande and Super-Kamiokande). The SMA solution values of $\sin^2 2\theta$ and Δm^2 thus excluded belong to the intervals $\sin^2 2\theta \cong (0.007 - 0.01)$ and $\Delta m^2 \cong (5.0 \times 10^{-6} - 10^{-5}) \text{ eV}^2$. In contrast, the current upper limit on the D-N asymmetry, derived by the Super-Kamiokande collaboration using the *whole night* data sample of solar neutrino events, does not permit to probe the SMA solution region: the predicted asymmetry is too small [2]. The oscillation length resonance leads also to a relatively large D-N asymmetry in the recoil - e^- spectrum which is being measured in the Super-Kamiokande experiment [2].

As was shown in [1], the conditions for the neutrino oscillation length resonance are not even approximately fulfilled if solar neutrinos take part in $\nu_e \rightarrow \nu_s$ transitions, and hence the effect of strong enhancement of the probability P_{e2} does not take place in this case. However, when the MSW resonance occurs in the Earth core, the purely MSW enhancement of P_{e2} at small mixing angles is rather strongly “assisted” by some of the additional interference terms present in P_{e2} (see ref. [1] for details) and at the corresponding maximum P_{e2} has a noticeably larger value (by a factor of $\sim (2 - 4)$) than if it were determined by the MSW effect only. Still, at $\sin^2 2\theta \lesssim 0.02$, the value of P_{e2} at its absolute maximum in the $\nu_e \rightarrow \nu_s$ case is substantially smaller (by a factor of $\sim (2.5 - 4.0)$ [1,3]) than the maximum value of P_{e2} due to the oscillation length resonance if $\nu_e \rightarrow \nu_{\mu(\tau)}$ transitions took place. In addition, due basically to the well-known difference between the $\nu_{\mu(\tau)}$ and ν_s effective potentials in matter and the fact that the Earth matter is approximately isotopically symmetric, for fixed Δm^2 and $\sin^2 2\theta$ the absolute maximum of P_{e2} occurs in the case of $\nu_e \rightarrow \nu_s$ transitions at values of the neutrino energy E exceeding approximately by a factor 2 the values at which the oscillation length resonance maximum takes place if the solar ν_e undergo transitions

⁴The possibility of enhancement of the Earth effect in the Super-Kamiokande sample of events generated by the core-crossing solar neutrinos was discussed in ref. [5], where on the basis of results obtained for few pairs of values of Δm^2 and $\sin^2 2\theta$ it was also suggested that the effect might be measurable even in the case of small neutrino mixing angle. However, no estimates of the magnitude of the core enhancement were given in this article and the enhancement was interpreted to be due to the MSW effect taking place in the Earth core.

into $\nu_{\mu(\tau)}$ [3]. As a consequence, the oscillation length resonance does not produce such a dramatic enhancement of the D-N asymmetry in the *core* sample of the Super-Kamiokande solar neutrino events as in the case of $\nu_e \rightarrow \nu_{\mu(\tau)}$ transitions. Thus, the possibility to probe the MSW $\nu_e \rightarrow \nu_s$ (SMA) solution of the solar neutrino problem via the measurement of the D-N effect related observables in the Super-Kamiokande experiment appears unlikely at present [3].

The oscillation length resonance enhancement can be present also in the $\nu_\mu \rightarrow \nu_e$ and $\nu_e \rightarrow \nu_{\mu(\tau)}$ transitions of atmospheric neutrinos crossing the Earth core [1]. It can take place practically for all neutrino trajectories through the core, in particular, for the trajectories with $h = (0^\circ - 23^\circ)$. In the case of two-neutrino mixing and at small mixing angles, the maximum in $P(\nu_\mu \rightarrow \nu_e) = P(\nu_e \rightarrow \nu_{\mu(\tau)})$ due to the oscillation length resonance is an absolute maximum and dominates in these probabilities⁵. This can be especially relevant for the interpretation of the results of the atmospheric neutrino experiments and for the future studies of the oscillations/transitions of atmospheric neutrinos crossing the Earth. As is well-known, the Super-Kamiokande collaboration has reported recently strong experimental evidences for oscillations of the atmospheric ν_μ ($\bar{\nu}_\mu$) neutrinos [8,9]. Assuming two-neutrino mixing, the data is best described in terms of $\nu_\mu \leftrightarrow \nu_\tau$ and $\bar{\nu}_\mu \leftrightarrow \bar{\nu}_\tau$ vacuum oscillations with parameters $\Delta m^2 \cong (5 \times 10^{-4} - 6 \times 10^{-3}) \text{ eV}^2$ and $\sin^2 2\theta \cong (0.8 - 1.0)$, although the hypothesis of large mixing $\nu_\mu \leftrightarrow \nu_s$ oscillations provides almost equally good fit to the data. At the same time, the possibility of two-neutrino $\nu_\mu \leftrightarrow \nu_e$ and $\bar{\nu}_\mu \leftrightarrow \bar{\nu}_e$ large mixing oscillations is disfavored by the presently existing Super-Kamiokande data [8,9]. At $\Delta m^2 \gtrsim 2 \times 10^{-3} \text{ eV}^2$ this possibility is ruled out by the results of the CHOOZ experiment [10].

It is a remarkable coincidence that, as was shown in [1], for values of $\Delta m^2 \sim (5 \times 10^{-4} - 5 \times 10^{-3}) \text{ eV}^2$ and small mixing angles, $\sin^2 2\theta \lesssim 0.10$, the neutrino oscillation length resonance in $P(\nu_\mu \rightarrow \nu_e)$ ($P(\nu_e \rightarrow \nu_{\mu(\tau)})$) occurs for values of the energy E of the atmospheric ν_e and ν_μ which contribute either to the sub-GeV or to the multi-GeV samples of e -like and μ -like events in the Super-Kamiokande experiment. For $\sin^2 2\theta = 0.01$, $\Delta m^2 = 5 \times 10^{-4}$; 10^{-3} ; $5 \times 10^{-3} \text{ eV}^2$, and $h = 0^\circ$ (Earth center crossing), for instance, the absolute maximum in $P(\nu_\mu \rightarrow \nu_e) = P(\nu_e \rightarrow \nu_{\mu(\tau)})$ due to the oscillation length resonance takes place at $E \cong 0.75$; 1.50 ; 7.5 GeV . Thus, for values of $\Delta m^2 \sim (5 \times 10^{-4} - 6 \times 10^{-3}) \text{ eV}^2$ of the region of the $\nu_\mu \leftrightarrow \nu_\tau$ oscillation solution of the atmospheric neutrino problem, the oscillation length resonance strongly enhances the $\nu_\mu \rightarrow \nu_e$ (and $\nu_e \rightarrow \nu_{\mu(\tau)}$) transitions of the atmospheric neutrinos crossing the Earth core, making the transition probabilities large and the transitions perhaps detectable even at small mixing angles. Actually, it was suggested in [1,11] that the small excess of e -like events in the region $-1 \leq \cos \theta_z \leq -0.6$, θ_z being the Zenith angle, either in the sub-GeV or in the multi-GeV sample of atmospheric neutrino events, observed (in both samples) in the Super-Kamiokande experiment [8,9], is due to $\nu_\mu \rightarrow \nu_e$ small mixing angle, $\sin^2 2\theta_{e\mu} \cong (0.01 - 0.10)$, transitions with $\Delta m^2 \sim (5 \times 10^{-4} - 10^{-3}) \text{ eV}^2$ or respectively $\Delta m^2 \sim (2 \times 10^{-3} - 6 \times 10^{-3}) \text{ eV}^2$, strongly enhanced by the neutrino oscillation length resonance as neutrinos cross the Earth core on the way to the

⁵Let us note that the oscillation length resonance enhancement of $P(\nu_\mu \rightarrow \nu_e)$ is operative at large mixing angles as well, at which the probabilities P_{e2} and $P(\nu_\mu \rightarrow \nu_e)$ exhibit different dependence on $E/\Delta m^2$ (see further).

detector. The same resonantly enhanced transitions with $\Delta m^2 \sim (2 \times 10^{-3} - 6 \times 10^{-3}) \text{ eV}^2$ ($\Delta m^2 \sim (5 \times 10^{-4} - 10^{-3}) \text{ eV}^2$) should produce [1,11] at least part of the strong Zenith angle dependence, exhibited by the μ -like multi-GeV (sub-GeV) Super-Kamiokande data.

The $\nu_\mu \rightarrow \nu_e$ and $\nu_e \rightarrow \nu_{\mu(\tau)}$ transitions of atmospheric neutrinos under discussion should exist if three-flavour-neutrino (or four-neutrino) mixing takes place in vacuum. More specifically, such transitions are naturally predicted to take place in the case of three-neutrino mixing [1] if large mixing angle $\nu_e \leftrightarrow \nu_\mu$ oscillations with $\Delta m_{21}^2 \sim 10^{-10} \text{ eV}^2$ or small mixing angle MSW $\nu_e \rightarrow \nu_\mu$ transitions with $\Delta m_{21}^2 \sim (4 - 8) \times 10^{-6} \text{ eV}^2$, provide the solution of the solar neutrino problem, and if the atmospheric neutrino anomaly is due to $\nu_\mu \leftrightarrow \nu_\tau$ large mixing angle oscillations with $\Delta m_{31}^2 \sim (5 \times 10^{-4} - 6 \times 10^{-3}) \text{ eV}^2$. If $\Delta m_{31}^2 \gg \Delta m_{21}^2$, which seems to be a plausible possibility in view of the neutrino oscillation interpretation of the solar and atmospheric neutrino data, the relevant three-neutrino $\nu_\mu \rightarrow \nu_e$ and $\nu_e \rightarrow \nu_{\mu(\tau)}$ transition probabilities reduce to a two-neutrino transition probability (see, e.g., [12]) with Δm_{31}^2 and $\sin^2 2\theta_{13} \equiv \sin^2 2\theta_{e\mu} = 4|U_{e3}|^2(1 - |U_{e3}|^2)$ playing the role of the relevant two-neutrino oscillation parameters, where U_{e3} is the element of the lepton mixing matrix U , coupling the electron and the third (heaviest) massive neutrino, ν_3 , in the charged lepton current. Under the above assumptions and taking into account the CHOOZ result [10] one finds that $|U_{e3}|^2$ cannot be large, but is also not necessarily exceedingly small: $\sin^2 2\theta_{13} \lesssim 0.20$. Thus, searching for the $\nu_\mu \rightarrow \nu_e$ and $\nu_e \rightarrow \nu_{\mu(\tau)}$ transitions of atmospheric neutrinos, amplified by the oscillation length resonance, can provide unique information, in particular, about the magnitude of the element U_{e3} of the lepton mixing matrix [13]. As is not difficult to show using the results of [12], the fluxes of atmospheric $\nu_{e,\mu}$ having energy E and crossing the Earth along a trajectory with Zenith angle θ_z before reaching the detector, $\Phi_{\nu_{e,\mu}}(E, \theta_z)$, are given by the following expressions in the three-neutrino mixing scheme under discussion [11]:

$$\Phi_{\nu_e}(E, \theta_z) \cong \Phi_{\nu_e}^0 \left(1 + [s_{23}^2 r(E, \theta_z) - 1] P_{2\nu}(E, \theta_z; \Delta m_{31}^2, \theta_{13}) \right), \quad (1a)$$

$$\begin{aligned} \Phi_{\nu_\mu}(E, \theta_z) \cong \Phi_{\nu_\mu}^0 (1 + s_{23}^4 [(s_{23}^2 r(E, \theta_z))^{-1} - 1] P_{2\nu}(E, \theta_z; \Delta m_{31}^2, \theta_{13}) \\ - 2c_{23}^2 s_{23}^2 [1 - \text{Re}(e^{-i\kappa} A_{2\nu}(\nu_\tau \rightarrow \nu_\tau))]), \end{aligned} \quad (1b)$$

Here $\Phi_{\nu_{e(\mu)}}^0 = \Phi_{\nu_{e(\mu)}}^0(E, \theta_z)$ is the $\nu_{e(\mu)}$ flux in the absence of neutrino transitions/oscillations,

$$s_{23}^2 \equiv \frac{|U_{\mu 3}|^2}{1 - |U_{e3}|^2} \leq 1, \quad r(E, \theta_z) \equiv \frac{\Phi_{\nu_\mu}^0(E, \theta_z)}{\Phi_{\nu_e}^0(E, \theta_z)}, \quad (1c)$$

$U_{\mu 3}$ being the μ - ν_3 element of U , $c_{23}^2 = 1 - s_{23}^2$, $P_{2\nu}(E, \theta_z; \Delta m_{31}^2, \theta_{13})$ is the probability of two-neutrino transitions in the Earth which coincides in form with $P(\nu_e \rightarrow \nu_\tau)$, $P_{2\nu} = P(\nu_e \rightarrow \nu_\tau)$, but describes $\nu_e \rightarrow \nu_\tau$ transitions only in a certain limit [12], and κ and $A_{2\nu}(\nu_\tau \rightarrow \nu_\tau)$ are known phase and two-neutrino transition probability amplitude⁶. The interpretation of the Super-Kamiokande atmospheric neutrino data in terms of $\nu_\mu \leftrightarrow \nu_\tau$ oscillations requires the parameter s_{23}^2 to lie approximately in the interval (0.30 - 0.70), with 0.5 being the statistically

⁶Analytic expressions for $P(\nu_e \rightarrow \nu_\tau)$, κ and $A_{2\nu}(\nu_\tau \rightarrow \nu_\tau)$ will be given later (see eqs. (13), (15) and (16)).

preferred value. For the predicted ratio $r(E, \theta_z)$ of the atmospheric ν_μ and ν_e fluxes for the Earth core crossing neutrinos, $-1 \leq \cos \theta_z \lesssim -0.8$, one has [14,15]: $r(E, \theta_z) \cong (2.0 - 2.5)$ for the neutrinos giving the contribution to the sub-GeV samples of Super-Kamiokande events, and $r(E, \theta_z) \cong (2.6 - 4.5)$ for those giving the main contribution to the multi-GeV samples. If $s_{23}^2 = 0.5$ and $r(E, \theta_z) \cong 2.0$ we have $(s_{23}^2 r(E, \theta_z) - 1) \cong 0$ and the possible effects of the $\nu_\mu \rightarrow \nu_e$ and $\nu_e \rightarrow \nu_{\mu(\tau)}$ transitions on the ν_e flux and correspondingly on the sub-GeV e -like sample of events, would be strongly suppressed even if these transitions are maximally enhanced by the oscillation length resonance. The indicated suppression may actually be taking place ⁷. However, one should keep in mind that the factor $(s_{23}^2 r(E, \theta_z) - 1)$ can be as large as ~ 0.6 for the sub-GeV neutrinos and that the effects of the resonantly enhanced $\nu_\mu \rightarrow \nu_e$ and $\nu_e \rightarrow \nu_{\mu(\tau)}$ transitions in the sub-GeV e -like event sample can be suppressed by the specific way this sample is selected from the data in the Super-Kamiokande experiment [13]. For the multi-GeV neutrinos we have $(s_{23}^2 r(E, \theta_z) - 1) \gtrsim 0.3$ (0.9) for $s_{23}^2 = 0.5$ (0.7). The factor $(s_{23}^2 r(E, \theta_z) - 1)$ amplifies the effect of the $\nu_\mu \rightarrow \nu_e$ transitions in the e -like sample for $E \gtrsim (5 - 6)$ GeV, for which $r(E, \theta_z) \gtrsim 4$ [14,15]. This discussion suggests that the effects of the neutrino oscillation length resonance in the Super-Kamiokande e -like multi-GeV data for $\Delta m_{31}^2 \sim (2 \times 10^{-3} - 6 \times 10^{-3})$ eV² can be much larger than those in the e -like sub-GeV data for $\Delta m_{31}^2 \sim (5 \times 10^{-4} - 10^{-3})$ eV² [11,13]. As similar analysis of the expression (1b) for Φ_{ν_μ} shows, they are also expected to be larger (within the three-neutrino mixing scheme considered) than the oscillation length resonance effects in the multi-GeV μ -like event sample [11,13].

In view of the possible important phenomenological implications of the neutrino oscillation length resonance, some of which have been discussed above, we continue in this article the studies of the resonance in the $\nu_2 \rightarrow \nu_e$ and $\nu_\mu \rightarrow \nu_e$ ($\nu_e \rightarrow \nu_{\mu(\tau)}$) transitions, began in ref. [1]. Assuming two-neutrino $\nu_e - \nu_{\mu(\tau)}$ or $\nu_e - \nu_s$ mixing (with nonzero-mass neutrinos) exists in vacuum, we study in greater detail the conditions under which the neutrino oscillation length resonance takes place in the $\nu_2 \rightarrow \nu_e$ and $\nu_\mu \rightarrow \nu_e$ ($\nu_e \rightarrow \nu_{\mu(\tau)}$) transitions of the solar and atmospheric neutrinos in the Earth. We give a graphical representation of both the necessary conditions for existence of the extrema in the probabilities P_{e2} and $P(\nu_\mu \rightarrow \nu_e)$ ($P(\nu_e \rightarrow \nu_{\mu(\tau)})$), associated with the resonance, and of the supplementary conditions ensuring that these extrema correspond to maxima. This permits, e.g., to determine all relevant values of the transition parameters, E , Δm^2 and $\sin^2 2\theta$, at which the resonance occurs for a given neutrino trajectory through the Earth core. Similar analysis is performed for the case of $\bar{\nu}_\mu \rightarrow \bar{\nu}_s$ transitions at small mixing angles. We also investigate the behavior of the probabilities P_{e2} and $P(\nu_\mu \rightarrow \nu_e)$ ($P(\nu_e \rightarrow \nu_{\mu(\tau)})$) in the region of the neutrino oscillation length resonance. We show, in particular, that at small mixing angles the resonance is relatively wide not only in the variable $E/\Delta m^2$, but also in the Nadir angle variable h . The implications of our results for the current and future experiments with solar and atmospheric neutrinos are also briefly discussed.

⁷Indeed, a more detailed investigation [13] performed within the indicated three-neutrino mixing scheme reveals, in particular, that the excess of e -like events in the Super-Kamiokande sub-GeV data at $-1 \leq \cos \theta_z \leq -0.6$ seems unlikely to be due to small mixing angle, $\sin^2 2\theta_{13} \lesssim 0.20$, $\nu_\mu \rightarrow \nu_e$ transitions amplified by the oscillation length resonance.

Let us note that the Earth enhancement of the two-neutrino $\nu_2 \rightarrow \nu_e$ and $\nu_{\mu(e)} \rightarrow \nu_{e(\mu)}$ ($\nu_e \rightarrow \nu_{\mu(\tau)}$) transitions of interest of the solar and atmospheric neutrinos in the case of relatively small mixing angles has been discussed in the past in, e.g., refs. [4,5,16–19]. Some of these articles contain plots of the probabilities P_{e2} and/or $P(\nu_\mu \rightarrow \nu_e)$ or $P(\nu_e \rightarrow \nu_{\mu(\tau)})$ on which one can clearly recognize now the dominating maximum due to the neutrino oscillation length resonance (see, e.g., [16–19]). However, this maximum was invariably interpreted to be due to the MSW effect in the Earth core before the appearance of the study [1].

2. The Earth Model, the Two-Layer Density Approximation and the Neutrino Oscillation Length Resonance

We begin with a brief summary of the main properties of the reference Earth model and of the results obtained in ref. [1], which will be utilized in our further analysis. Following [1–4,17] we will use the Stacey model from 1977 [20] as a reference Earth model. The density distribution in the Stacey model is, as in all Earth models known to us, spherically symmetric and there are two major density structures - the core and the mantle, and a certain number of substructures (shells or layers). The core has a radius $R_c = 3485.7$ km, the Earth mantle depth is approximately $R_{man} = 2885.3$ km, and the Earth radius in the Stacey model is $R_\oplus = 6371$ km. The mean values of the matter densities of the core and of the mantle read, respectively: $\bar{\rho}_c \cong 11.5$ g/cm³ and $\bar{\rho}_{man} \cong 4.5$ g/cm³. The density distribution in the 1977 Stacey model practically coincides with that in the more recent PREM model [21].

All the interesting features of the solar and atmospheric neutrino transitions in the Earth, including those related to the neutrino oscillation length resonance, can be understood quantitatively in the framework of the two-layer model of the Earth density distribution [1]. The density profile of the Earth in the two-layer model is assumed to consist of two structures - the mantle and the core, having different densities, ρ_{man} and ρ_c , and different electron fraction numbers, Y_e^{man} and Y_e^c , none of which however vary within a given structure. The core radius and the depth of the mantle are known with a rather good precision and these data are incorporated in the Earth models [20,21]. The densities ρ_{man} and ρ_c in the case of interest should be considered as mean effective densities along the neutrino trajectories, which can vary somewhat with the change of the trajectory ⁸: $\rho_{man} = \bar{\rho}_{man}$ and $\rho_c = \bar{\rho}_c$. In the Stacey model one has: $\bar{\rho}_{man} \cong (4 - 5)$ g/cm³ and $\bar{\rho}_c \cong (11 - 12)$ g/cm³. For the electron fraction numbers in the mantle and in the core one can use the standard values [20–22] (see also [2]) $Y_e^{man} = 0.49$ and $Y_e^c = 0.467$. Numerical calculations show [23] (see also [17]) that, e.g., the (time-averaged probability P_{e2} calculated within the two-layer model of the Earth with $\bar{\rho}_{man}$ and $\bar{\rho}_c$ taken from the Stacey 1977 model [20] reproduces with a remarkably high precision the probability calculated by solving numerically the relevant system of evolution equations with the much more sophisticated Earth density profile of the Stacey model [20].

The probability of the $\nu_2 \rightarrow \nu_e$ transition in the Earth, P_{e2} , which accounts for the Earth effect in the solar neutrino survival probability, has the following form in the two-layer model

⁸Let us note that because of the spherical symmetry of the Earth, a given neutrino trajectory through the Earth is completely specified by its Nadir angle (see, e.g., [4]).

of the Earth density distribution [1]:

$$\begin{aligned}
P_{e2} = & \sin^2 \theta + \frac{1}{2} [1 - \cos \Delta E'' X''] [\sin^2(2\theta''_m - \theta) - \sin^2 \theta] \\
& + \frac{1}{4} [1 - \cos \Delta E'' X''] [1 - \cos \Delta E' X'] [\sin^2(2\theta''_m - 4\theta'_m + \theta) - \sin^2(2\theta''_m - \theta)] \\
& - \frac{1}{4} [1 - \cos \Delta E'' X''] [1 - \cos 2\Delta E' X'] [\sin^2(2\theta'_m - \theta) - \sin^2 \theta] \cos^2(2\theta''_m - 2\theta'_m) \\
& + \frac{1}{4} [1 + \cos \Delta E'' X''] [1 - \cos 2\Delta E' X'] [\sin^2(2\theta'_m - \theta) - \sin^2 \theta] \\
& + \frac{1}{2} \sin \Delta E'' X'' \sin 2\Delta E' X' [\sin^2(2\theta'_m - \theta) - \sin^2 \theta] \cos(2\theta''_m - 2\theta'_m) \\
& + \frac{1}{4} [\cos(\Delta E' X' - \Delta E'' X'') - \cos(\Delta E' X' + \Delta E'' X'')] \sin(4\theta'_m - 2\theta) \sin(2\theta''_m - 2\theta'_m). \quad (2)
\end{aligned}$$

Here

$$\Delta E' (\Delta E'') = \frac{\Delta m^2}{2E} \sqrt{\left(1 - \frac{\bar{\rho}_{man(c)}}{\rho_{man(c)}^{res}}\right)^2 \cos^2 2\theta + \sin^2 2\theta}, \quad (3)$$

is the difference between the energies of the two energy- eigenstate neutrinos in the mantle (core), θ'_m and θ''_m are the mixing angles in matter in the mantle and in the core, respectively,

$$\sin^2 2\theta'_m (\sin^2 2\theta''_m) = \frac{\sin^2 2\theta}{\left(1 - \frac{\bar{\rho}_{man(c)}}{\rho_{man(c)}^{res}}\right)^2 \cos^2 2\theta + \sin^2 2\theta}, \quad (4)$$

X' is half of the distance the neutrino travels in the mantle and X'' is the length of the path of the neutrino in the core, and ρ_{man}^{res} and ρ_c^{res} are the resonance densities in the mantle and in the core. The latter can be obtained from the expressions

$$\rho^{res} = \frac{\Delta m^2 \cos 2\theta}{2E\sqrt{2}G_F f(Y_e)} m_N, \quad (5)$$

$$f(Y_e) = Y_e, \quad \nu_e \rightarrow \nu_{\mu(\tau)} \quad (\nu_\mu \rightarrow \nu_e) \text{ transitions}, \quad (6a)$$

$$f(Y_e) = \frac{1}{2}(3Y_e - 1), \quad \nu_e \rightarrow \nu_s \quad (\nu_s \rightarrow \nu_e) \text{ transitions}, \quad (6b)$$

m_N being the nucleon mass, by using the specific values of Y_e in the mantle and in the core. We have $\rho_{man}^{res} \neq \rho_c^{res}$ (but $\rho_{man}^{res} \sim \rho_c^{res}$) because $Y_e^c = 0.467$ and $Y_e^{man} = 0.49$. Obviously, one has: $f(Y_e^c)\rho_c^{res} = f(Y_e^{man})\rho_{man}^{res}$.

We will present some of our results (obtained for fixed $\sin^2 2\theta$) utilizing the density parameter

$$\rho_r = \frac{\Delta m^2 \cos 2\theta}{2E\sqrt{2}G_F C_{a(s)}} m_N, \quad (7a)$$

where the constant $C_{a(s)} = 0.50$ (0.25) for the $\nu_e \rightarrow \nu_{\mu(\tau)}$ ($\nu_e \rightarrow \nu_s$) transitions. The parameter ρ_r would coincide with the resonance density if Y_e were equal to 1/2 both in the

mantle and in the core, so $\rho_r \cong \rho_{man}^{res}$; for given $\sin^2 2\theta$ it is equivalent to $E/\Delta m^2$, but gives an idea about the densities at which one has an enhancement of the transition probabilities of interest when the neutrinos cross the Earth and we have used it for the latter purpose in [2–4] and in [1]. Clearly, $C_a \rho_r = Y_e^c \rho_c^{res} = Y_e^{man} \rho_{man}^{res}$, or $C_s \rho_r = 0.5(3Y_e^c - 1)\rho_c^{res} = 0.5(3Y_e^{man} - 1)\rho_{man}^{res}$ depending on whether $\nu_e - \nu_{\mu(\tau)}$ or $\nu_e - \nu_s$ mixing takes place. The relation between ρ_r and $\Delta m^2/E$, expressed in units of g/cm³ and eV²/MeV, respectively, has the form:

$$\rho_r[g/cm^3] = 1.32 \times 10^7 \frac{0.5}{C_{a(s)}} \frac{\Delta m^2[eV^2]}{E[MeV]} \cos 2\theta. \quad (7b)$$

For a neutrino trajectory which is specified by a given Nadir angle h we have:

$$X' = R_\oplus \cosh -\sqrt{R_c^2 - R_\oplus^2 \sin^2 h}, \quad X'' = 2\sqrt{R_c^2 - R_\oplus^2 \sin^2 h}. \quad (8)$$

The conditions for the presence of a neutrino oscillation length resonance maximum in P_{e2} read [1]:

$$\Delta E' X' = \pi(2k + 1), \quad \Delta E'' X'' = \pi(2k' + 1), \quad k, k' = 0, 1, 2, \dots, \quad (9)$$

and

$$\sin^2(2\theta''_m - 4\theta'_m + \theta) - \sin^2 \theta > 0, \quad (10a)$$

$$\begin{aligned} & \sin^2(2\theta''_m - 4\theta'_m + \theta) \sin(2\theta''_m - 2\theta'_m) \sin(2\theta'_m - \theta) \cos(2\theta''_m - 4\theta'_m + \theta) \\ & + \frac{1}{4} \sin^2 \theta \sin(4\theta''_m - 8\theta'_m + 2\theta) \sin(4\theta''_m - 4\theta'_m) < 0. \end{aligned} \quad (10b)$$

When equalities (9) hold, conditions (10a) and (10b) ensure that P_{e2} has a maximum⁹. At the resonance maximum the probability P_{e2} takes the value [1]:

$$P_{e2}^{max} = \sin^2(2\theta''_m - 4\theta'_m + \theta). \quad (11)$$

If instead of inequality (10a) we have

$$\sin^2(2\theta''_m - 4\theta'_m + \theta) - \sin^2 \theta < 0, \quad (12)$$

and inequality (10b) is fulfilled (together with equalities (9)), the neutrino oscillation resonance extrema in P_{e2} correspond to minima.

As was already indicated in the Introduction, the oscillation length resonance is present in the $\nu_\mu \rightarrow \nu_e$ (and $\nu_e \rightarrow \nu_{\mu(\tau)}$) transitions of atmospheric neutrinos as well [1]. The probability of the $\nu_\mu \rightarrow \nu_e$ ($\nu_e \rightarrow \nu_{\mu(\tau)}$) transitions, $P(\nu_\mu \rightarrow \nu_e) = P(\nu_e \rightarrow \nu_{\mu(\tau)})$, can be obtained¹⁰ from eq. (1) by formally setting $\theta = 0$ while keeping $\theta'_m \neq 0$ and $\theta''_m \neq 0$:

$$P(\nu_\mu \rightarrow \nu_e) = P(\nu_e \rightarrow \nu_{\mu(\tau)}) = \frac{1}{2} [1 - \cos \Delta E'' X''] \sin^2 2\theta''_m$$

⁹Note that the factor 1/4 in the second term in the left-hand side of the inequality (10b) is missing in the same inequality given in [1] (see eq. (12b) in [1]).

¹⁰All subsequent results for the $\nu_\mu \rightarrow \nu_e$ and $\nu_e \rightarrow \nu_{\mu(\tau)}$ transitions will be formulated for the probability $P(\nu_\mu \rightarrow \nu_e)$.

$$\begin{aligned}
& + \frac{1}{4} [1 - \cos \Delta E'' X''] [1 - \cos \Delta E' X'] [\sin^2(2\theta''_m - 4\theta'_m) - \sin^2 2\theta''_m] \\
& - \frac{1}{4} [1 - \cos \Delta E'' X''] [1 - \cos 2\Delta E' X'] \sin^2 2\theta'_m \cos^2(2\theta''_m - 2\theta'_m) \\
& + \frac{1}{4} [1 + \cos \Delta E'' X''] [1 - \cos 2\Delta E' X'] \sin^2 2\theta'_m \\
& + \frac{1}{2} \sin \Delta E'' X'' \sin 2\Delta E' X' \sin^2 2\theta'_m \cos(2\theta''_m - 2\theta'_m) \\
& + \frac{1}{4} [\cos(\Delta E' X' - \Delta E'' X'') - \cos(\Delta E' X' + \Delta E'' X'')] \sin 4\theta'_m \sin(2\theta''_m - 2\theta'_m). \quad (13)
\end{aligned}$$

Correspondingly, the maximum conditions (9) are the same as for P_{e2} , while the analogs of the conditions (10a) and (10b) for this probability change: condition (10a) becomes $\sin^2(2\theta''_m - 4\theta'_m) > 0$ and is always fulfilled, while condition (10b) transforms into [1]

$$\cos(2\theta''_m - 4\theta'_m) < 0. \quad (14)$$

Obviously, in contrast to P_{e2} , the probability $P(\nu_\mu \rightarrow \nu_e)$ cannot have minima associated with conditions (9).

At small mixing angles, $\sin^2 2\theta < 0.10$, the maxima in the probabilities P_{e2} and $P(\nu_\mu \rightarrow \nu_e)$ associated with the conditions (9) and (10a), (10b), and (9) and (14), are absolute maxima. For given $\sin^2 2\theta$ and trajectory crossing the Earth core, the neutrino oscillation length resonance is relatively wide in the variable $E/\Delta m^2$ (or ρ_r , see Figs. 1 and 2 in [1]).

The analytic expression and the resonance conditions (13) and (14) derived for the probability $P(\nu_\mu \rightarrow \nu_e)$ are valid, with minor modifications, for the probabilities of the i) $\nu_e \rightarrow \nu_s$ ($\bar{\nu}_e \rightarrow \bar{\nu}_s$) and ii) $\nu_\mu \rightarrow \nu_s$ ($\bar{\nu}_\mu \rightarrow \bar{\nu}_s$) transitions, $P(\nu_e \rightarrow \nu_s)$ ($P(\bar{\nu}_e \rightarrow \bar{\nu}_s)$) and $P(\nu_\mu \rightarrow \nu_s)$ ($P(\bar{\nu}_\mu \rightarrow \bar{\nu}_s)$): one has to use in eqs. (3), (4), (9) and (14) and in the formula for $P(\nu_\mu \rightarrow \nu_e)$, the expressions for the resonance densities $\rho_{man,c}^{res}$ with i) $f(Y_e)$ given by eq. (6) ($f(Y_e) = 0.5(1 - 3Y_e)$) and ii) $f(Y_e) = 0.5(Y_e - 1)$ ($f(Y_e) = 0.5(1 - Y_e)$), respectively. Since Y_e for the Earth is close to 0.5, only the probabilities $P(\nu_e \rightarrow \nu_s)$ and $P(\bar{\nu}_\mu \rightarrow \bar{\nu}_s)$ can, in principle, be amplified for $\cos 2\theta > 0$ by the oscillation length resonance if $\Delta m^2 > 0$, which is assumed throughout this study. Note, however, that in the case of two-neutrino mixing, the probability $P(\nu_e \rightarrow \nu_s)$ ($P(\bar{\nu}_\mu \rightarrow \bar{\nu}_s)$) for $\Delta m^2 > 0$ coincides, as can be easily shown, with the probability $P(\bar{\nu}_e \rightarrow \bar{\nu}_s)$ ($P(\nu_\mu \rightarrow \nu_s)$) for $\Delta m^2 < 0$ for any given values of E , $|\Delta m^2|$ and θ , and that conditions (9) and (14) are identical in the two cases.

The phase κ and the probability amplitude $A_{2\nu}(\nu_\tau \rightarrow \nu_\tau)$, which appear in eq. (1b) for the flux of atmospheric ν_μ in the case of three-flavour neutrino mixing and strong hierarchy between the neutrino mass squared differences and therefore can play important role in the interpretation of the, e.g., Super-Kamiokande atmospheric neutrino data, have the following form in the two-layer model of the Earth density distribution [1,11,12]:

$$\kappa \cong \frac{1}{2} \left[\frac{\Delta m_{31}^2}{2E} X + \sqrt{2} G_F \frac{1}{m_N} (X'' Y_e^c \bar{\rho}_c + 2X' Y_e^{man} \bar{\rho}_{man}) - 2\Delta E' X' - \Delta E'' X'' \right] - \frac{\Delta m_{21}^2}{2E} X \cos 2\varphi_{12}, \quad (15)$$

$$A_{2\nu}(\nu_\tau \rightarrow \nu_\tau) = 1 + \left(e^{-i2\Delta E' X'} - 1 \right) \left[1 + \left(e^{-i\Delta E'' X''} - 1 \right) \cos^2(\theta'_m - \theta''_m) \right] \cos^2 \theta'_m$$

$$+ \left(e^{-i\Delta E'' X''} - 1 \right) \cos^2 \theta''_m + \frac{1}{2} \left(e^{-i\Delta E'' X''} - 1 \right) \left(e^{-i\Delta E' X'} - 1 \right) \sin(2\theta'_m - 2\theta''_m) \sin 2\theta'_m. \quad (16)$$

where $X = X'' + 2X'$ and ¹¹ $\cos 2\varphi_{12} = (|U_{e1}|^2 - |U_{e2}|^2)/(1 - |U_{e3}|^2)$.

Let us note finally that the neutrino oscillation length resonance arises when the conditions specified above are fulfilled, due basically to the interference between the probability amplitudes describing the neutrino transitions in the Earth core and in the Earth mantle.

3. The Oscillation Length Resonance Conditions and the

Probabilities P_{e2} , $P(\nu_\mu \rightarrow \nu_e)$ ($P(\nu_e \rightarrow \nu_{\mu(\tau)})$) and $P(\bar{\nu}_\mu \rightarrow \bar{\nu}_s)$

3.1. The Resonance Conditions

The quantities $\Delta E' X'$ and $\Delta E'' X''$ represent the phase differences the states of the energy-eigenstate neutrinos acquire after the neutrinos have crossed the mantle and the core, respectively. Thus, the neutrino oscillation length resonance can take place only when these phases are correlated, being odd multiples of π , eq. (9). Since

$$\Delta E' (\Delta E'') = \frac{2\pi}{L_{man(c)}^m}, \quad (17)$$

where $L_{man(c)}^m$ is the neutrino oscillation length in matter in the Earth mantle (core), and X' and X'' are fixed for a given neutrino trajectory, conditions (9) are constraints on the oscillation lengths L_{man}^m and L_c^m . When these constraints are satisfied, the oscillating factors in the first two terms in the expressions (2) and (13) for P_{e2} and $P(\nu_\mu \rightarrow \nu_e)$ are maximized. If in addition inequalities (10a) and (10b) or (14) hold, this produces the resonance maximum of interest in P_{e2} or $P(\nu_\mu \rightarrow \nu_e)$. For these *two* reasons the term “neutrino oscillation length resonance” was used in [1] to denote the effect under discussion. Although this term may not be perfect, it underlines the physical essence of the effect.

Conditions (9) and conditions (10a) and (10b) are shown graphically in Figs. 1a - 1f and in Figs. 2a - 2b, respectively, while condition (14) is shown in Figs. 3a - 3b. Figures 1a - 1f, 2a - 2b and 3a - 3b correspond to the case of $\nu_e - \nu_{\mu(\tau)}$ mixing. We will discuss first conditions (10a), (10b) and (14). As was noticed in [1], at small mixing angles, $\sin^2 2\theta \lesssim 0.10$, (10a) is fulfilled for

$$\rho_{man}^{res} < (2r - 1)\bar{\rho}_{man}, \quad \rho_{man}^{res} \neq \bar{\rho}_{man}, \quad (18a)$$

where

$$r \equiv \frac{\bar{\rho}_c Y_e^c}{\bar{\rho}_{man} Y_e^{man}}. \quad (18b)$$

For the standard values of $\bar{\rho}_{man,c}$ and $Y_e^{man,c}$ given earlier one has $r \cong 2.44$ and (18a) corresponds to $\rho_{man}^{res} < 17.4 \text{ g/cm}^3$, which is in very good agreement with our numerical results (Fig. 2a). Actually, as Figs. 2a - 2b show, (10a) is fulfilled for any θ in a subregion

¹¹The expression for $A_{2\nu}(\nu_\tau \rightarrow \nu_\tau)$ can be obtained from eq. (1) in ref. [1] by formally setting $\theta = \pi/2$ while keeping θ'_m and θ''_m arbitrary, and then interchanging $\sin \theta'_m$ ($\sin \theta''_m$) and $\cos \theta'_m$ ($\cos \theta''_m$).

of the region determined by (18a). Condition (10b) holds in two practically disconnected regions (Figs. 2a - 2b). In the region where (10a) is satisfied, condition (10b) reduces to the simple inequality [1]:

$$\cos(2\theta''_m - 4\theta'_m + \theta) < 0. \quad (18c)$$

Thus, condition (18c) determines effectively the region where both inequalities (10a) and (10b) are valid at $\sin^2 2\theta \lesssim 0.10$. Condition (18c) can be satisfied for [1]

$$\bar{\rho}_{man} < \rho_{man,c}^{res} < \bar{\rho}_c, \quad (19a)$$

as well as for

$$0 < \rho_{man}^{res} < \bar{\rho}_m. \quad (19b)$$

Only the first region, (19a), is relevant for the transitions of solar neutrinos with parameters corresponding to the small mixing angle MSW solution of the solar neutrino problem [1]. At large mixing angles the oscillation length resonance enhancement of P_{e2} can take place only in the second region, (19b) (see further).

In the region $\rho_{man}^{res} > (2r-1)\bar{\rho}_{man}$, where inequality (12) holds, condition (10b) is satisfied at small mixing angles for

$$\frac{2r}{3(r-1)} \left(\sqrt{1 + \frac{4r}{9(r-1)^2}} - 1 \right)^{-1} \bar{\rho}_{man} < \rho_{man}^{res} < \frac{3r-1}{3-r} \bar{\rho}_{man}. \quad (20)$$

For $r \cong 2.44$, (20) gives $21.7 \text{ g/cm}^3 < \rho_{man}^{res} < 50.3 \text{ g/cm}^3$ - in very nice agreement with our numerical results (Fig. 2a). Note that, as it follows from Fig. 2a, condition (10b) is fulfilled in most of the region determined by (20) even at relatively large mixing angles.

Condition (14) holds at small mixing angles for (Fig. 3a)

$$\rho_{man,c}^{res} < \bar{\rho}_c, \quad \rho_{man}^{res} \neq \bar{\rho}_{man}. \quad (21)$$

The regions determined by the two inequalities (10a), (10b) and by the inequality (14) differ at large mixing angles.

At small mixing angles, $\sin^2 2\theta \lesssim 0.10$, conditions (9) can be fulfilled only for $k = k' = 0$ [1]. For the $\nu_2 \rightarrow \nu_e$ transitions in the case of $\nu_e - \nu_{\mu(\tau)}$ mixing, and for the $\nu_\mu \rightarrow \nu_e$ and $\nu_e \rightarrow \nu_{\mu(\tau)}$ transitions, taking place along the trajectories with $h = 0^\circ; 13^\circ; 23^\circ$, one has $\Delta E' X' = \pi$ and $\Delta E'' X'' = \pi$ at $\sin^2 2\theta \cong 0.045; 0.05; 0.08$ and $\rho_r \cong 9.7; 9.4; 8.5 \text{ g/cm}^3$, respectively. As can be easily seen from Figs. 1a - 1c, Fig. 2a and Fig. 3a, all the three points lie rather close to, but outside the regions determined by the inequality (10b) (or (18c)) and by the inequality (14). Thus, for $\sin^2 2\theta < 0.040$ conditions (9) are never exactly satisfied for the trajectories of neutrinos crossing the Earth core [1]: one has either $\Delta E' X' = \pi$ and $\Delta E'' X''$ relatively close but different from π , or *vice versa*. This can also be seen from the fact that at $\sin^2 2\theta \lesssim 0.02$, one of the two conditions in (9) is equivalent to the following physical condition [1]:

$$\pi \left[\frac{1}{X'} + \frac{1}{X''} \right] \cong \sqrt{2} G_F \frac{1}{m_N} (Y_e^c \bar{\rho}_c - Y_e^{man} \bar{\rho}_{man}) = \sqrt{2} G_F (\bar{N}_e^c - \bar{N}_e^{man}), \quad (22)$$

\bar{N}_e^c and \bar{N}_e^{man} being the average core and mantle electron number densities along the chosen neutrino trajectory. One can easily convince oneself using eq. (8), the values of the core

and Earth radii R_c and R_\oplus and the values of Y_e^c , $\bar{\rho}_c$, Y_e^{man} and $\bar{\rho}_{man}$ that the above equality cannot be exactly satisfied for the trajectories of neutrinos crossing the Earth core.

Conditions (9) are fulfilled for certain values of $\sin^2 2\theta$ from the interval $(0.04 - 0.10)$, but in this case inequality (10b) (or (18c)) and inequality (14), which guarantee that the relevant neutrino transition probabilities have maxima, are not fulfilled. Nevertheless, the probabilities P_{e2} and $P(\nu_\mu \rightarrow \nu_e)$ are strongly (resonantly) enhanced even when conditions (9) are only approximately satisfied due to the fact that the neutrino oscillation length resonance is relatively wide [1].

As Figs. 1a - 1c, 2a and 3a demonstrate, the point where $\Delta E'X' = \pi$ and $\Delta E''X'' = \pi$, which is closest to the regions determined by (10a), (10b) or by (14), corresponds to $h = 0^\circ$. As a consequence, the values of P_{e2} and $P(\nu_\mu \rightarrow \nu_e)$ at their corresponding maxima for the trajectory with $h = 0^\circ$ and small mixing angles ($\sin^2 2\theta \lesssim 0.02$) are bigger than $\max P_{e2}$ and $\max P(\nu_\mu \rightarrow \nu_e)$ for the other trajectories crossing the Earth core: $\max P_{e2}$ and $\max P(\nu_\mu \rightarrow \nu_e)$ decrease with the increase of h . This is illustrated in Figs. 4a and 4b showing the dependence of the probability P_{e2} on h for $\rho_r = 10 \text{ g/cm}^3$ (Fig. 4a) and on h and ρ_r (Fig. 4b) for $\sin^2 2\theta = 0.01$. Figure 4a clearly demonstrates also that i) the neutrino oscillation length resonance can take place only if the neutrinos cross the Earth core, ii) this resonance is relatively wide in the Nadir angle variable h as well, and that iii) the resonance of interest is distinctly different from the MSW resonance in the mixing as the enhancement of P_{e2} due to the latter cannot and does not take place at $\rho_r = 10 \text{ g/cm}^3$ [1].

Comparing Fig. 2a (2b) and Fig. 3a (3b) one notices that the regions allowed by the inequalities (10b) or (18c) and (14) for values of the resonance densities from the interval (19a) differ somewhat even for $\sin^2 2\theta \cong (0.01 - 0.10)$. This difference is due to the presence of θ in the argument of the cosine in (18c). As a result, the points at which we have $\Delta E'X' = \pi$ and $\Delta E''X'' = \pi$ for the different trajectories through the Earth core are closer to the region where (18c) holds than to the region of validity of (14). Correspondingly, we can expect that for given $h \lesssim 28^\circ$, $\sin^2 2\theta \cong (0.01 - 0.10)$, and transitions involving active neutrinos only, the maxima associated with the neutrino oscillation length resonance satisfy $\max P_{e2} \gtrsim \max P(\nu_\mu \rightarrow \nu_e)$ and/or that the width of the resonance in P_{e2} is larger than that in $P(\nu_\mu \rightarrow \nu_e)$. The dependence of the probability $P(\nu_\mu \rightarrow \nu_e)$ on $E/\Delta m^2$ and h for three values of $\sin^2 2\theta$, 0.005, 0.01 and 0.05, is shown graphically in Figs. 5a - 5c.

Similar analysis can be performed for the $\nu_2 \rightarrow \nu_e$ small mixing angle (solar) neutrino transitions in the Earth in the case of $\nu_e - \nu_s$ mixing. Equations (18a), (18c), (19a) - (19b) and (20) - (22) and the discussions associated with them remain valid in this case after a minor change: we have to replace Y_e by $0.5(3Y_e - 1)$ and use for the ratio r the expression

$$r \equiv \frac{\bar{\rho}_c (3Y_e^c - 1)}{\bar{\rho}_{man}(3Y_e^{man} - 1)} \quad (23)$$

in these equations. The numerical values of the parameter r and of the upper and lower limits (18a) and in (20) now read, respectively: $r \cong 2.180$, $\rho_{man}^{res} < 15.1 \text{ g/cm}^3$ and $18.3 \text{ g/cm}^3 < \rho_{man}^{res} < 30.4 \text{ g/cm}^3$. The lines of $\Delta E'X' = \pi(2k + 1)$ and $\Delta E''X'' = \pi(2k' + 1)$ in the $\Delta m^2/E - \sin^2 2\theta$ plane are shown in Figs. 6a - 6c for the trajectories with $h = 0^\circ$; 13° ; 23° , while the regions where conditions (10a) and (10b) are satisfied are depicted in Fig. 7. As we have already indicated [1], the oscillation length resonance conditions (9) and (10a) - (10b) are not even approximately fulfilled simultaneously for the $\nu_2 \rightarrow \nu_e$ transitions of

interest at small mixing angles. This is well illustrated by Figs. 6a - 6c and 7. Conditions (9) with $k = k' = 0$ can¹² both be satisfied only for $h \gtrsim 15^\circ$. At $h = 16^\circ$, for example, we have $\Delta E'X' = \pi$ and $\Delta E''X'' = \pi$ at $\sin^2 2\theta \sim 0.01$ for $\Delta m^2/E \sim 5.5 \times 10^{-7}$ eV²/MeV ($\rho_r \sim 14.3$ g/cm³), but this point is located rather far from the region where (10a) - (10b) hold (Fig. 7). With the increase of h the point where one has $\Delta E'X' = \pi$ and $\Delta E''X'' = \pi$ is moving further away from the region where (10a) - (10b) are fulfilled (Fig. 6c). As a consequence, the effect of the oscillation length resonance on the $\nu_2 \rightarrow \nu_e$ transitions at small $\sin^2 2\theta$ is considerably weaker if the latter are triggered by $\nu_e - \nu_s$ mixing in vacuum. In spite of that, the $\nu_2 \rightarrow \nu_e$ transition probability is noticeably enhanced in the region of the MSW effect in the Earth core by interference terms present in P_{e2} in addition to the MSW terms and the dominant term associated with the oscillation length resonance [1] - notably by the contribution of the last term in eq. (2). Analogous results are valid for the $\nu_e \rightarrow \nu_s$ transitions at small mixing.

It is quite interesting that, in contrast to the case just considered, the oscillation length resonance conditions (9) with $k = 0$ and $k' = 0$ can both be satisfied for the $\bar{\nu}_\mu \rightarrow \bar{\nu}_s$ transitions at small mixing angles ($\sin^2 2\theta \lesssim 0.10$) for the trajectories with $h \lesssim 15^\circ$. These transitions are strongly enhanced for $h \lesssim 15^\circ$ in spite of the fact that the points where the equalities $\Delta E'X' = \pi$ and $\Delta E''X'' = \pi$ hold lie outside the region determined by the inequality (14) (Figs. 8a, 8b, 9, 10a-10b). For $h = 0^\circ$, for instance, one has $\Delta E'X' = \pi$, $\Delta E''X'' = \pi$ for $\sin^2 2\theta \cong 0.05$ and $\Delta m^2/E \cong 6 \times 10^{-7}$ eV²/MeV ($\rho_r \cong 15.8$ g/cm³). However, the dominating absolute maximum of $P(\bar{\nu}_\mu \rightarrow \bar{\nu}_s)$ occurs in the region of the MSW resonance in the Earth core, i.e., at $\Delta m^2/E \sim 4.1 \times 10^{-7}$ eV²/MeV ($\rho_r \sim 10.8$ g/cm³). Actually, at the point where conditions (9) hold one has $P(\bar{\nu}_\mu \rightarrow \bar{\nu}_s) = \sin^2(2\theta''_m - 4\theta'_m)$, but the function $\sin^2(2\theta''_m - 4\theta'_m)$ takes a relatively small value and $P(\bar{\nu}_\mu \rightarrow \bar{\nu}_s)$ is strongly suppressed. At the same time in the example we are considering $\max P(\bar{\nu}_\mu \rightarrow \bar{\nu}_s) \cong 0.94$. The strong enhancement of $P(\bar{\nu}_\mu \rightarrow \bar{\nu}_s)$ at small mixing angles is due to the term in the expression for $P(\bar{\nu}_\mu \rightarrow \bar{\nu}_s)$, describing the MSW effect in the Earth core and to an equally important interference term - the analog of the last term in eq. (13) for $P(\nu_\mu \rightarrow \nu_e)$. Thus, the mechanism of enhancement of $P(\bar{\nu}_\mu \rightarrow \bar{\nu}_s)$ at small mixing angles is similar to the mechanism of enhancement of P_{e2} in the case of $\nu_e - \nu_s$ mixing. Note that, e.g., for $h = 0^\circ$, $\sin^2 2\theta \cong 0.01$ and $\Delta m^2 = 5 \times 10^{-4}$; 10^{-3} ; 4×10^{-3} eV², the dominating absolute maximum in $P(\bar{\nu}_\mu \rightarrow \bar{\nu}_s)$ takes place at $E \cong 1.2$; 2.3 ; 9.6 GeV, which fall in the intervals of energies of $\bar{\nu}_\mu$ contributing either to the sub-GeV or to the multi-GeV μ -like samples of Super-Kamiokande atmospheric neutrino events. Obviously, the discussed strong enhancement of $P(\bar{\nu}_\mu \rightarrow \bar{\nu}_s)$ (or of $P(\nu_\mu \rightarrow \nu_s)$ if $\Delta m^2 < 0$) can be utilized to perform a rather sensitive search for, and might allow to detect, $\bar{\nu}_\mu \rightarrow \bar{\nu}_s$ (or $\nu_\mu \rightarrow \nu_s$) transitions of, e.g., the atmospheric $\bar{\nu}_\mu$ (or ν_μ) at small mixing angles. For $\sin^2 2\theta = 0.01$; 0.05 the dependence of the probability $P(\bar{\nu}_\mu \rightarrow \bar{\nu}_s)$ on h and $E/\Delta m^2$ is shown in Figs. 10a and 10b.

At large mixing angles, $\sin^2 2\theta \gtrsim 0.10$, and $\nu_e - \nu_{\mu(\tau)}$ mixing, inequalities (10a) and (10b)

¹²Among the lines on the $\Delta m^2/E - \sin^2 2\theta$ plane determined by the conditions $\Delta E'X' = \pi(2k+1)$ and $\Delta E''X'' = \pi(2k'+1)$, those corresponding to $k = 0$ and $k' = 0$ are located at small mixing angles closer to the region where conditions (10a) and (10b) (or (14)) hold, than the lines for $k \neq 0$ and $k' \neq 0$.

or (14) can be satisfied only in the interval (19b) (Fig. 2a). The corresponding regions of maxima of P_{e2} and $P(\nu_\mu \rightarrow \nu_e)$ differ somewhat (compare Fig. 2a (2b) and Fig. 3a (3b)). In the regions where (10a) and (10b) hold or (14) is satisfied, conditions (9) are fulfilled only for $k = 0$ and $k' = 1$, and only for $h \gtrsim 20^\circ$: we have $\Delta E' X' = \pi$ and $\Delta E'' X'' = 3\pi$ for the trajectory with $h = 23^\circ$, for instance, at $\sin^2 2\theta \cong 0.88$ and $\rho_r \cong 1.23 \text{ g/cm}^3$ ($E/\Delta m^2 \cong 3.695 \times 10^6 \text{ MeV/eV}^2$). Correspondingly, the probability $P(\nu_\mu \rightarrow \nu_e)$ has a maximum at the indicated point due to the neutrino oscillation length resonance¹³.

Conditions (9) can be satisfied for $k \geq 0$ and $k' \geq 1$ at large mixing angles in the region $\rho_m^{res} > \bar{\rho}_m$ as well, as Figs. 1a - 1c illustrate. For the trajectory with $h = 13^\circ$, for example, we have $\Delta E' X' = \pi$ and $\Delta E'' X'' = 3\pi$ at $\sin^2 2\theta \cong 0.52$ and $\rho_r \cong 5.4 \text{ g/cm}^3$; $\Delta E' X' = 3\pi$ and $\Delta E'' X'' = 5\pi$ at $\sin^2 2\theta \cong 0.4$ and $\rho_r \cong 15 \text{ g/cm}^3$; and $\Delta E' X' = 5\pi$ and $\Delta E'' X'' = 9\pi$ at $\sin^2 2\theta \cong 0.42$ and $\rho_r \cong 23 \text{ g/cm}^3$. All these points correspond, however, to minima in P_{e2} : now conditions (12) (instead of (10a)) and (10b) are fulfilled. They correspond to saddle points in $P(\nu_\mu \rightarrow \nu_e)$. Some of the minima can be very deep. This is clearly seen in Fig. 11 showing the dependence of P_{e2} on ρ_r for $\sin^2 2\theta = 0.4$. Only the minimum at $\rho_r \sim (6.0 - 7.0) \text{ g/cm}^3$ ($h = 0^\circ; 13^\circ$) is an absolute one: we have $P_{e2} = 0$ at this minimum. Note that such a deep minimum is not present in the same region for the trajectory with $h = 23^\circ$, in accord with the results shown in Figs. 1a - 1c. Nevertheless, the indicated minimum in P_{e2} at $h \lesssim 16^\circ$ leads to the "island" of somewhat reduced values of the D-N asymmetry in the vicinity of the point $\sin^2 2\theta \cong 0.45$, $\Delta m^2 \cong 5 \times 10^{-5} \text{ eV}^2$ in the *core* sample of the solar neutrino events in the Super-Kamiokande detector (see Fig. 3c in [2]). The wide deep minimum in P_{e2} in the case of $\nu_e \rightarrow \nu_s$ transitions of the core-crossing solar neutrinos, taking place at $\sin^2 2\theta \cong (0.30 - 0.55)$ and $\rho_r \cong (6 - 10) \text{ g/cm}^3$ (Fig. 12), has apparently a similar origin¹⁴. The other minima in P_{e2} at $\rho_r > 10 \text{ g/cm}^3$ are relatively shallow.

It should be noted that the large mixing angle (LMA) MSW $\nu_e \rightarrow \nu_{\mu(\tau)}$ transition solution of the solar neutrino problem is possible, as the analyzes of the solar neutrino data show, for $\Delta m^2 \gtrsim 10^{-5} \text{ eV}^2$ and $0.60 \lesssim \sin^2 2\theta \lesssim 0.96$. As we have seen, the oscillation length resonance maxima in P_{e2} can take place at large mixing angles only for $\rho_r < \bar{\rho}_{man} \cong 4.5 \text{ g/cm}^3$. Correspondingly, P_{e2} can be enhanced due to this resonance only for neutrino energies

$$E \gtrsim 30 \text{ MeV} \cos 2\theta, \quad (24)$$

which can fall in the range of (5 - 14) MeV, causing substantial D-N asymmetry in the spectrum of ^8B neutrinos, only for $0.80 \lesssim \sin^2 2\theta \lesssim 0.95$ and only for the trajectories with $h \gtrsim 20^\circ$. Figure 13 illustrates the dependence of the probability P_{e2} on ρ_r for $\sin^2 2\theta = 0.9$.

Let us emphasize in conclusion of this Section that for most of the neutrino trajectories crossing the Earth core the neutrino oscillation length resonance takes place at values of the

¹³Conditions (9) (and (14) or (10a) - (10b)) are also satisfied for the $\nu_{\mu(e)} \rightarrow \nu_{e(\mu)}$ and $\nu_2 \rightarrow \nu_e$ transitions at $\sin^2 2\theta \cong 1$. The study of this specific case will be reported elsewhere.

¹⁴The existence of this minimum is reflected in the prediction of a spectacularly large in absolute value but *negative* D-N asymmetry at $\sin^2 2\theta \sim 0.50$, $\Delta m^2 \sim 3.5 \times 10^{-6} \text{ eV}^2$ in the *core* sample of the the Super-Kamiokande solar neutrino induced events (see footnote 11 and Figs. 3.11, 3.12 and 6a - 6d in [3]).

resonance density which differ from the values of the density met, according to the Earth models, in the Earth mantle and in the Earth core.

3.2. Properties of the Probabilities P_{e2} , $P(\nu_\mu \rightarrow \nu_e)$ ($P(\nu_e \rightarrow \nu_{\mu(\tau)})$) and $P(\bar{\nu}_\mu \rightarrow \bar{\nu}_s)$ in the Oscillation Length Resonance Regions

As one can easily check utilizing Figs. 1d - 1f, 2b and 3b, practically all maxima of P_{e2} and $P(\nu_\mu \rightarrow \nu_e)$ associated with the neutrino oscillation length resonance, take place along the line $\Delta E' X' = \pi$. For $\Delta E' X' = \pi(2k + 1)$, the probabilities P_{e2} and $P(\nu_\mu \rightarrow \nu_e)$ have for any θ the following form [1]:

$$P_{e2} = \sin^2 \theta + \frac{1}{2} [1 - \cos \Delta E'' X''] [\sin^2(2\theta''_m - 4\theta'_m + \theta) - \sin^2 \theta], \quad \Delta E' X' = \pi(2k + 1), \quad (25)$$

$$P(\nu_\mu \rightarrow \nu_e) = P(\nu_e \rightarrow \nu_{\mu(\tau)}) = \frac{1}{2} [1 - \cos \Delta E'' X''] \sin^2(2\theta''_m - 4\theta'_m), \quad \Delta E' X' = \pi(2k + 1). \quad (26)$$

Expressions (25) and (26) describe P_{e2} and $P(\nu_\mu \rightarrow \nu_e)$ in the region of the neutrino oscillation length resonance; they determine, in particular, the width of the resonance. Obviously, many of the properties of, e.g., the probability P_{e2} in the resonance region are determined by the properties of the function $\sin^2(2\theta''_m - 4\theta'_m + \theta)$ in eq. (25).

The dependence of the function $\sin^2(2\theta''_m - 4\theta'_m + \theta)$ on ρ_r is shown graphically in Fig. 14 for $\sin^2 2\theta = 0.005; 0.01; 0.05; 0.10; 0.50; 0.90$. At small mixing angles, $\sin^2 2\theta \lesssim 0.02$, $\sin^2(2\theta''_m - 4\theta'_m + \theta)$ has three distinct maxima [1]: at $\rho_c^{res} \cong \bar{\rho}_c$ where $2\theta''_m \cong \pi/2$ and $4\theta'_m - \theta \cong 5.6\theta \lesssim 0.13\pi \ll 2\theta''_m$, and at the points where

$$2\theta'_m \cong \frac{\pi}{4}, \quad \frac{3\pi}{4}, \quad (27a)$$

which is realized for

$$\rho_{man}^{res} \cong \frac{\bar{\rho}_{man}}{1 \pm 2\sqrt{2}\theta}. \quad (27b)$$

At these two points $2\theta''_m \cong \pi$. The same function has two distinct minima in the interval $0 < \rho_{man}^{res} < \bar{\rho}_c$: at $\rho_{man}^{res} \cong \bar{\rho}_{man}$ ($4\theta'_m \cong \pi$, $2\theta''_m \cong \pi$) and at [1]

$$\rho_{man}^{res} \cong \kappa \bar{\rho}_{man}, \quad (28a)$$

where

$$\kappa \cong \frac{r\sqrt{2} + \sqrt{r}}{\sqrt{2} + \sqrt{r}}. \quad (28b)$$

The first minimum is rather deep, while the second one is relatively shallow [1]. At the first minimum $\sin^2(2\theta''_m - 4\theta'_m + \theta) \cong \sin^2 \theta$, and at the second

$$\min \sin^2(2\theta''_m - 4\theta'_m + \theta) \cong \sin^2 \left[\pi - 2\theta\kappa((r - \kappa)^{-1} + 2(\kappa - 1)^{-1}) + \theta \right]. \quad (28c)$$

For $r \cong 2.44$ ($\nu_e - \nu_{\mu(\tau)}$ mixing) one finds $\kappa \cong 1.68$, and correspondingly $\rho_{man}^{res} = \kappa \bar{\rho}_{man} \cong 7.57 \text{ g/cm}^3$ and $\min \sin^2(2\theta''_m - 4\theta'_m + \theta) \cong \sin^2(\pi - 13.3\theta)$, which is in excellent agreement

with our numerical results¹⁵. Note that the positions of both minima depend very weakly on θ at small mixing angles.

The oscillation length resonance maximum in P_{e2} occurs for given $\sin^2 2\theta \lesssim 0.05$ and the different neutrino trajectories through the Earth core at values of $\rho_r \cong (8.0-9.7) \text{ g/cm}^3$. The precise position of the maximum is determined by the factor $0.5(1 - \cos \Delta E'' X'')$ in eq. (25) and it does not coincide with the position of the maximum of the function $\sin^2(2\theta''_m - 4\theta'_m + \theta)$ [1]. Actually, the maximum of P_{e2} falls in the interval of values of ρ_r between the minimum at $\rho_{man}^{res} \cong \kappa \bar{\rho}_{man} \cong 7.57 \text{ g/cm}^3$ and the maximum at $\rho_c^{res} \cong \bar{\rho}_c \cong 11.5 \text{ g/cm}^3$ of the factor $[\sin^2(2\theta''_m - 4\theta'_m + \theta) - \sin^2 \theta]$, where the latter rises steeply (Fig. 14). For this reason, in particular, the width of the neutrino oscillation length resonance in P_{e2} is determined at $\sin^2 2\theta \lesssim 0.05$ by the expression (25) and not only by the function $\sin^2(2\theta''_m - 4\theta'_m + \theta)$, as one might have expected on the basis of eq. (11). The same considerations apply to the position of the oscillation length resonance maximum and the width of the resonance in the probability $P(\nu_\mu \rightarrow \nu_e)$ in the indicated range of values of $\sin^2 2\theta$.

The minimum of $\sin^2(2\theta''_m - 4\theta'_m + \theta)$ at $\rho_{man}^{res} \cong \kappa \bar{\rho}_{man}$ becomes shallower as $\sin^2 2\theta$ increases starting, say, from the value 0.001. At $\sin^2 2\theta = 0.05$ ($\theta \cong 0.11$) it is still visible (Fig. 14), but $\min \sin^2(2\theta''_m - 4\theta'_m + \theta) \cong 0.98$. As $\sin^2 2\theta$ increases further this minimum disappears and the two maxima it separated, at $\rho_{man}^{res} \cong \bar{\rho}_{man}/(1 - 2\sqrt{2}\theta)$ ($2\theta'_m \cong \pi/4$) and at $\rho_c^{res} \cong \bar{\rho}_c$ ($2\theta''_m \cong \pi/2$), merge to form one maximum. The latter is located practically at the position of the indicated minimum, i.e., at $\rho_{man}^{res} \cong \kappa \bar{\rho}_{man}$, as this is clearly seen in the case of $\sin^2 2\theta = 0.10$ in Fig. 14: at this point $2\theta''_m - 4\theta'_m + \theta$ is just close to $\pi/2$ due to the relatively large value of θ . As $\sin^2 2\theta$ increases beyond 0.10, this maximum diminishes since $2\theta''_m - 4\theta'_m + \theta$ decreases and at $\sin^2 2\theta = 0.50$, where $2\theta''_m - 4\theta'_m + \theta \cong 0$, it does not exist.

The maximum of $\sin^2(2\theta''_m - 4\theta'_m + \theta)$ in the region $\rho_{man}^{res} \sim \kappa \bar{\rho}_{man} \cong 7.57 \text{ g/cm}^3$ for $\sin^2 2\theta \sim (0.05 - 0.10)$ is remarkably wide (Fig. 14). However, the oscillating factor $0.5(1 - \cos \Delta E'' X'')$ in eqs. (25) and (26) goes through zero in the same region, thus reducing considerably the effect of the large width of this maximum on the probabilities P_{e2} , $P(\nu_\mu \rightarrow \nu_e)$ and $P(\bar{\nu}_\mu \rightarrow \bar{\nu}_s)$ (Figs. 5c and 10b).

The position of the minimum of $\sin^2(2\theta''_m - 4\theta'_m + \theta)$ at $\rho_{man}^{res} \cong \bar{\rho}_{man}$, where $4\theta'_m \cong \pi$, is very stable with respect to the change of $\sin^2 2\theta$ up to $\sin^2 2\theta \cong 0.5$.

The maximum and the minimum of $\sin^2(2\theta''_m - 4\theta'_m + \theta)$, which at small mixing angles are located at $\rho_{man}^{res} \cong \bar{\rho}_{man}/(1 + 2\sqrt{2}\theta)$ and at $\rho_{man}^{res} \cong \bar{\rho}_{man}$, respectively, “survive” at large mixing angles, but change their positions moving to somewhat smaller values of ρ_{man}^{res} . These are the only extrema $\sin^2(2\theta''_m - 4\theta'_m + \theta)$ has at large mixing angles. At $\sin^2 2\theta \gtrsim 0.4$ the function $[\sin^2(2\theta''_m - 4\theta'_m + \theta) - \sin^2 \theta]$ “shrinks” essentially to the region $\rho_{man}^{res} \lesssim \bar{\rho}_{man}$, where it can take relatively large values (Fig. 14). This is also the region where the two extrema of $[\sin^2(2\theta''_m - 4\theta'_m + \theta) - \sin^2 \theta]$ are located: the maximum occurs at $\rho_r \lesssim 2.0 \text{ g/cm}^3$, while the minimum takes place at $\rho_r \cong (3.5 - 4.5) \text{ g/cm}^3$, depending on the neutrino trajectory. Outside the indicated region $[\sin^2(2\theta''_m - 4\theta'_m + \theta) - \sin^2 \theta]$ is close to 0.

At $\rho_c^{res} \gg \bar{\rho}_c$ and at $\rho_{man}^{res} \ll \bar{\rho}_{man}$ we have for small mixing angles $\sin^2(2\theta''_m - 4\theta'_m + \theta) \cong$

¹⁵If $\nu_e - \nu_s$ mixing takes place we have $r \cong 2.18$, $\kappa \cong 1.58$ and this minimum occurs at $\rho_{man}^{res} \cong 7.1 \text{ g/cm}^3$. In the case of $\bar{\nu}_\mu \rightarrow \bar{\nu}_s$ transitions, $r \cong 2.67$ and $\kappa \cong 1.76$, so the minimum is at $\rho_{man}^{res} \cong 8.0 \text{ g/cm}^3$.

$\sin^2(\theta(1 - \epsilon))$, where $\epsilon > 0$ is a small quantity, $\epsilon \ll 1$, so that $\sin^2(\theta(1 - \epsilon)) \cong \sin^2 \theta$. Nevertheless, one always has $\sin^2(2\theta''_m - 4\theta'_m + \theta) < \sin^2 \theta$ in the indicated regions, although the difference between the two sines is very small. Obviously, the probabilities P_{e2} and $P(\nu_\mu \rightarrow \nu_e)$ are rather strongly suppressed at small mixing angles when $\rho_c^{res} \gg \bar{\rho}_c$ or $\rho_{man}^{res} \ll \bar{\rho}_{man}$. The same conclusion is valid at large mixing angles, $\sin^2 2\theta \gtrsim 0.2$, for the probability P_{e2} ; it is valid also in the region $\rho_{man}^{res} \ll \bar{\rho}_{man}$ for the probability $P(\nu_\mu \rightarrow \nu_e)$. However, as can be shown (and Fig. 14 suggests), $P(\nu_\mu \rightarrow \nu_e)$ can take relatively large values at $\sin^2 2\theta \gtrsim 0.2$ for $\rho_c^{res} \gg \bar{\rho}_c$. The behavior of the probability $P(\nu_\mu \rightarrow \nu_e)$ as a function of ρ_r for several different values of $\sin^2 2\theta$ and for $h = 0^\circ; 13^\circ; 23^\circ$ is illustrated in Figs. 15a - 15c.

Let us note finally that the probabilities P_{e2} in the case of $\nu_e - \nu_s$ mixing, $P_{e2,s}$, $P(\nu_e \rightarrow \nu_s)$ and $P(\bar{\nu}_\mu \rightarrow \bar{\nu}_s)$ are given by somewhat more complicated expressions than (25) and (26) in the regions of their strong (resonance-like) enhancement at small mixing angles [1]:

$$\begin{aligned}
P_{e2,s}^{res} &\cong \frac{1}{2} [1 - \cos \Delta E'' X''] \sin^2(2\theta''_m - \theta) \\
&+ \frac{1}{4} [1 - \cos \Delta E'' X''] [1 - \cos \Delta E' X'] [\sin^2(2\theta''_m - 4\theta'_m + \theta) - \sin^2(2\theta''_m - \theta)] \\
&+ \frac{1}{4} [\cos(\Delta E' X' - \Delta E'' X'') - \cos(\Delta E' X' + \Delta E'' X'')] \sin(4\theta'_m - 2\theta) \sin(2\theta''_m - 2\theta'_m). \quad (29)
\end{aligned}$$

The expressions for $P(\nu_e \rightarrow \nu_s)$ and $P(\bar{\nu}_\mu \rightarrow \bar{\nu}_s)$ can be obtained by setting formally $\theta = 0$, but keeping $\theta'_m \neq 0$ and $\theta''_m \neq 0$ in eq. (29) and using the definitions of $\rho_{man,c}^{res}$ given at the end of Section 2. The first and the last terms in eq. (29) and the corresponding terms in the expressions for $P(\nu_e \rightarrow \nu_s)$ and $P(\bar{\nu}_\mu \rightarrow \bar{\nu}_s)$ give the dominant contributions. Obviously, they determine the properties of $P_{e2,s}$, $P(\nu_e \rightarrow \nu_s)$ and $P(\bar{\nu}_\mu \rightarrow \bar{\nu}_s)$ in the region of interest.

4. Conclusions

The neutrino oscillation length resonance should be present in the $\nu_2 \rightarrow \nu_e$ transitions taking place when the solar neutrinos cross the Earth core on the way to the detector, if the solar neutrino problem is due to small mixing angle MSW $\nu_e \rightarrow \nu_\mu$ transitions in the Sun. The same resonance should be operative also in the $\nu_\mu \rightarrow \nu_e$ ($\nu_e \rightarrow \nu_{\mu(\tau)}$) small mixing angle transitions of the atmospheric neutrinos crossing the Earth core if the atmospheric ν_μ and $\bar{\nu}_\mu$ indeed take part in large mixing vacuum $\nu_\mu \leftrightarrow \nu_\tau$, $\bar{\nu}_\mu \leftrightarrow \bar{\nu}_\tau$ oscillations with $\Delta m^2 \sim (5 \times 10^{-4} - 5 \times 10^{-3}) \text{ eV}^2$, as is strongly suggested by the Super-Kamiokande atmospheric neutrino data, and if all three flavour neutrinos are mixed in vacuum. The existence of three-flavour-neutrino mixing in vacuum is a very natural possibility in view of the present experimental evidences for oscillations/transitions of the flavour neutrinos. In both cases the oscillation length resonance produces a strong enhancement of the corresponding transitions probabilities, making the transitions observable even at rather small mixing angles [1]. Actually, the resonance may have already manifested itself in the excess of e-like events at $-1 \leq \cos \theta_z \leq -0.6$ observed in the Super-Kamiokande atmospheric neutrino data [1,11,13]. And it can be responsible for at least part of the strong zenith angle dependence present in the Super-Kamiokande multi-GeV and sub-GeV μ -like data [1,11,13].

In view of the important role the oscillation length resonance can play in the interpretation of the results of the experiments with solar and atmospheric neutrinos as well as in obtaining information about possible small mixing angle oscillations/transitions of the (atmospheric) ν_μ ($\bar{\nu}_\mu$) and ν_e ($\bar{\nu}_e$), we have performed in the present article a rather detailed

study of the conditions under which the resonance takes place in the $\nu_2 \rightarrow \nu_e$, and in the $\nu_\mu \rightarrow \nu_e$ ($\nu_e \rightarrow \nu_{\mu(\tau)}$) and $\bar{\nu}_\mu \rightarrow \bar{\nu}_s$ transitions of neutrinos in the Earth. We have examined also some of the properties of the resonance. This was done under the simplest assumption of existence of two-neutrino mixing (with nonzero-mass neutrinos) in vacuum: $\nu_e - \nu_{\mu(\tau)}$ or $\nu_e - \nu_s$, or else $\nu_\mu - \nu_s$. However, in many cases of practical interest the probabilities of the relevant three- (or four-) neutrino mixing transitions in the Earth reduce effectively to two-neutrino transition probabilities for which our results are valid. Thus, our findings have a wider application than it may seem.

Using our Figs. 1a - 1f, 2a - 3b, 6a - 8c and 9, in particular, one can determine practically all relevant values of the neutrino oscillation parameters, E , Δm^2 and $\sin^2 2\theta$, at which the oscillation length resonance occurs for a given neutrino trajectory through the Earth core in the cases of $\nu_2 \rightarrow \nu_e$, $\nu_\mu \rightarrow \nu_e$ ($\nu_e \rightarrow \nu_{\mu(\tau)}$) and $\bar{\nu}_\mu \rightarrow \bar{\nu}_s$ transitions. The sets of such values for the transitions of solar and atmospheric neutrinos can be easily identified. We have shown, for instance, that the oscillation length resonance conditions (9) with $k = 0$ and $k' = 0$ can both be satisfied at small $\sin^2 2\theta$ for the $\nu_2 \rightarrow \nu_e$ transitions in the case of $\nu_e - \nu_s$ mixing only for $h \gtrsim 15^\circ$ (Figs. 6a - 6c). In contrast, conditions (9) can be simultaneously fulfilled at $\sin^2 2\theta \lesssim 0.10$ for the $\bar{\nu}_\mu \rightarrow \bar{\nu}_s$ transitions at $h \lesssim 15^\circ$ (Figs. 8a - 8c). However, the points where conditions (9) hold lie outside the regions determined by the inequalities (10a) - (10b) and by (14). Nevertheless, as like $P_{e2,s}$ [1], the probability of the $\bar{\nu}_\mu \rightarrow \bar{\nu}_s$ transitions is strongly enhanced at small mixing angles in the region of the MSW resonance in the Earth core (Figs. 10a - 10b). This resonance-like enhancement is due to the interplay of certain interference terms present in the expression for $P(\bar{\nu}_\mu \rightarrow \bar{\nu}_s)$ - notably by the analog of the last term in eq. (13), and the term describing the MSW effect in the Earth core. For, e.g., $h = 0^\circ$, $\sin^2 2\theta \cong 0.01$ and $\Delta m^2 = 5 \times 10^{-4}$; 10^{-3} ; 4×10^{-3} eV², the dominating absolute maximum in $P(\bar{\nu}_\mu \rightarrow \bar{\nu}_s)$ takes place at $E \cong 1.2$; 2.3; 9.6 GeV, which fall in the intervals of energies of $\bar{\nu}_\mu$ contributing either to the sub-GeV or to the multi-GeV μ -like samples of Super-Kamiokande atmospheric neutrino events. The strong (resonance-like) enhancement of $P(\bar{\nu}_\mu \rightarrow \bar{\nu}_s)$ (or of $P(\nu_\mu \rightarrow \nu_s)$ if $\Delta m^2 < 0$) found in this study can make possible the detection of the $\bar{\nu}_\mu \rightarrow \bar{\nu}_s$ (or $\nu_\mu \rightarrow \nu_s$) transitions of, e.g., the atmospheric $\bar{\nu}_\mu$ (or ν_μ) at small mixing angles.

We have also investigated the behavior of the probabilities P_{e2} and $P(\nu_\mu \rightarrow \nu_e)$ ($P(\nu_e \rightarrow \nu_{\mu(\tau)})$) in the region of the neutrino oscillation length resonance. Simple analytic expressions which describe P_{e2} and $P(\nu_\mu \rightarrow \nu_e)$ ($P(\nu_e \rightarrow \nu_{\mu(\tau)})$) in the region of the resonance and determine, in particular, the width of the resonance, and the probabilities $P_{e2,s}$, $P(\nu_e \rightarrow \nu_s)$ and $P(\bar{\nu}_\mu \rightarrow \bar{\nu}_s)$ in the region of their resonance-like enhancement at small mixing angles, are identified. We have shown that at small mixing angles i) the resonance is relatively wide not only in the variable $E/\Delta m^2$, but also in the Nadir angle variable h , and that ii) the values of P_{e2} and $P(\nu_\mu \rightarrow \nu_e)$ ($P(\nu_e \rightarrow \nu_{\mu(\tau)})$) at the maxima associated with the resonance decrease monotonically with the increase of h . Thus, at small mixing angles the enhancement of these probabilities due to the neutrino oscillation length resonance is maximal for the Earth center crossing trajectories, i.e., for $h = 0^\circ$. These conclusions are valid for the enhancement of the probabilities $P_{e2,s}$, $P(\nu_e \rightarrow \nu_s)$ and $P(\bar{\nu}_\mu \rightarrow \bar{\nu}_s)$ as well.

As the results obtained in refs. [1,2] and the present study indicate, it is not excluded that some of the current or future high statistics solar and/or atmospheric neutrino experiments will be able to observe directly the neutrino oscillation length resonance. Experiments located

at lower geographical latitudes than the existing ones or those under construction [19] would be better suited for this purpose. An atmospheric neutrino detector capable of reconstructing with relatively good precision, e.g., the energy and the direction of the momentum of the incident neutrino in each neutrino-induced event, would allow to study in detail the effects of the oscillation length resonance in the transitions/oscillations of the atmospheric neutrinos crossing the Earth.

Acknowledgements.

Part of the work of S.P.T. for the present study was done at the Aspen Center for Physics during the Workshop on Neutrino Physics and Astrophysics (June 15 - July 12, 1998). S.T.P. would like to thank the organizers of the Workshop, and especially L. Wolfenstein, for the kind hospitality extended to him, and L. Wolfenstein, B. Kayser, H. Goldberg, T. Weiler, G. Fuller, A. Balantekin, J. Beacom and F. Vissani for the interest in the present study and useful discussions. This work was supported in part by the Italian MURST under the program “Fisica Teorica delle Interazioni Fondamentali” and by Grant PH-510 from the Bulgarian Science Foundation.

REFERENCES

- [1] S.T. Petcov, Phys. Lett. B**434**, 321 (1998).
- [2] M. Maris and S.T. Petcov, Phys. Rev. D **56**, 7444 (1997).
- [3] M. Maris and S.T. Petcov, Report SISSA 154/97/EP, March 1998 (hep-ph/9803244, to be published in Phys. Rev. D).
- [4] Q.Y. Liu, M. Maris and S.T. Petcov, Phys. Rev. D **56**, 5991 (1997).
- [5] A. Baltz and J. Weneser, Phys. Rev. D **50**, 5971 (1994).
- [6] Y. Suzuki (Super-Kamiokande Collaboration), Talk given at the “Neutrino ’98” International Conference on Neutrino Physics and Astrophysics, June 3 - 9, 1998, Takayama, Japan (to be published in the Proceedings of the Conference).
- [7] M. Nakahata (Super-Kamiokande Collaboration), Talk given at the International Symposium “New Era in Neutrino Physics”, June 11 - 12, 1998, Tokyo, Japan (to be published in the Proceedings of the Symposium).
- [8] T. Kajita (Super-Kamiokande Collaboration), Talk given at the “Neutrino ’98” International Conference on Neutrino Physics and Astrophysics, June 3 - 9, 1998, Takayama, Japan (to be published in the Proceedings of the Conference).
- [9] Y. Fukuda et al. (Super-Kamiokande Collaboration), Boston Univ. Report BU-98-17, hep-ex/9807003, 3 July, 1998 (submitted for publication to Phys. Rev. Lett.).
- [10] M. Appolonio et al. (CHOOZ Collaboration), Phys. Lett. B**420**, 397 (1998).
- [11] S.T. Petcov, “Earth Matter Effects in the Atmospheric and Solar Neutrino Transitions”, Talk given at the Workshop “Neutrino Physics and Astrophysics: from Solar to Ultra-High Energy”, Aspen Center for Physics, June 29 - July 12, 1998, Aspen, U.S.A.
- [12] S.T. Petcov, Phys. Lett. B**214**, 259 (1988).
- [13] S.T. Petcov, L. Wolfenstein and O. Yasuda, work in progress.
- [14] M. Honda et al., Phys. Rev. D **52**, 4985 (1995).
- [15] V. Agraval et al., D **53**, 1314 (1996).
- [16] S.P. Mikheyev and A.Yu. Smirnov, Proceedings of the Moriond Workshop on Massive Neutrinos in Astrophysics and in Particle Physics, 1986, Tignes, Savoie, France, (eds. O. Fackler and J. Tran Thanh Van Editions Frontières, Gif-sur-Yvette, France, 1986), p. 355; E.D. Carlson, Phys. Rev. D**34**, 1454 (1986); A. Dar et al., Phys. Rev. D**35**, 3607 (1987); G. Auriemma et al., D**37**, 665 (1988).
- [17] P.I. Krastev and S.T. Petcov, Phys. Lett. B**205**, 84 (1988).
- [18] M. Cribier et al., Phys. Lett. B**182**, 89 (1986); A.J. Baltz and J. Weneser, Phys. Rev. D**35**, 528 (1987); J.M. LoSecco, Phys. Rev. D**47**, 2032 (1993).
- [19] J.M. Gelb, W. Kwong and S.P. Rosen, Phys. Rev. Lett. **78**, 2296 (1997).
- [20] F.D. Stacey, *Physics of the Earth, 2nd edition*, John Wiley and Sons, London, New York, 1977.
- [21] A.D. Dziewonski and D.L. Anderson, Physics of the Earth and Planetary Interiors **25**, 297 (1981).
- [22] R. Jeanloz, Annu. Rev. Earth Planet. Sci. **18**, 356 (1990); C.J. Allègre et al., Earth Planet. Sci. Lett. **134**, 515 (1995); W.F. McDonough and S.-s. Sun, Chemical Geology **120**, 223 (1995).
- [23] M. Maris and S.T. Petcov, in preparation; M. Maris, Q.Y. Liu and S.T. Petcov, preliminary study performed in December of 1996 (unpublished).

Figure Captions

Figures 1a - 1f. Lines in the $\sin^2 2\theta - \rho_r$ (a - c) and $\sin^2 2\theta - \Delta m^2/E$ (d - f) planes on which conditions $\Delta E'X' = \pi(2k+1)$, $k = 0, 1, 2, \dots$ (dotted lines), and $\Delta E''X'' = \pi(2k'+1)$, $k' = 0, 1, 2, \dots$ (black solid lines), are fulfilled for $h = 0^\circ$ (center crossing, (a),(d)), $h = 13^\circ$ (winter solstice for the Super-Kamiokande detector, (b),(e)), and $h = 23^\circ$ ((c),(f)). The parameters ρ_r and $\Delta m^2/E$ (the vertical axes in figures (a) - (c) and (d) - (f), respectively) are in units of g/cm^3 and $10^{-7} \text{ eV}^2/\text{MeV}$. The results shown correspond to $\nu_e \rightarrow \nu_{\mu(\tau)}$ and $\nu_2 \rightarrow \nu_e$ transitions in the case of $\nu_e - \nu_{\mu(\tau)}$ mixing.

Figures 2a - 2b. Regions of values of $\sin^2 2\theta$ and ρ_r (a) or $\Delta m^2/E$ (b) of validity of conditions (10a) (A + B), (10b) (A + C), and of both (10a) and (10b) (A) for the $\nu_2 \rightarrow \nu_e$ transitions in the case of $\nu_e - \nu_{\mu(\tau)}$ mixing. Conditions (10b) and (12) hold simultaneously in the region C.

Figures 3a - 3b. Regions of validity of condition (14) in the $\sin^2 2\theta - \rho_r$ (a) and $\sin^2 2\theta - \Delta m^2/E$ (b) planes (A) for the $\nu_e \rightarrow \nu_{\mu(\tau)}$ transitions.

Figures 4a - 4b. The probability P_{e2} as a function of the Nadir angle h ((a), upper frame), and of ρ_r and h (b), for $\sin^2 2\theta = 0.01$ in the case of $\nu_e \rightarrow \nu_{\mu(\tau)}$ transitions of solar neutrinos. The lower frame in figure (a) shows the dependence on h of the derivative of P_{e2} with respect to h in the Stacey 1977 model of the Earth.

Figures 5a - 5b. The probability $P(\nu_e \rightarrow \nu_{\mu(\tau)}) = P(\nu_\mu \rightarrow \nu_e)$ as a function of the Nadir angle h and $E/\Delta m^2$, for $\sin^2 2\theta = 0.005$ (a), 0.01 (b) and 0.05 (c).

Figures 6a - 6c. Lines of validity of the conditions $\Delta E'X' = \pi(2k+1)$, $k = 0, 1, 2, \dots$ (dotted lines), and $\Delta E''X'' = \pi(2k'+1)$, $k' = 0, 1, 2, \dots$ (black solid lines) in the $\sin^2 2\theta - \Delta m^2/E$ plane in the case of $\nu_e \rightarrow \nu_s$ and $\nu_2 \rightarrow \nu_e$ transitions ($\nu_e - \nu_s$ mixing). The three figures correspond to $h = 0^\circ$ (a), $h = 13^\circ$ (b), and $h = 23^\circ$ (c).

Figure 7. The same as in figure 2b for $\nu_2 \rightarrow \nu_e$ transitions induced by $\nu_e - \nu_s$ mixing in vacuum.

Figures 8a - 8c. Lines of validity of the conditions $\Delta E'X' = \pi(2k+1)$, $k = 0, 1, 2, \dots$ (dotted lines), and $\Delta E''X'' = \pi(2k'+1)$, $k' = 0, 1, 2, \dots$ (black solid lines) in the $\sin^2 2\theta - \Delta m^2/E$ plane for $\bar{\nu}_\mu \rightarrow \bar{\nu}_s$ transitions and $h = 0^\circ$ (a), $h = 13^\circ$ (b), and $h = 23^\circ$ (c).

Figure 9. The same as in figure 3b for the case of $\bar{\nu}_\mu \rightarrow \bar{\nu}_s$ transitions.

Figures 10a - 10b. The probability $P(\bar{\nu}_\mu \rightarrow \bar{\nu}_s)$ as a function of the Nadir angle h and $E/\Delta m^2$, for $\sin^2 2\theta = 0.01$ (a) and 0.05 (b).

Figure 11. The probability P_{e2} as a function of ρ_r in the case of $\nu_e - \nu_{\mu(\tau)}$ mixing with $\sin^2 2\theta = 0.4$.

Figure 12. The probability P_{e2} as a function of ρ_r for $\sin^2 2\theta = 0.5$ in the case of $\nu_e - \nu_s$ mixing.

Figure 13. The same as in figure 11 for $\sin^2 2\theta = 0.9$.

Figure 14. The dependence of the function $\sin^2(2\theta''_m - 4\theta'_m + \theta)$ on ρ_r for $\sin^2 2\theta = 0.005; 0.01; 0.05; 0.10; 0.50; 0.90$.

Figures 15a - 15c. The dependence of the probability $P(\nu_\mu \rightarrow \nu_e) = P(\nu_e \rightarrow \nu_{\mu(\tau)}) = P_{e\mu}$ on ρ_r for $h = 0^\circ$ (a); 13° (b); 23° (c) and $\sin^2 2\theta = 0.005; 0.01; 0.050; 0.10; 0.50; 0.70$.

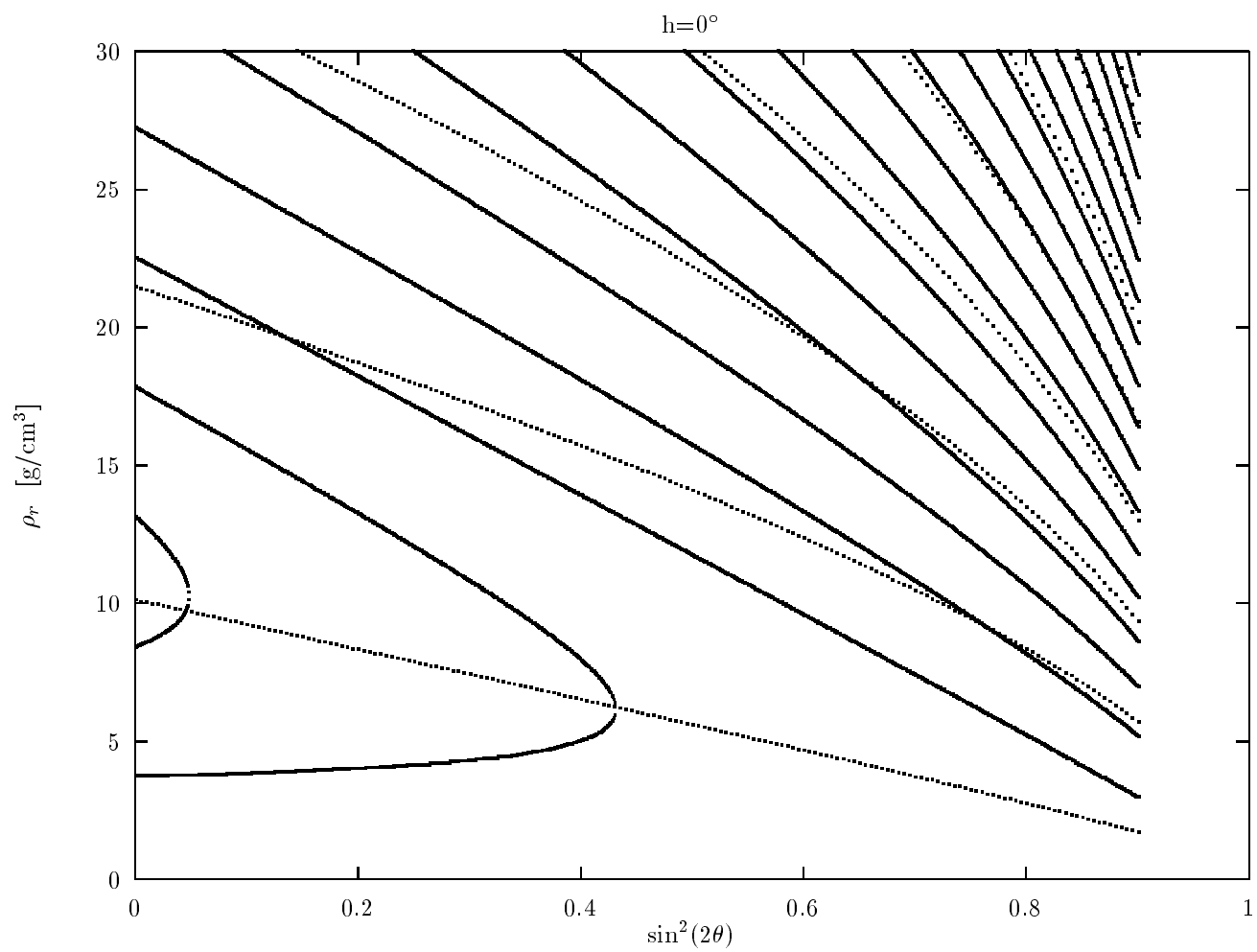


Figure 1a

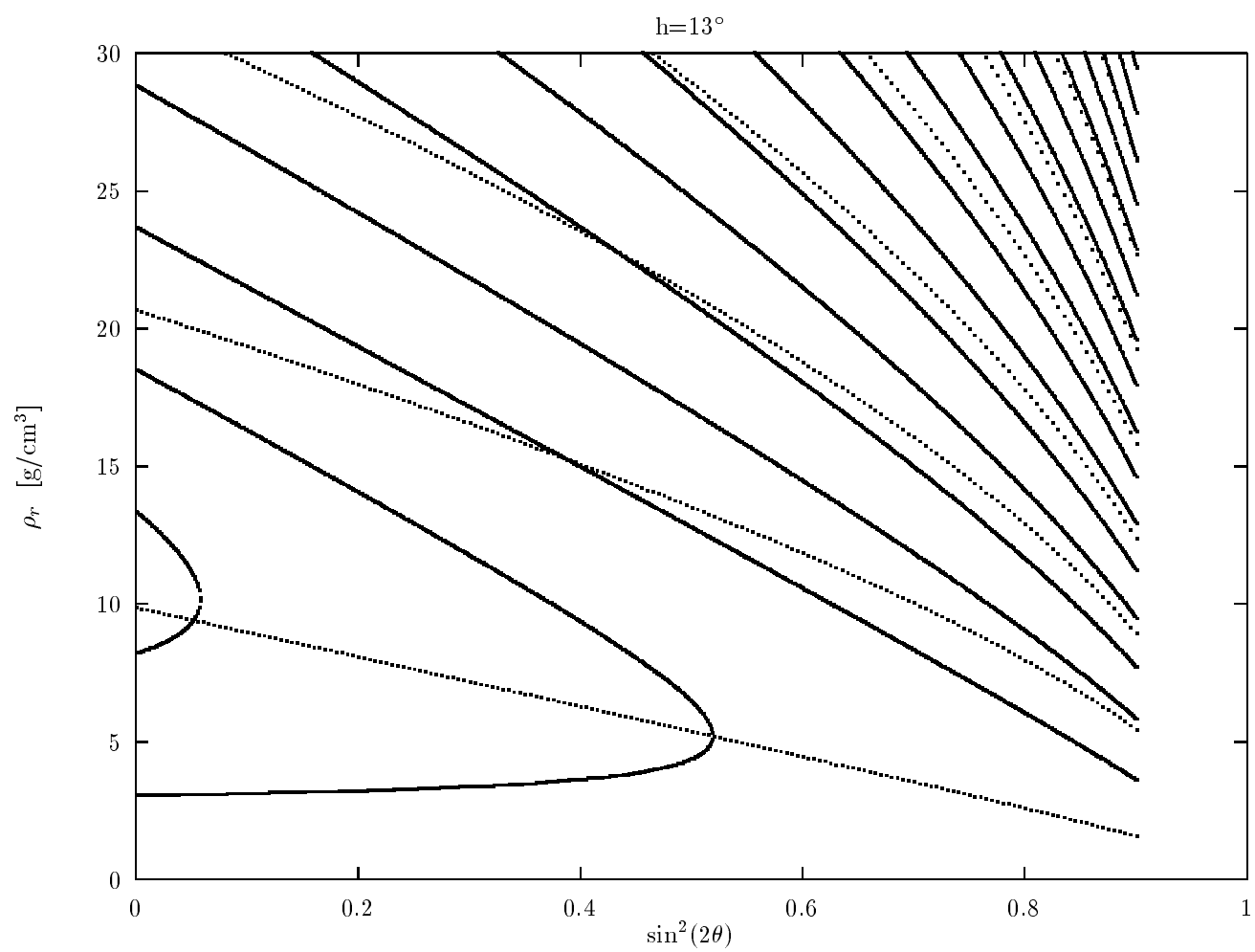


Figure 1b

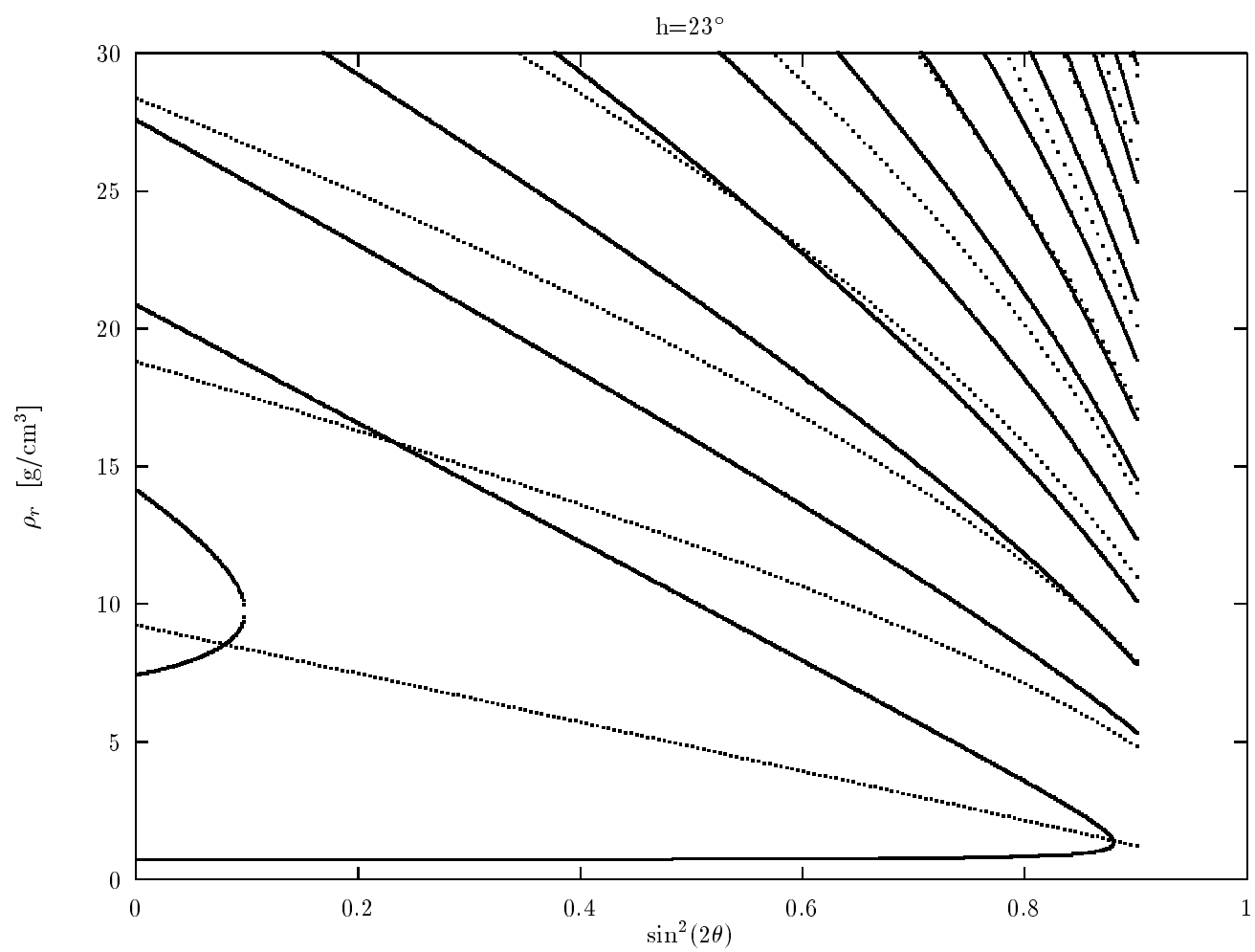


Figure 1c

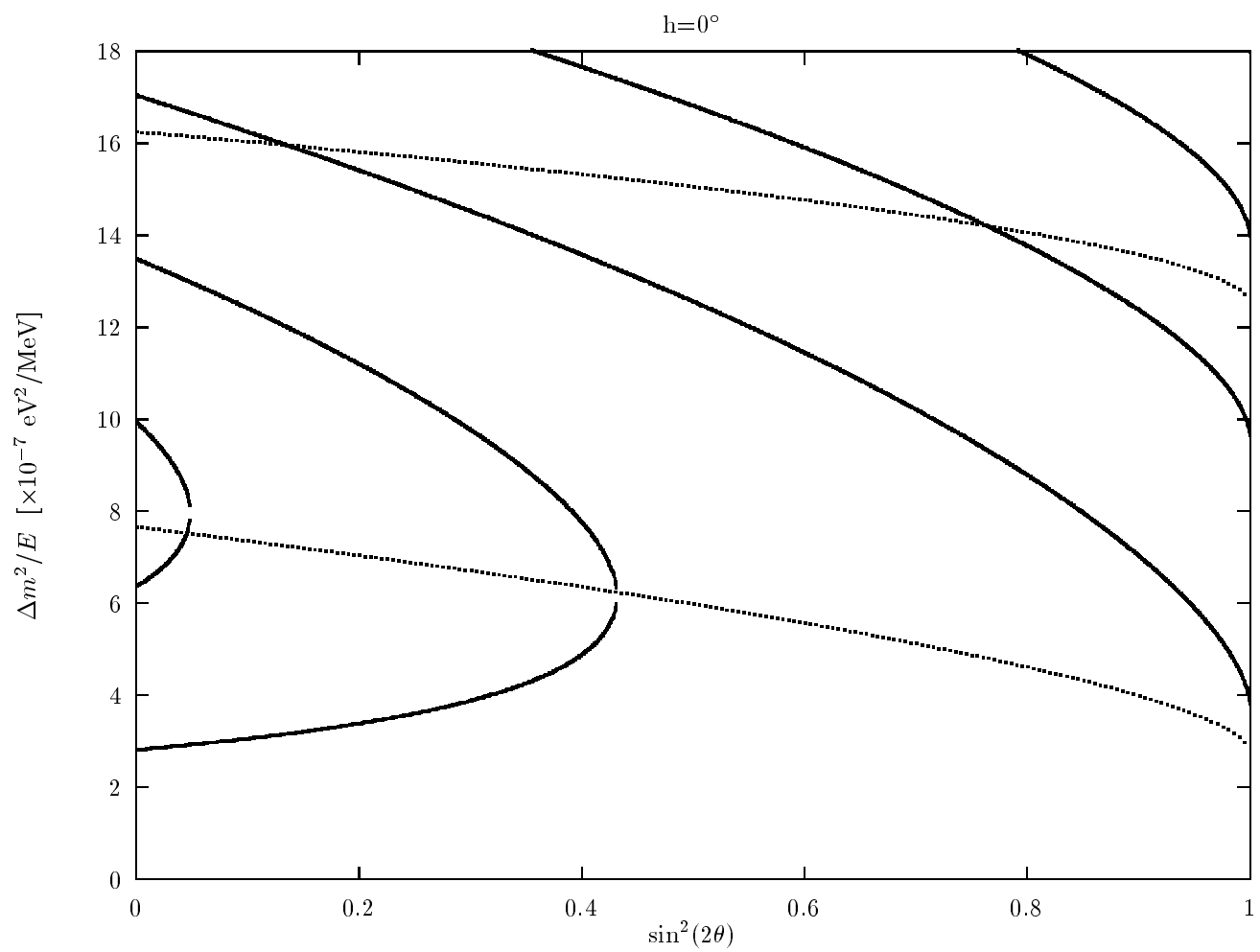


Figure 1d

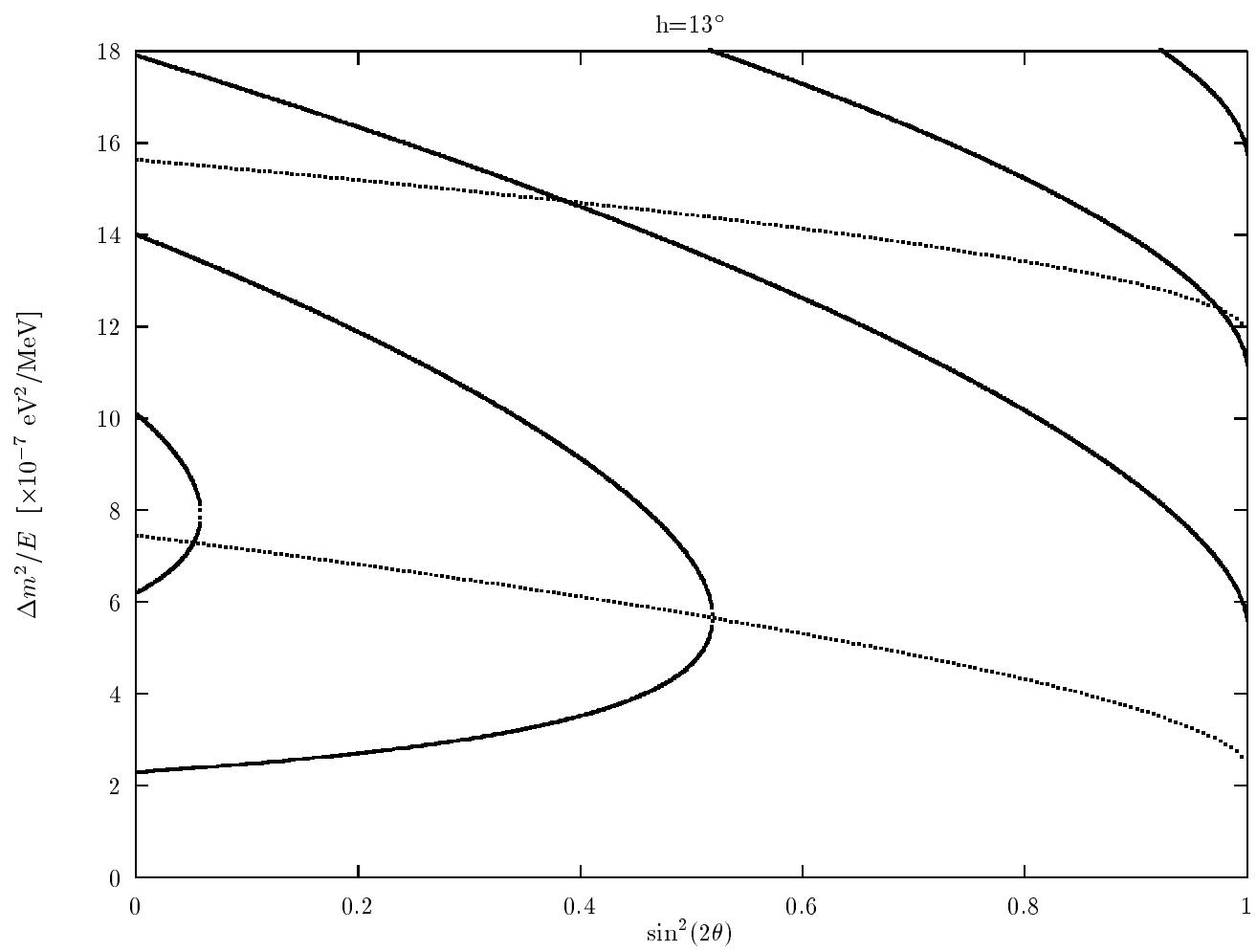


Figure 1e

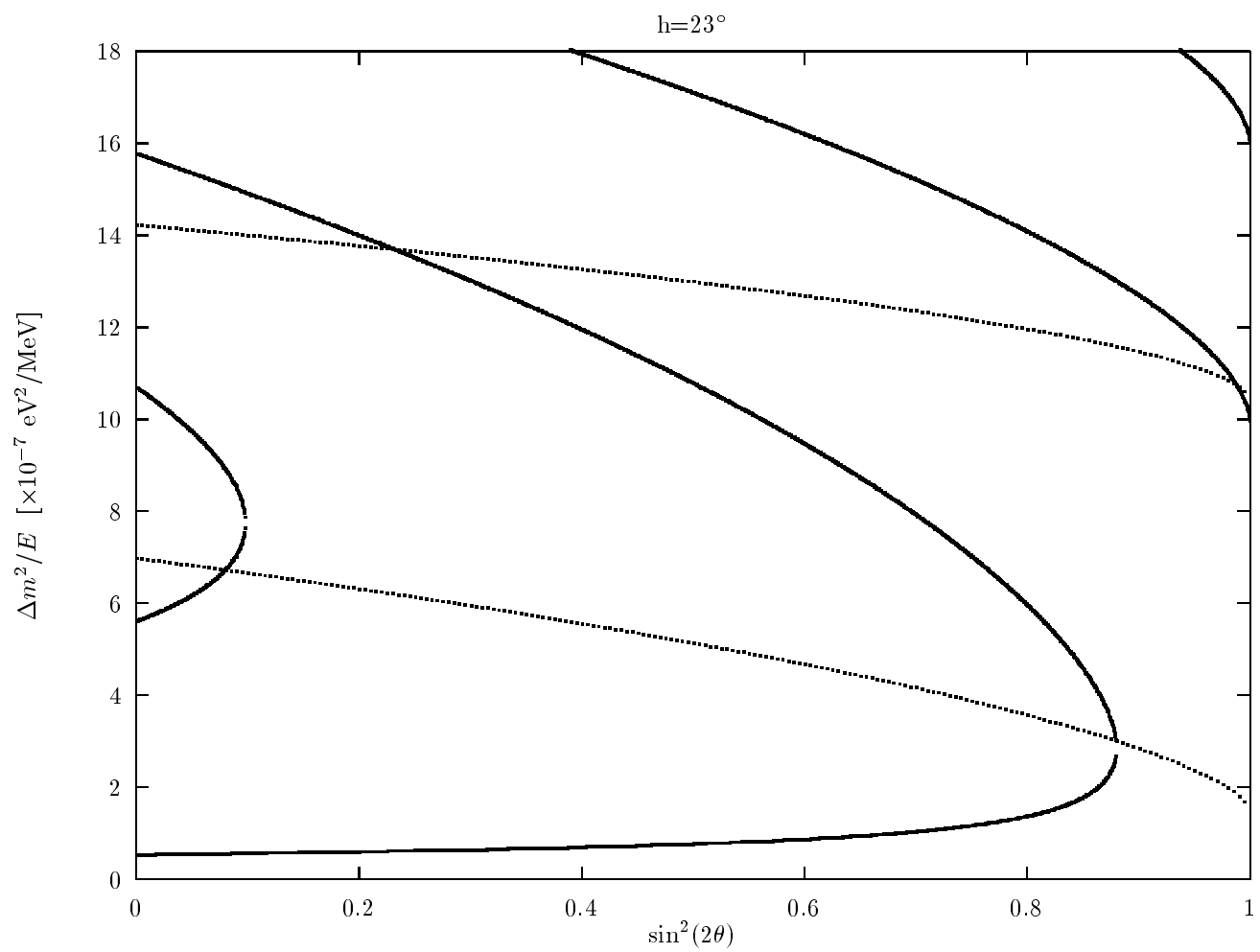
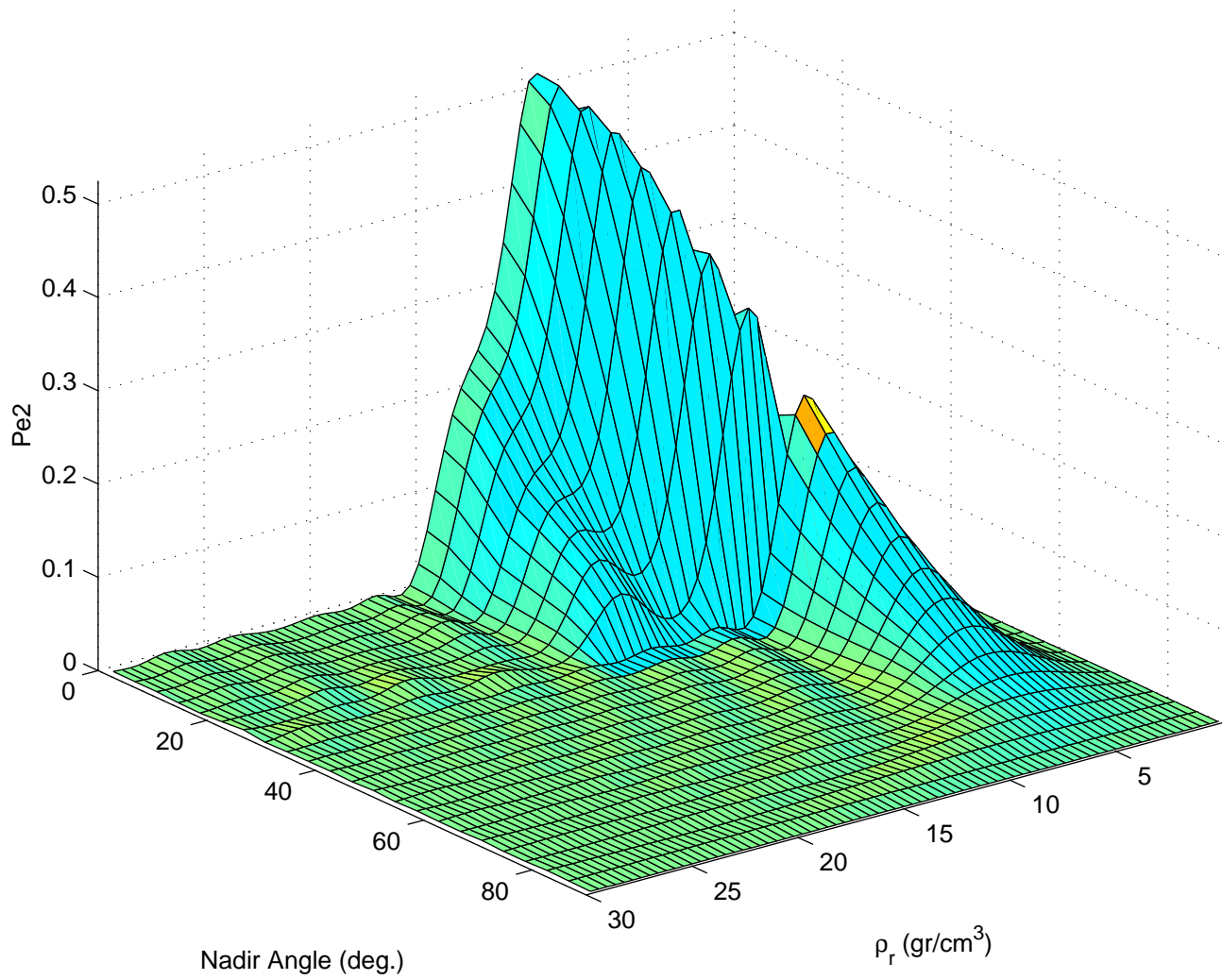
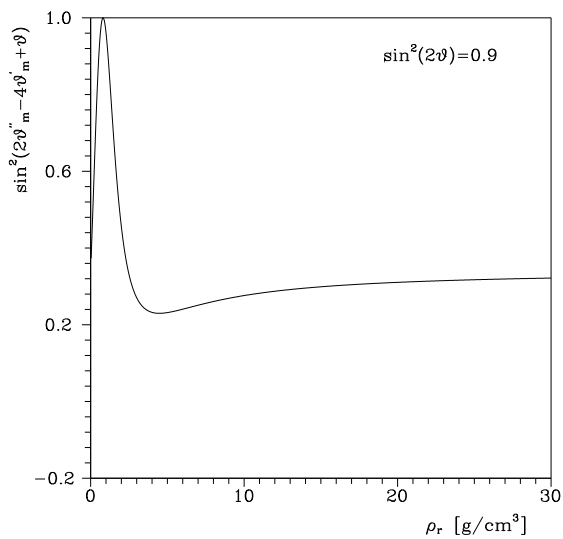
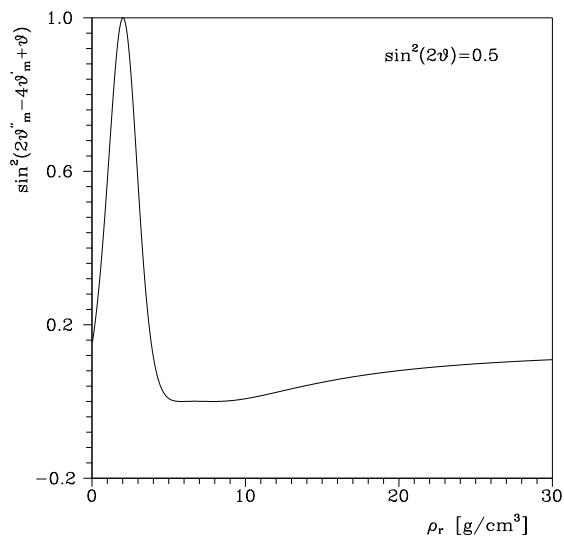
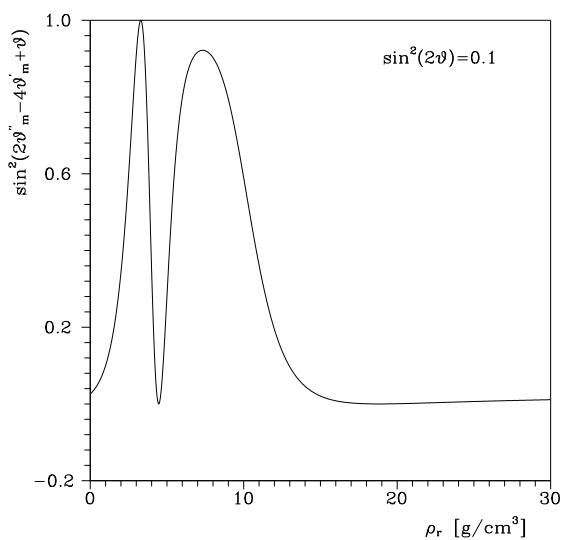
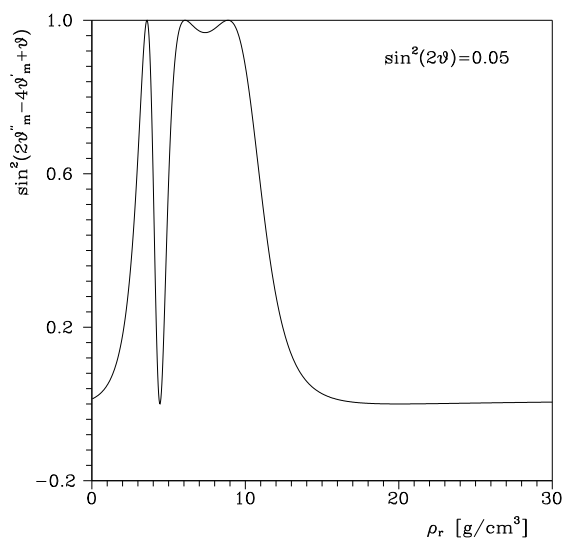
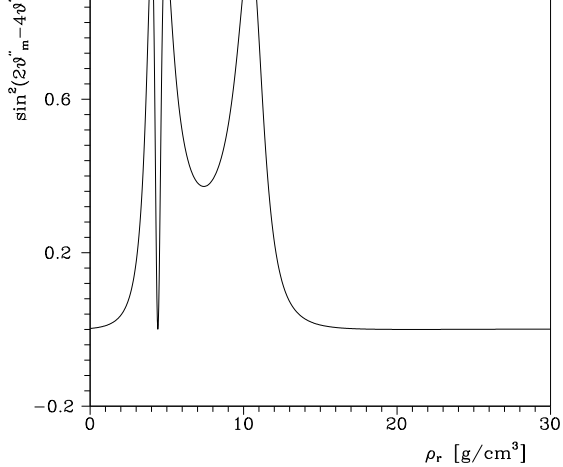
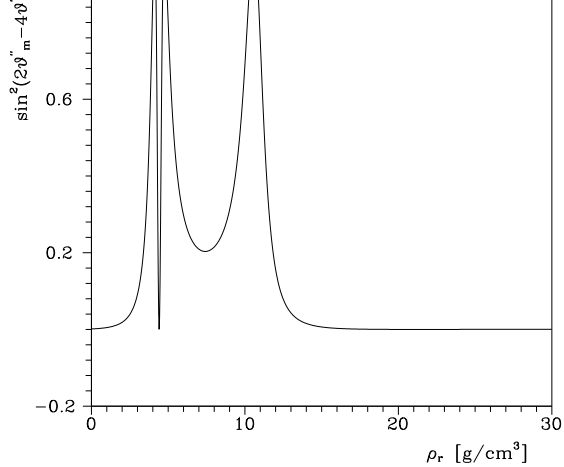


Figure 1f

$\sin^2 2\theta_v = 0.01$ Active $Y_e = 0.467$





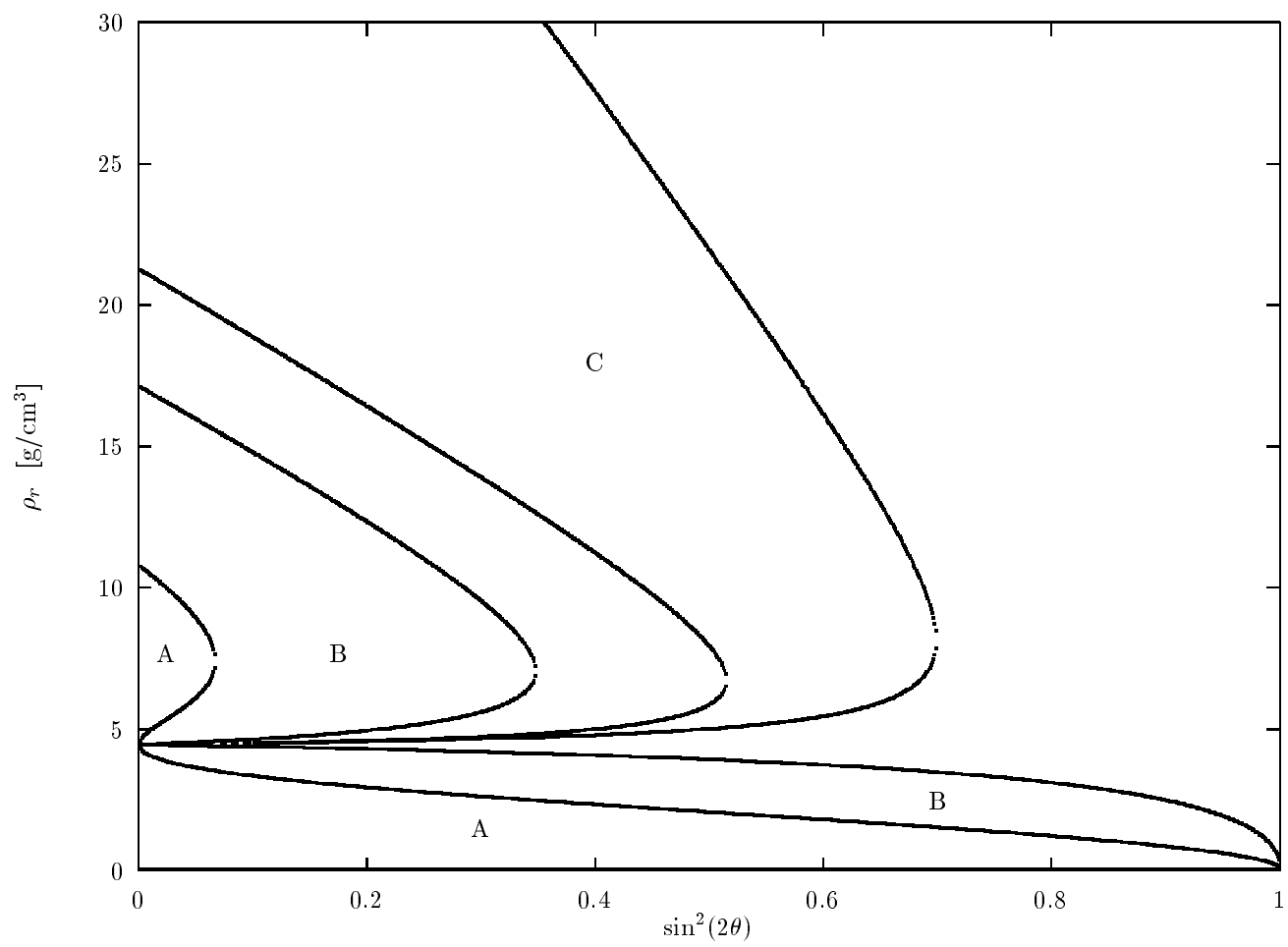


Figure 2a

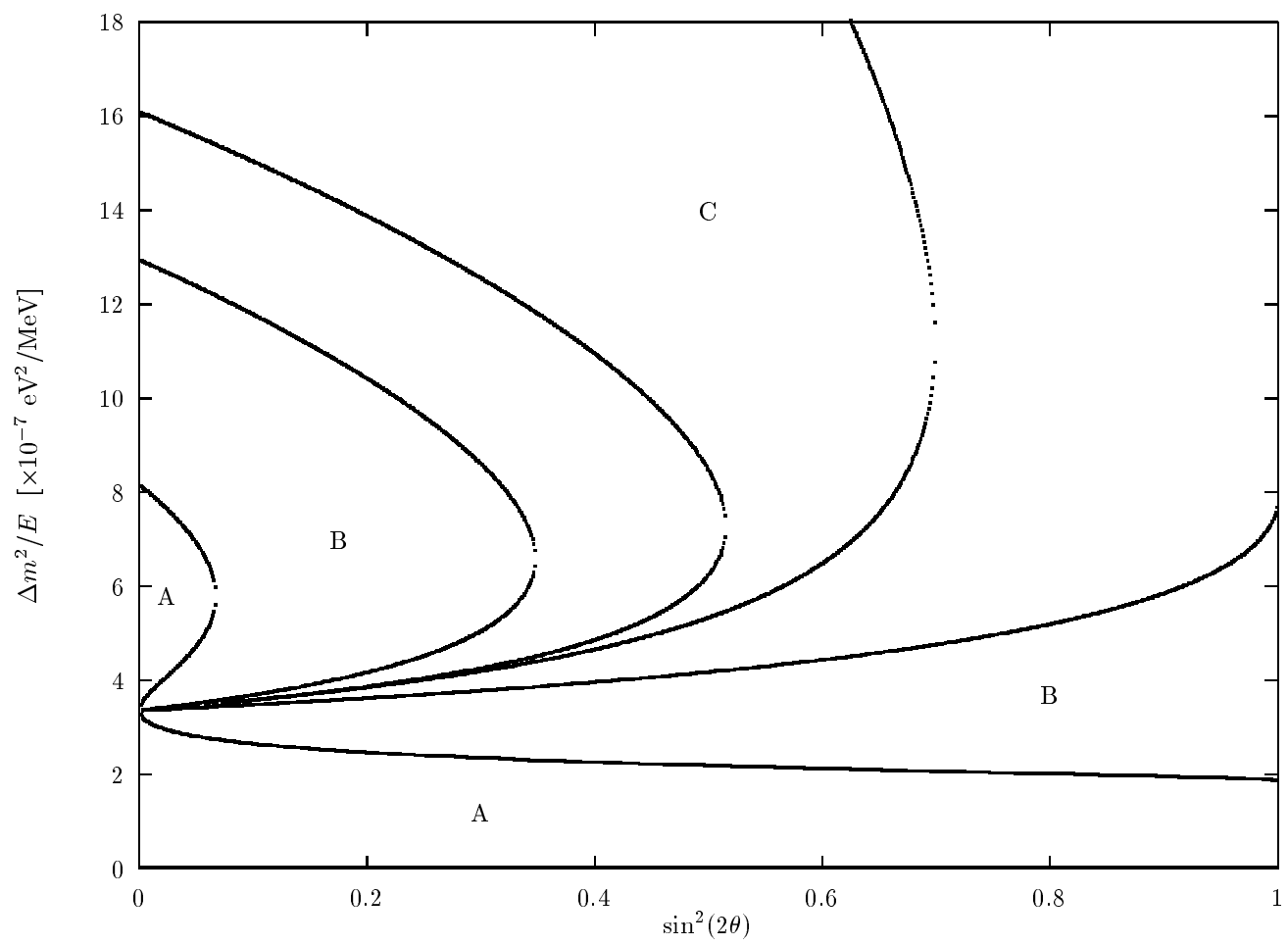


Figure 2b

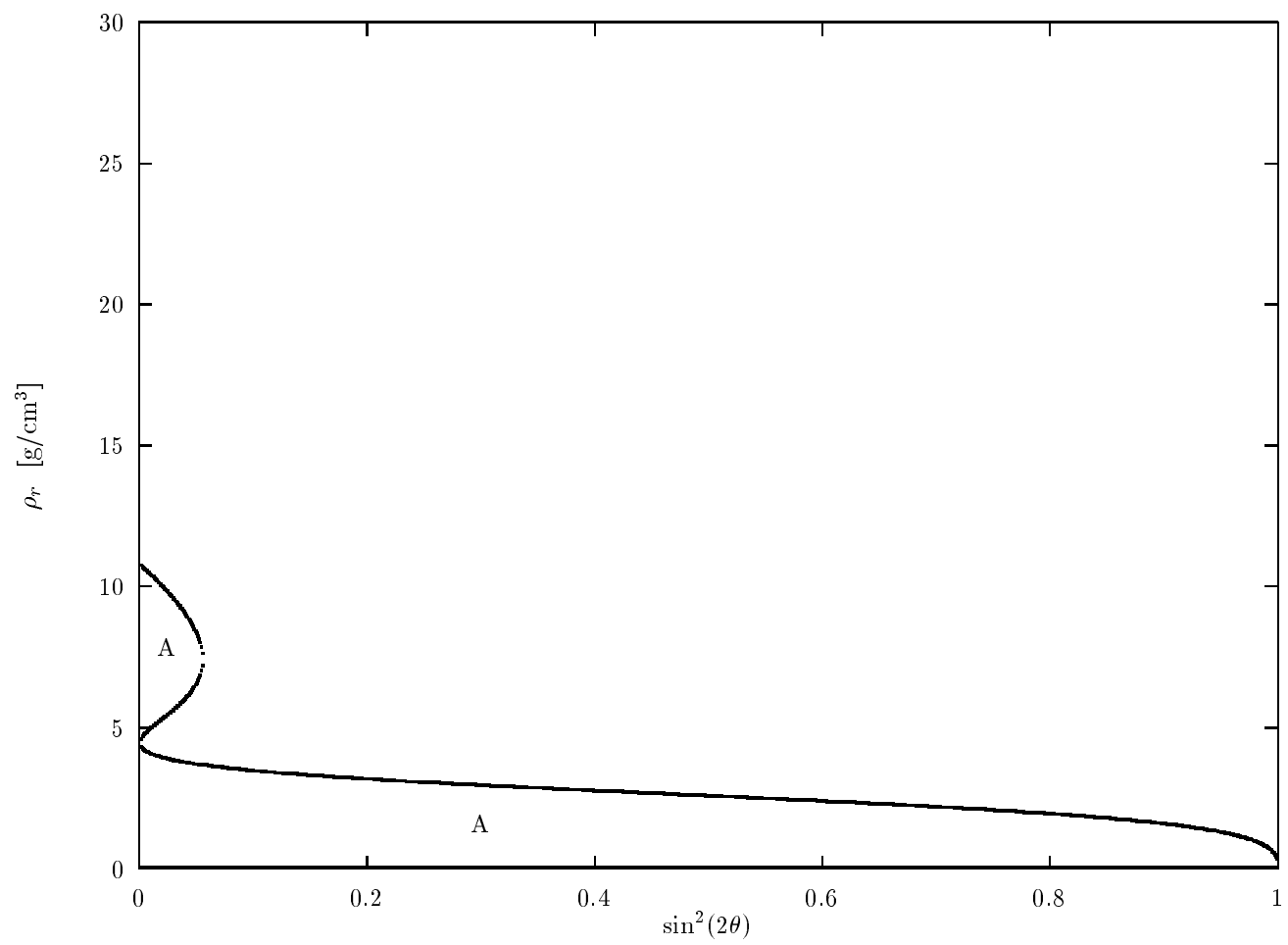


Figure 3a

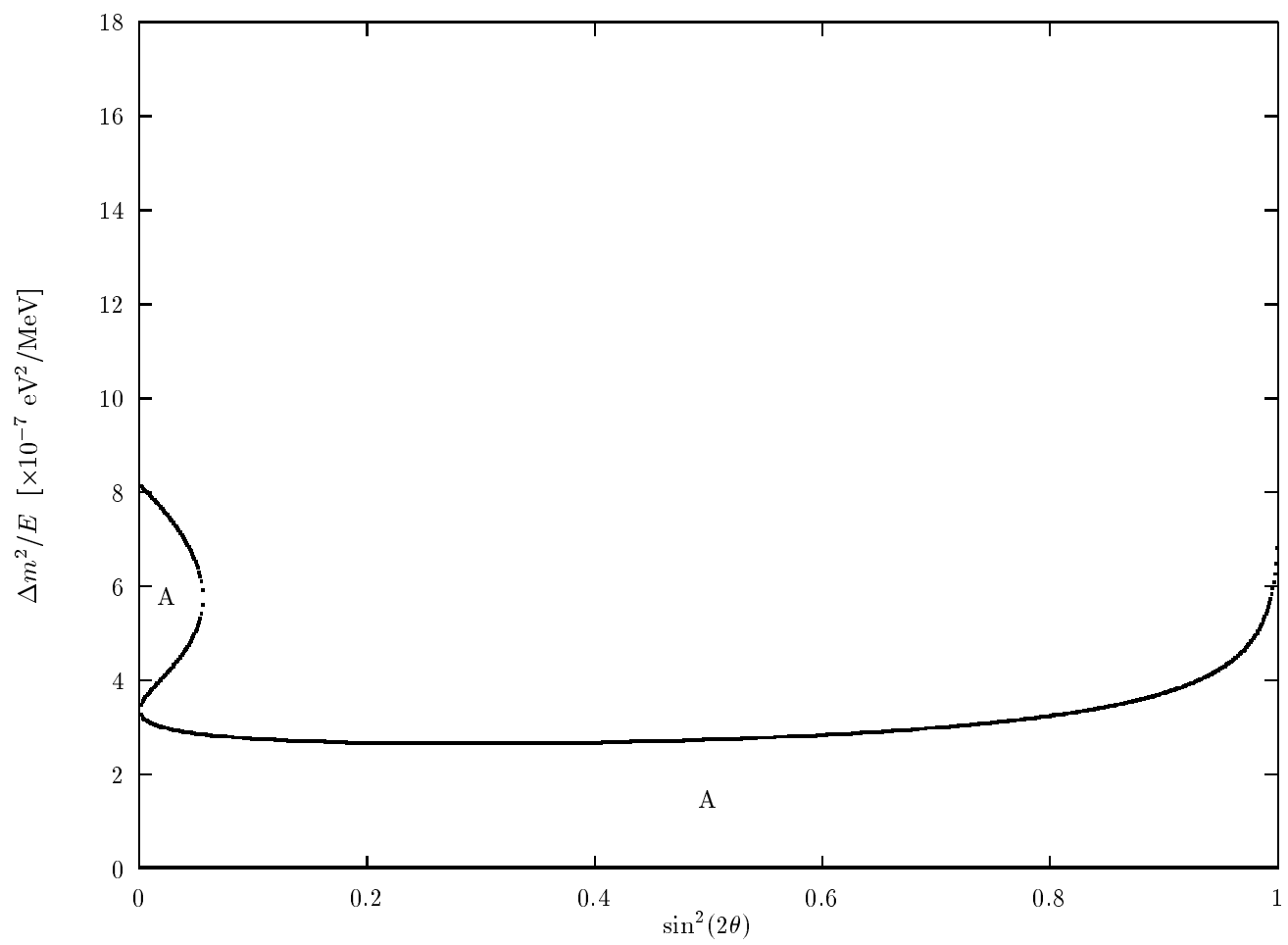
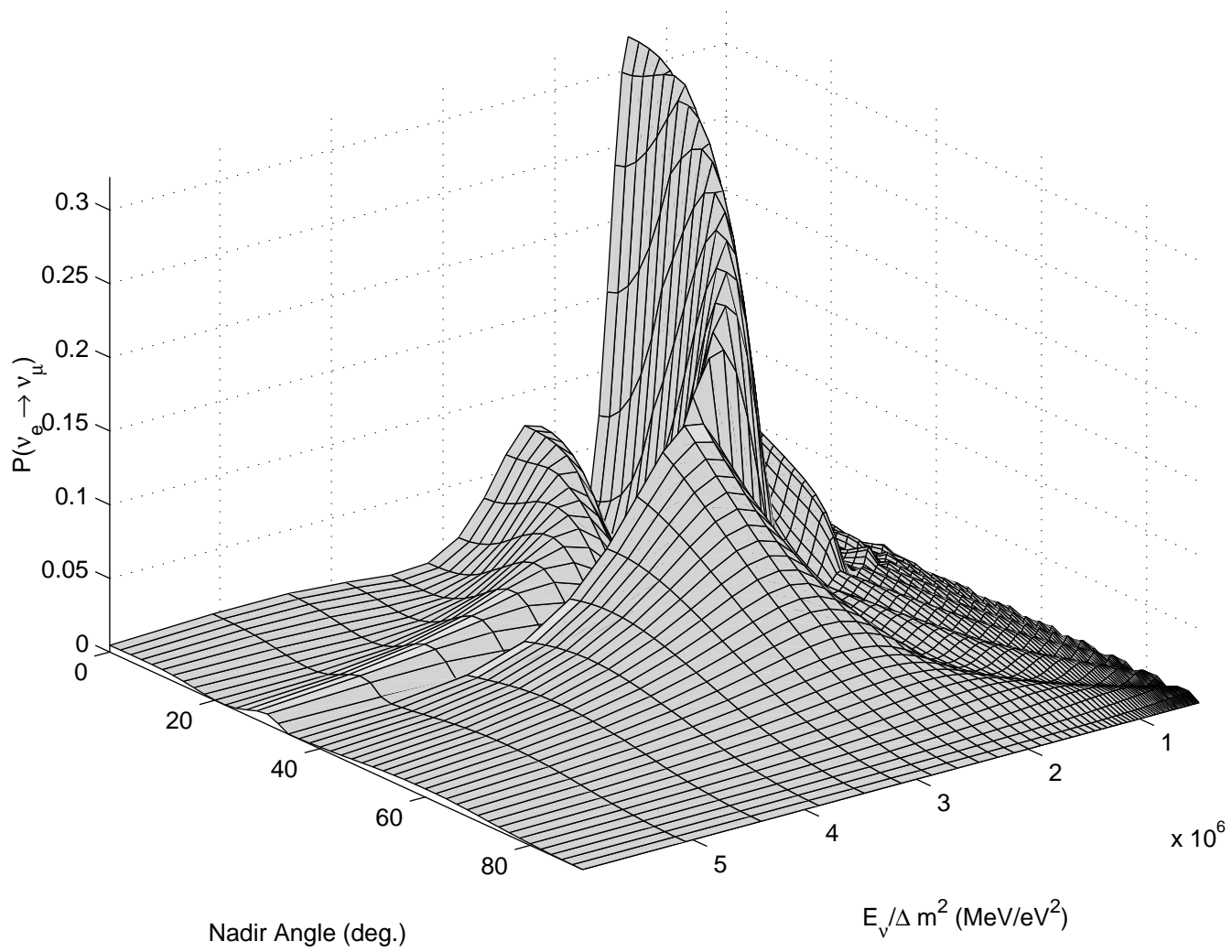


Figure 3b

$$\sin^2 2\theta_\nu = 0.005$$



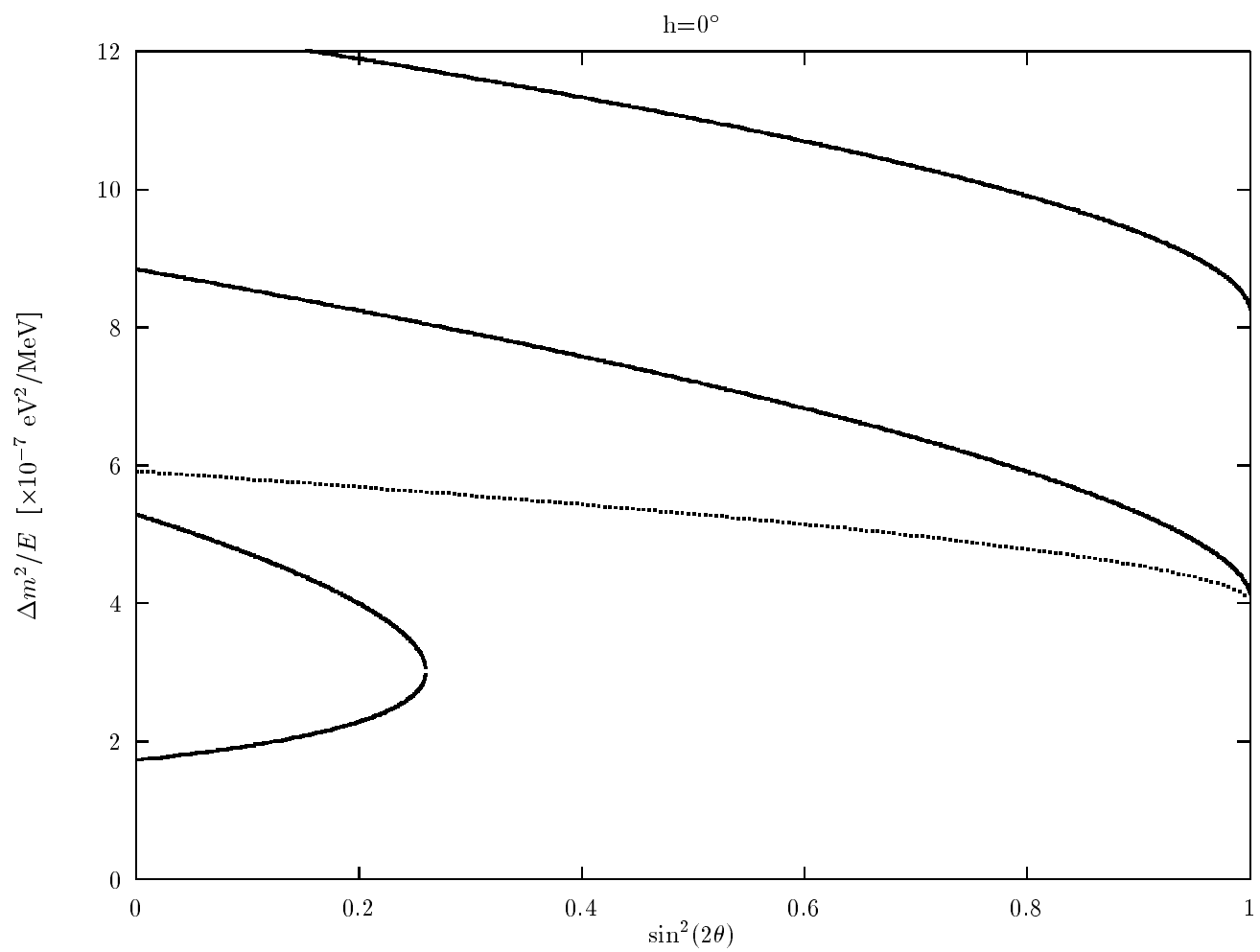


Figure 6a

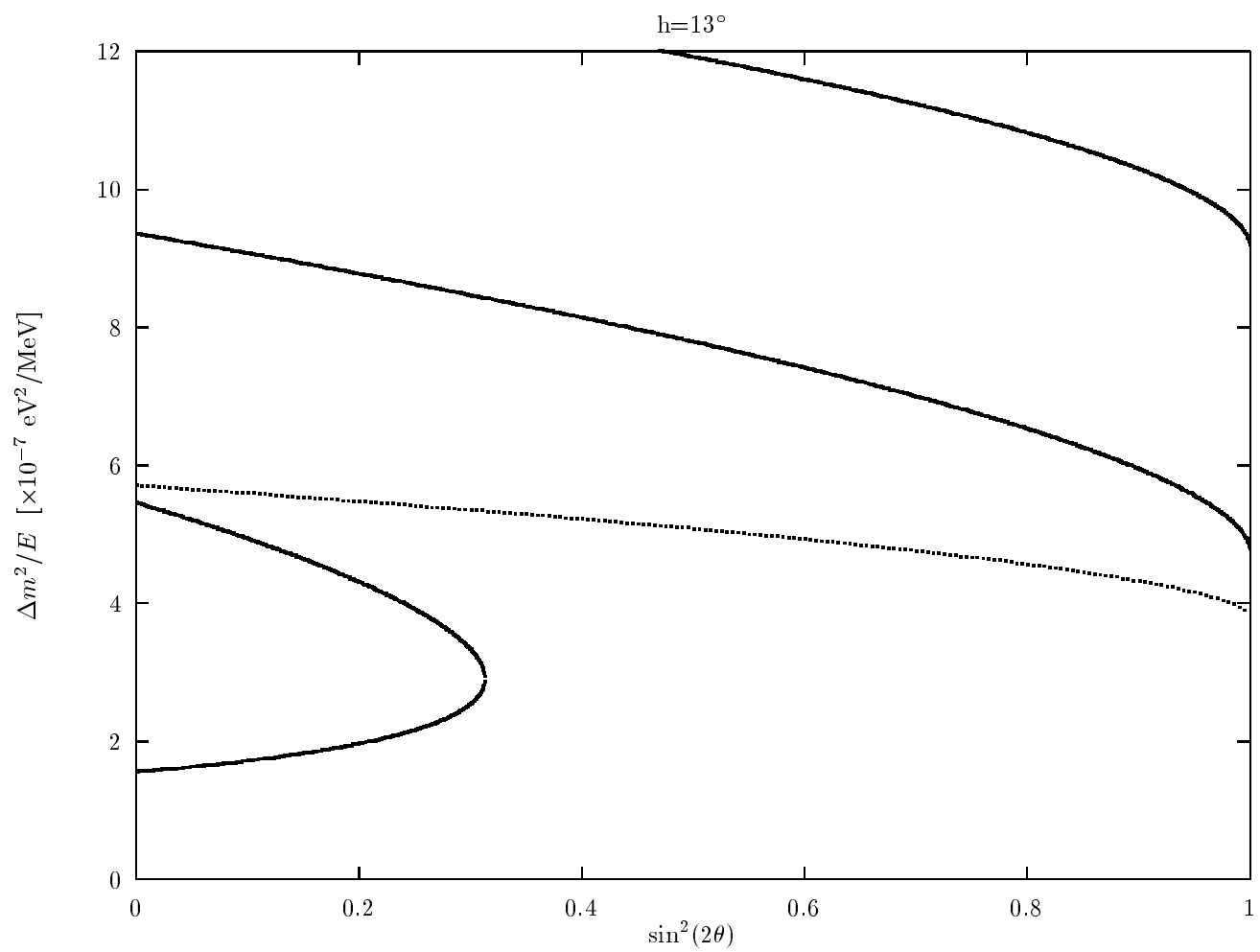


Figure 6b

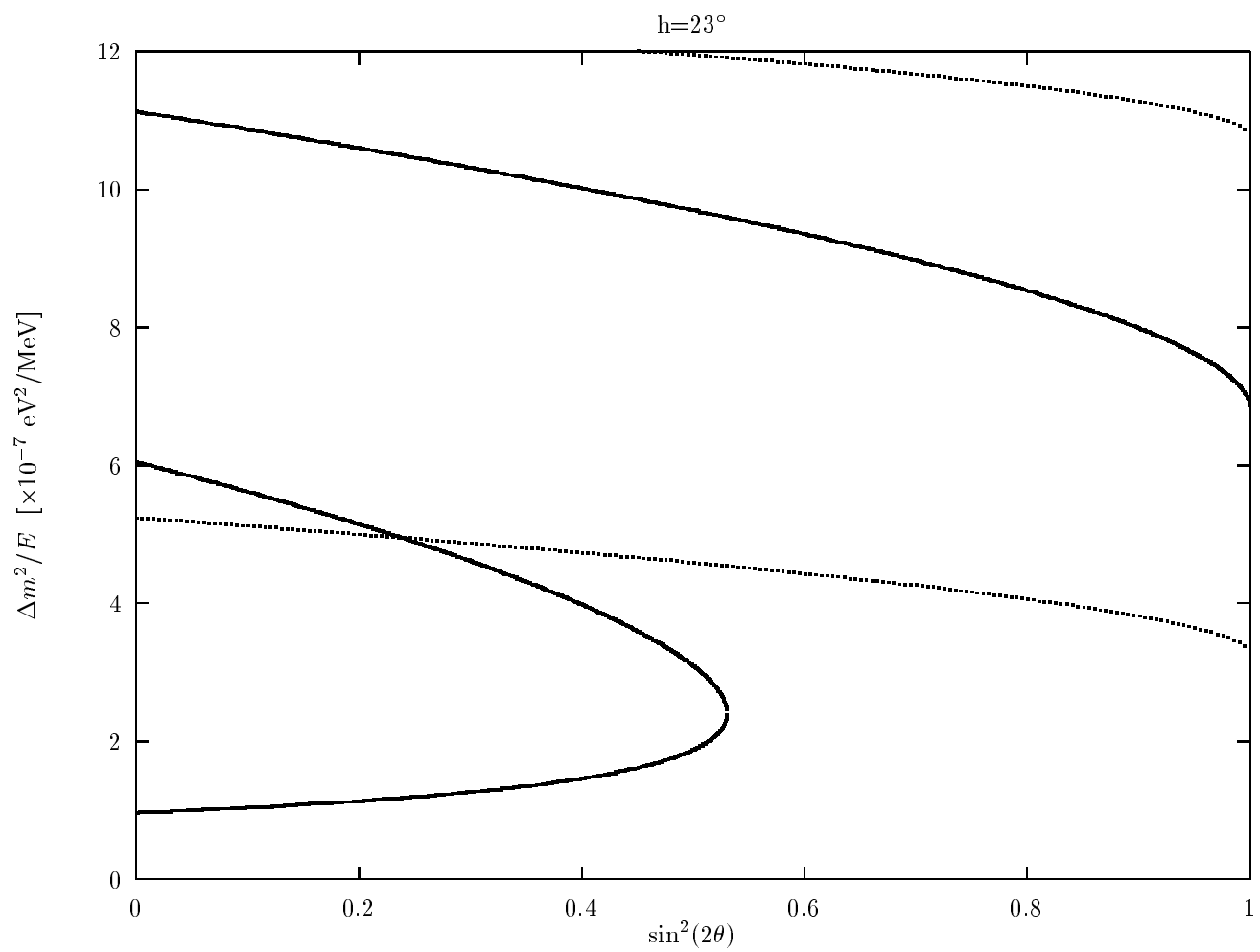


Figure 6c

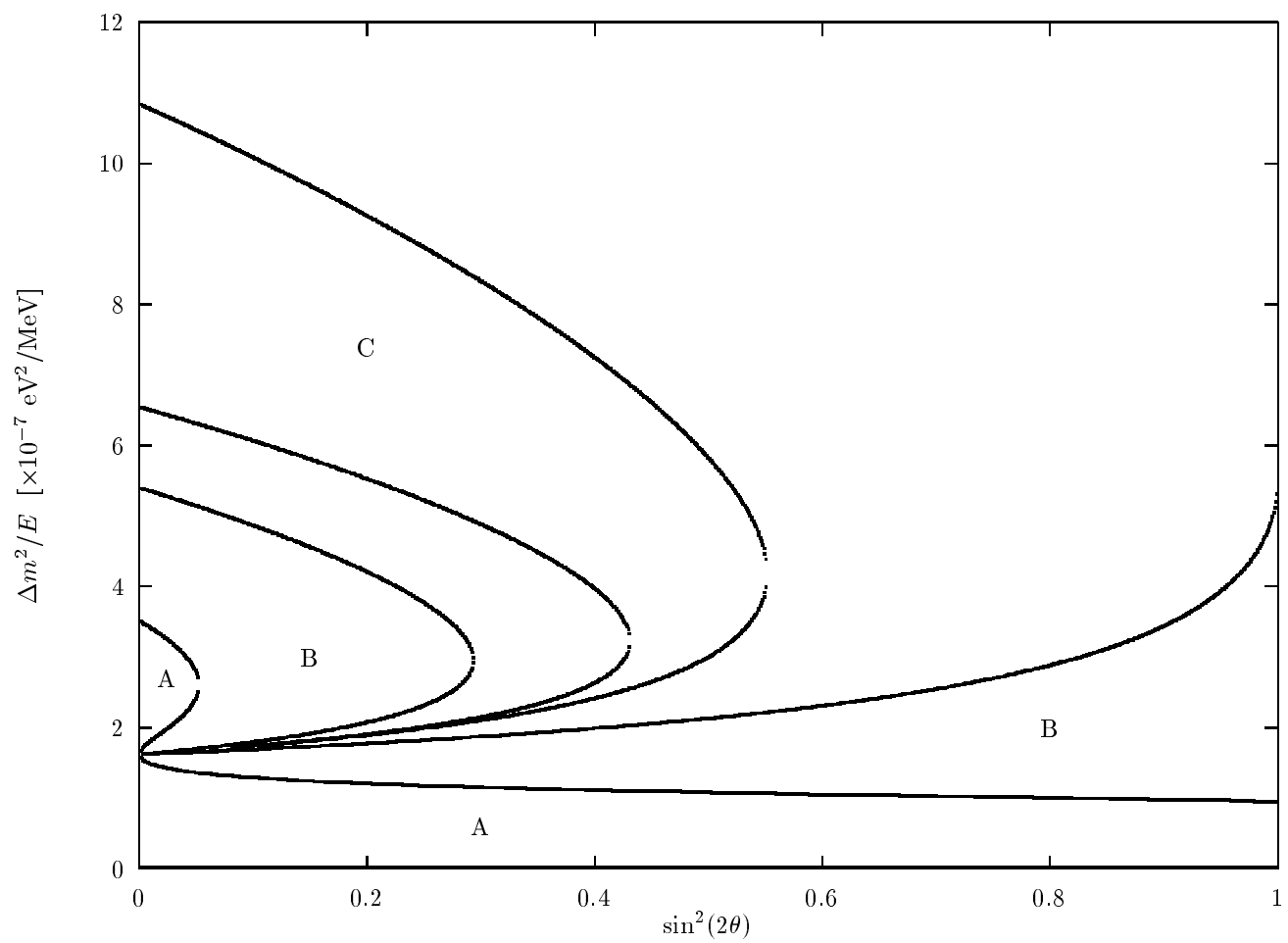


Figure 7

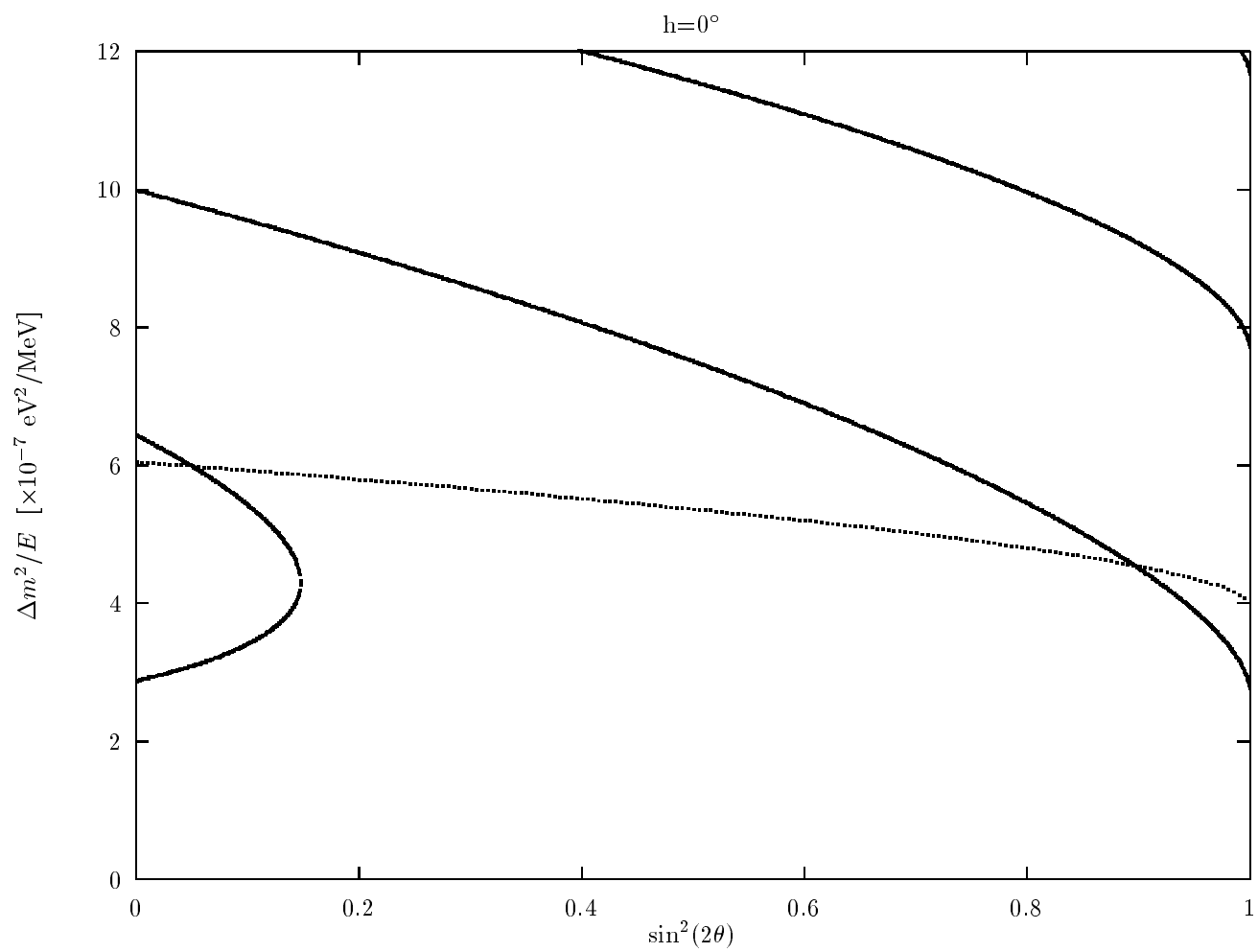


Figure 8a

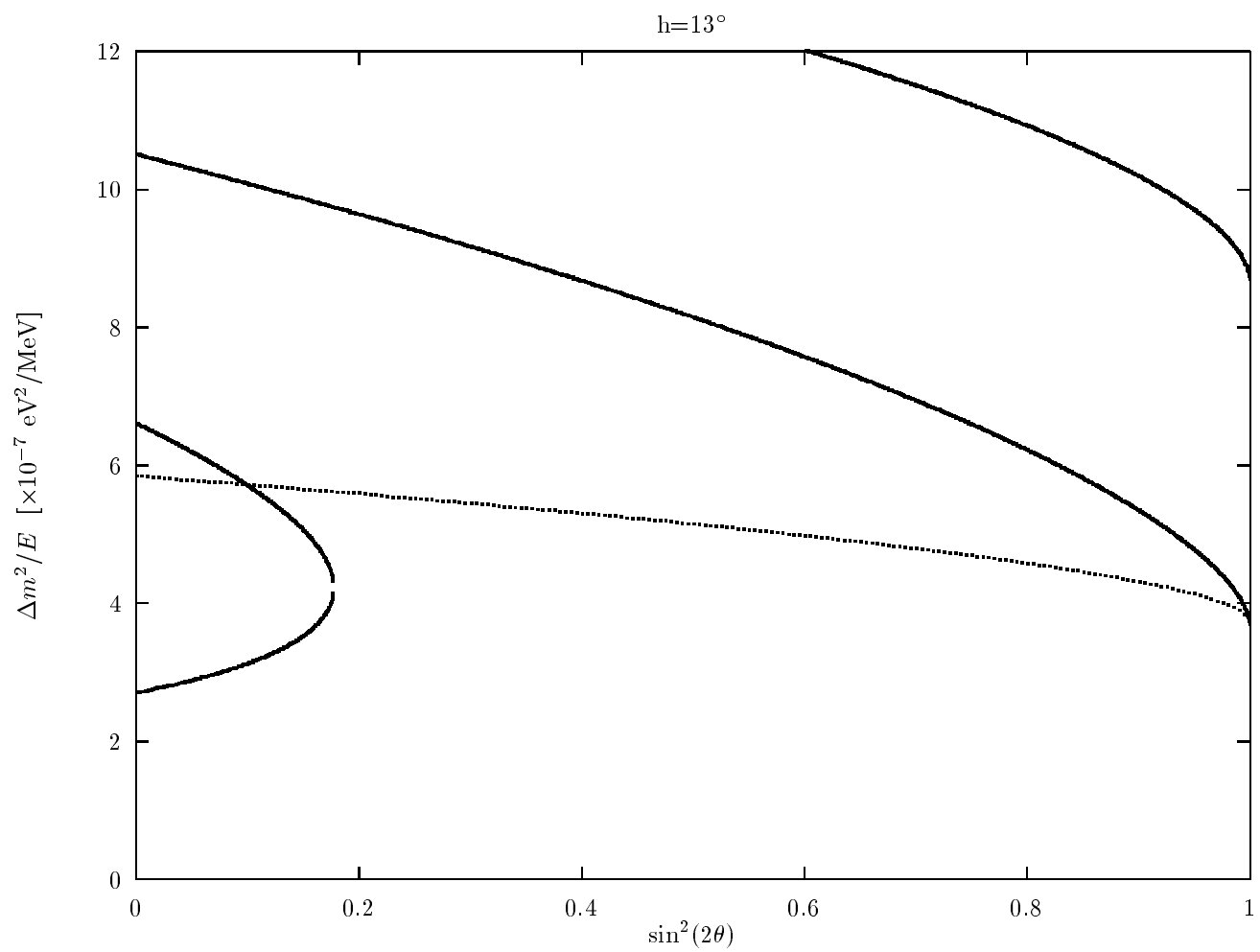


Figure 8b

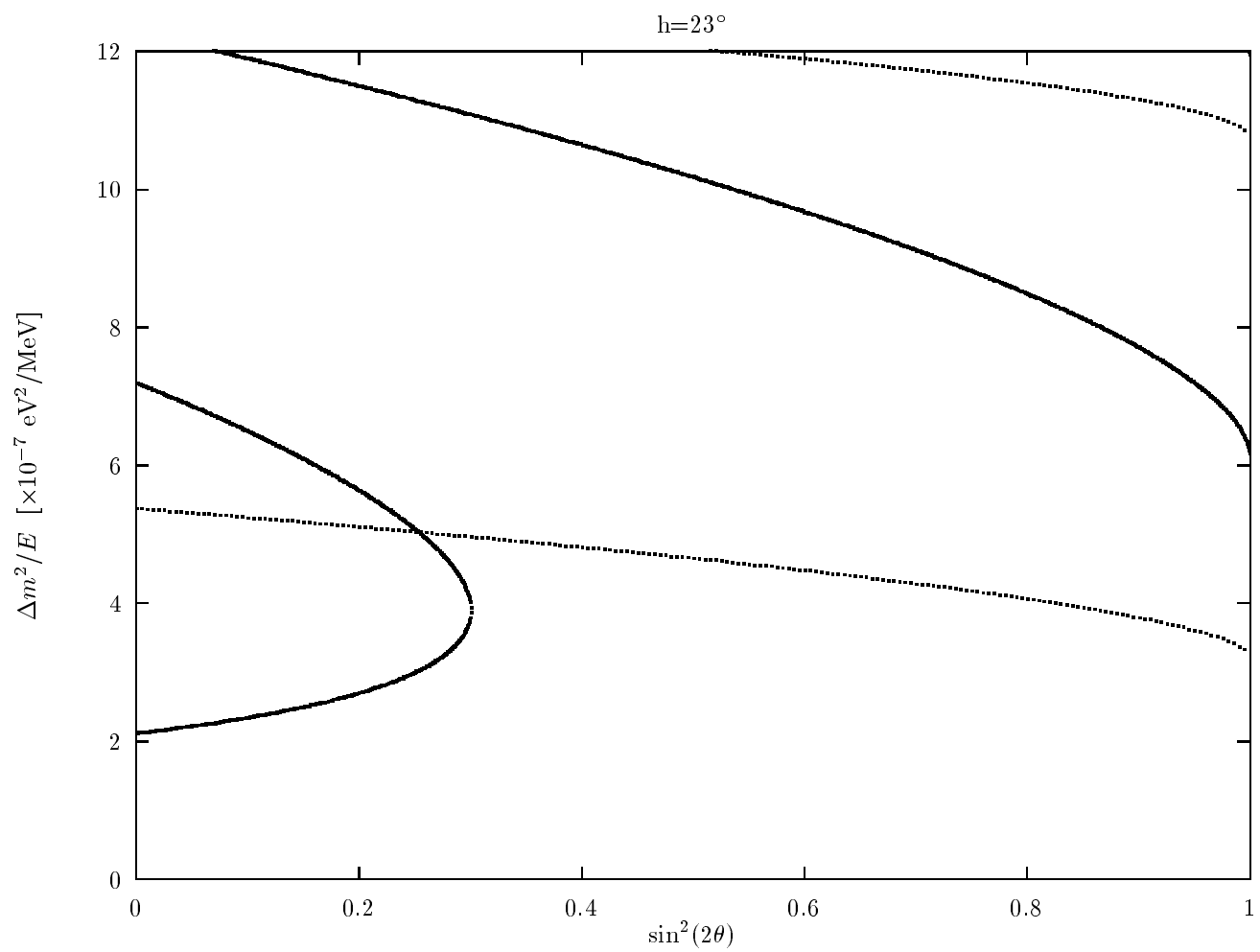


Figure 8c

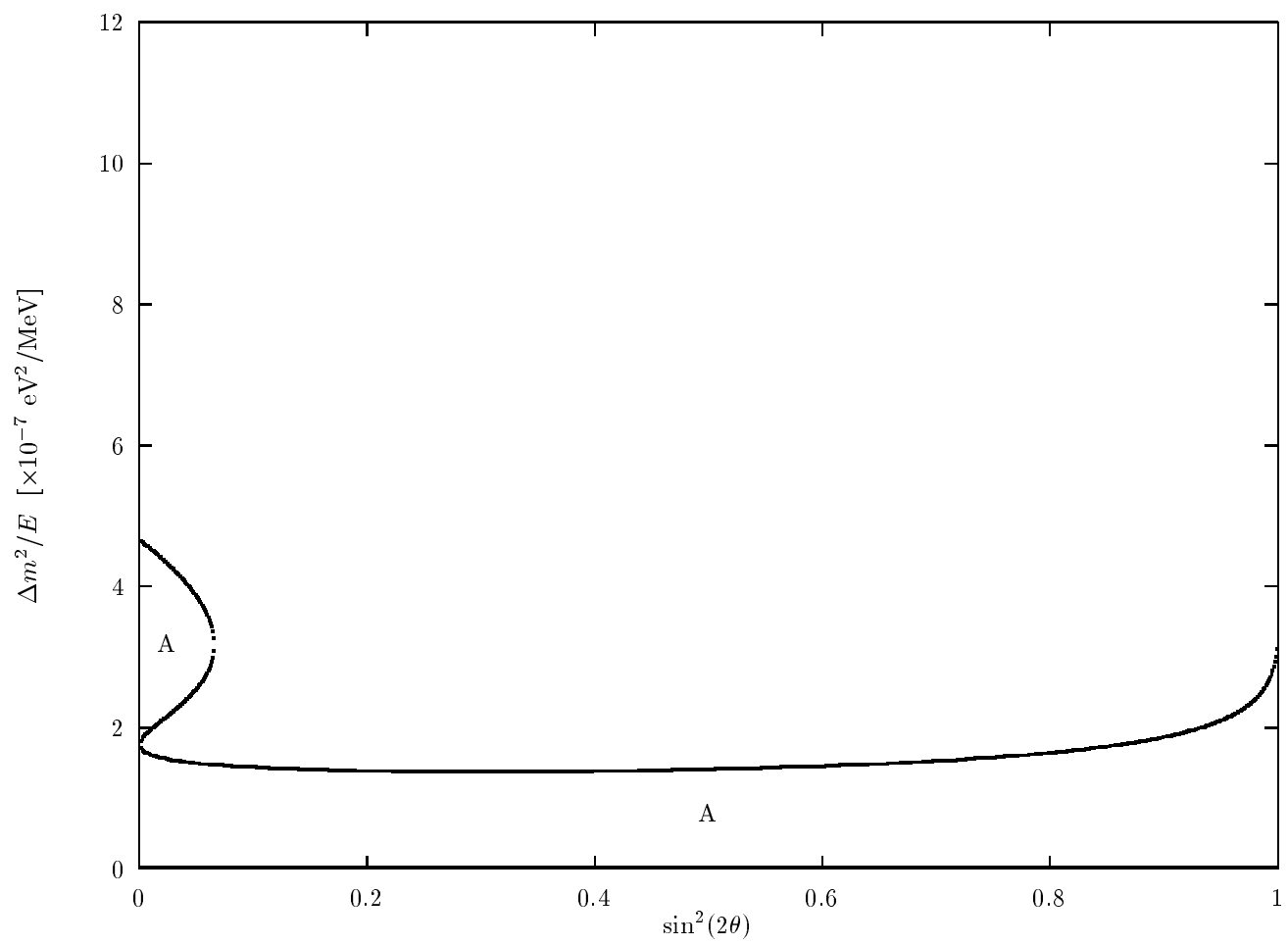
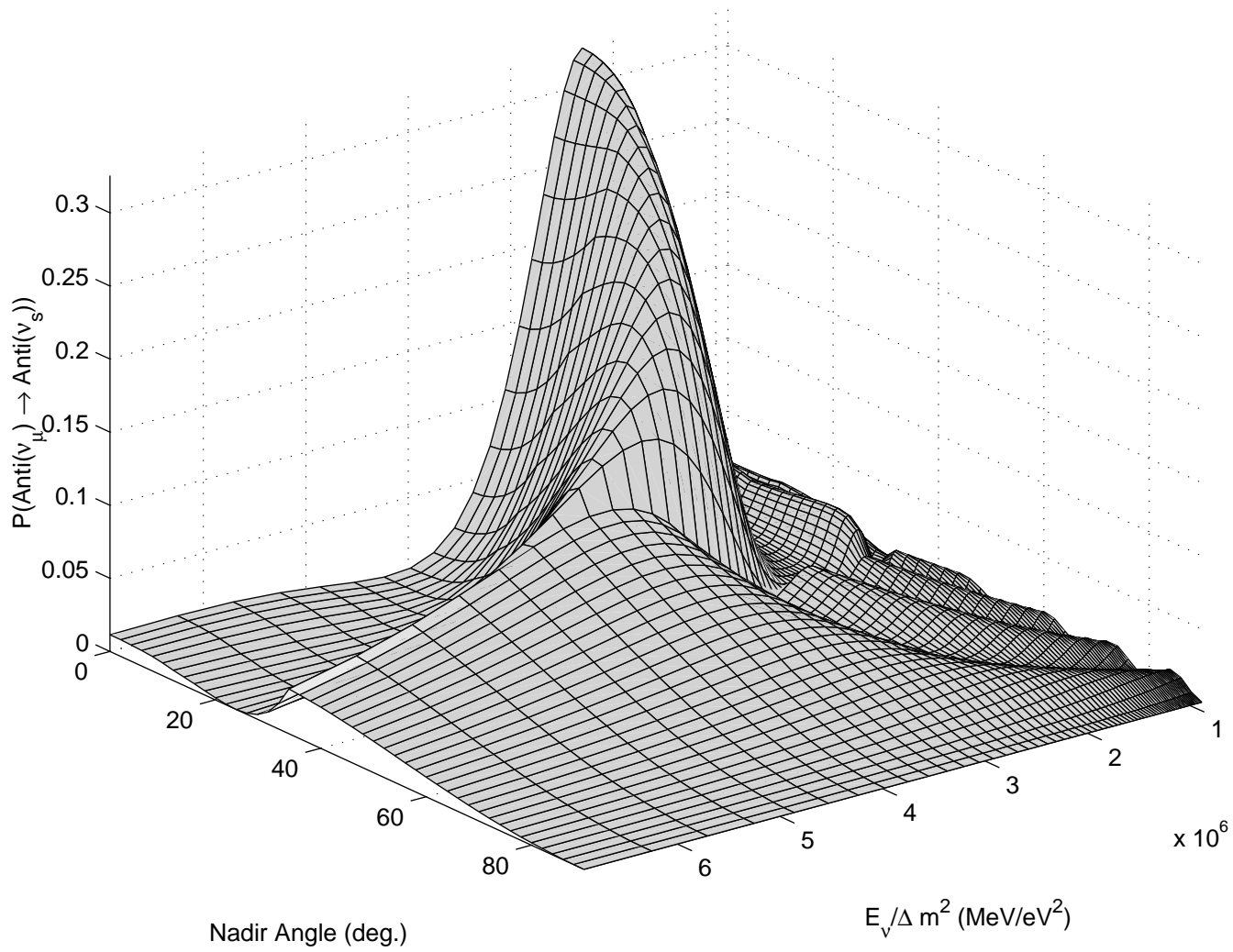
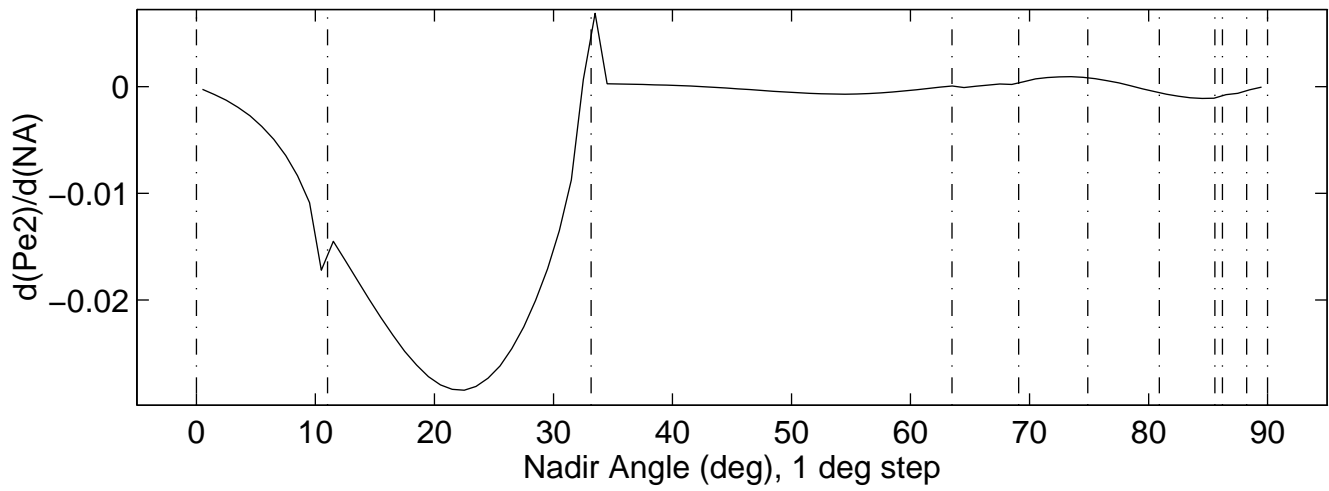
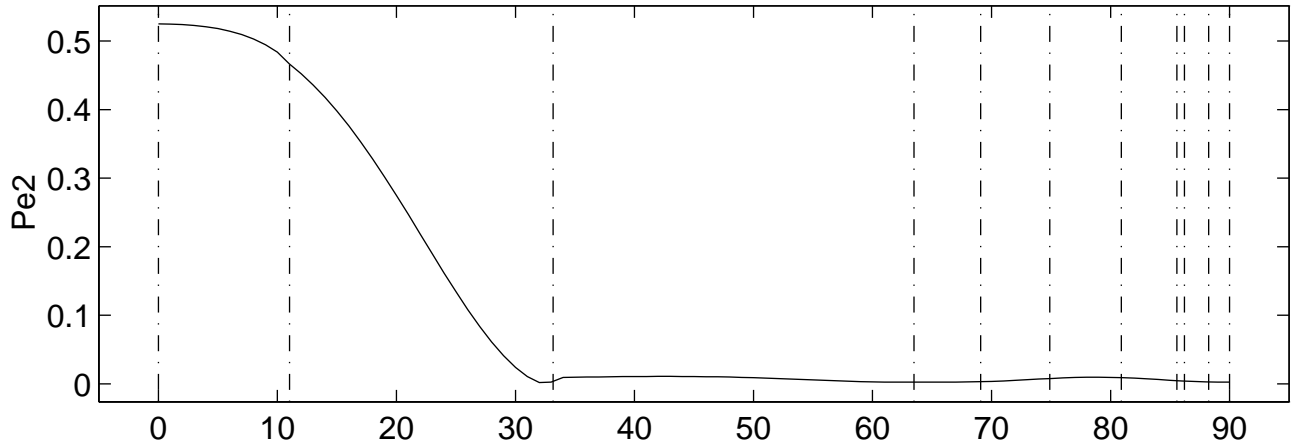


Figure 9

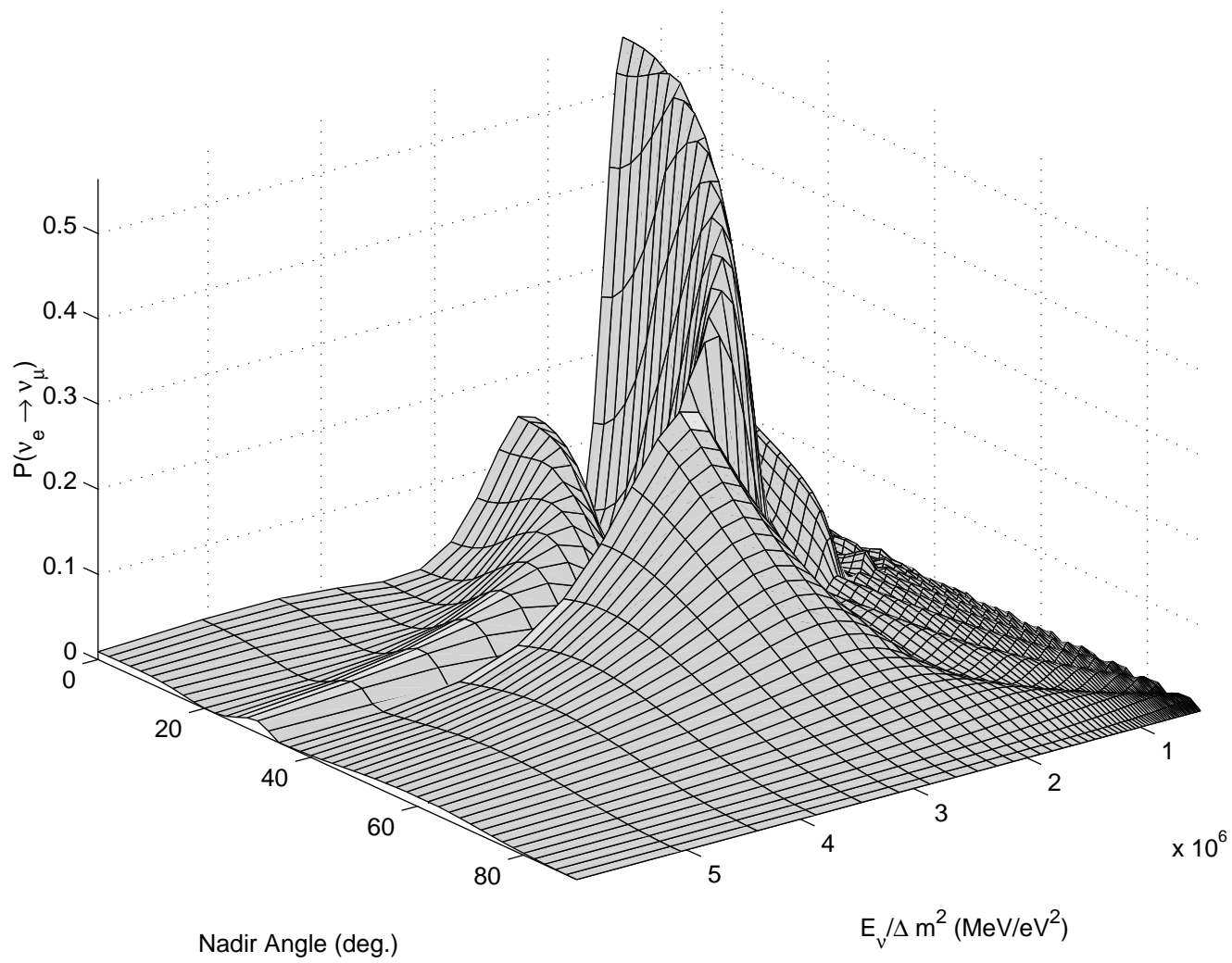
$$\sin^2 2\theta_\nu = 0.010$$

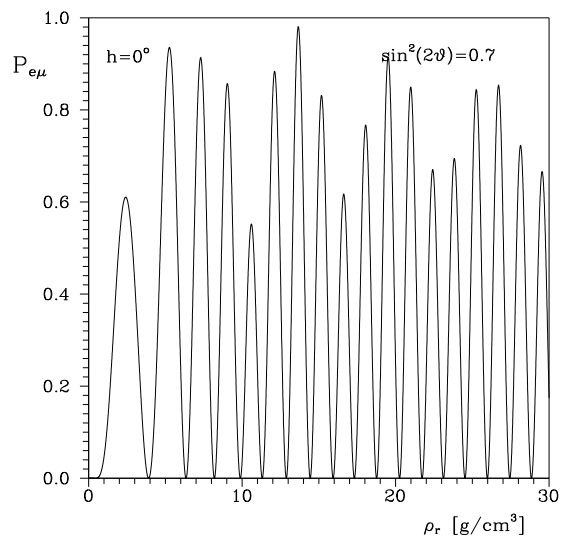
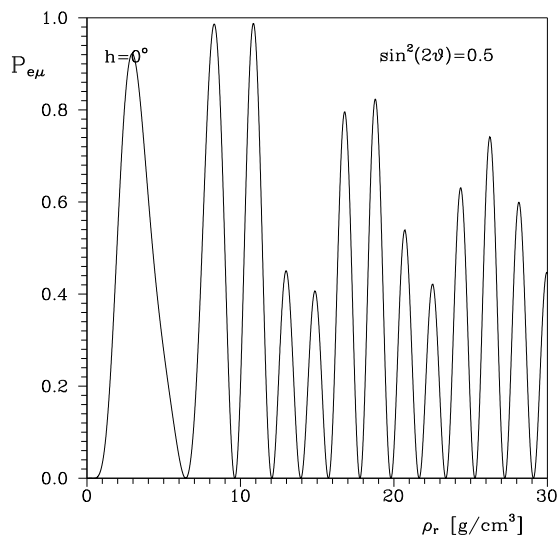
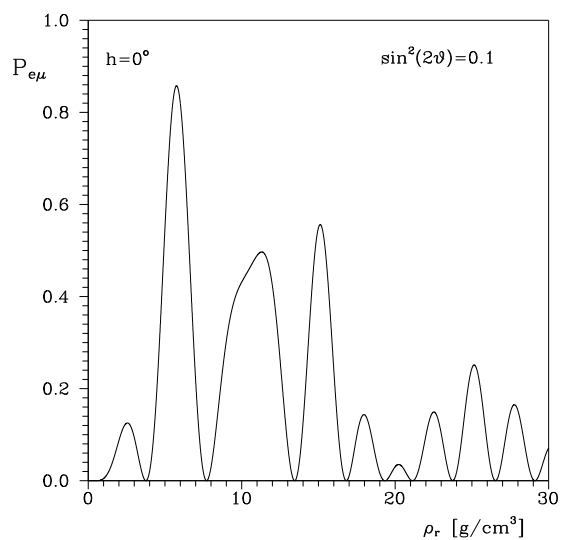
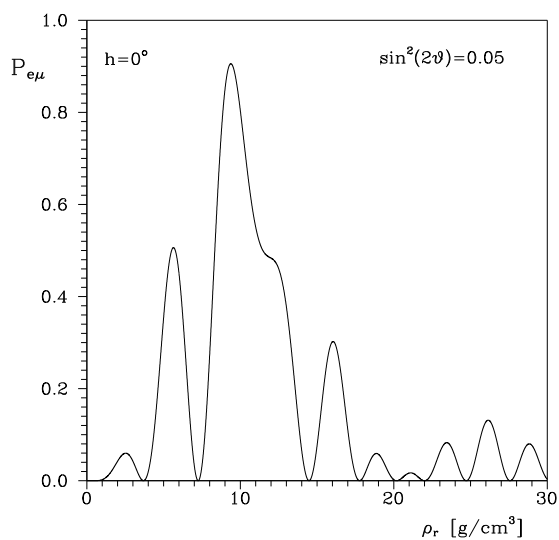
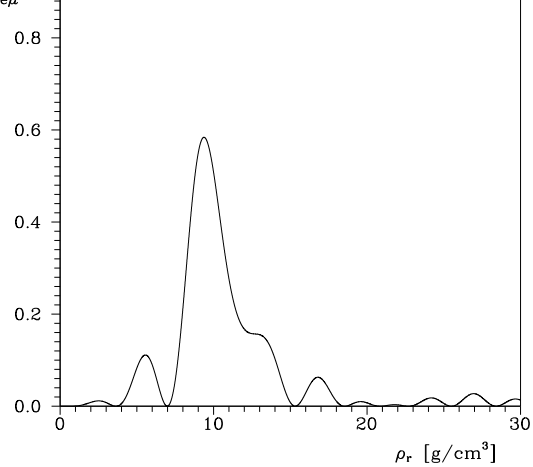
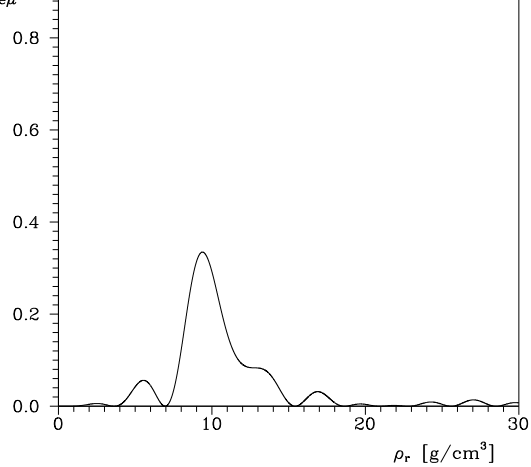


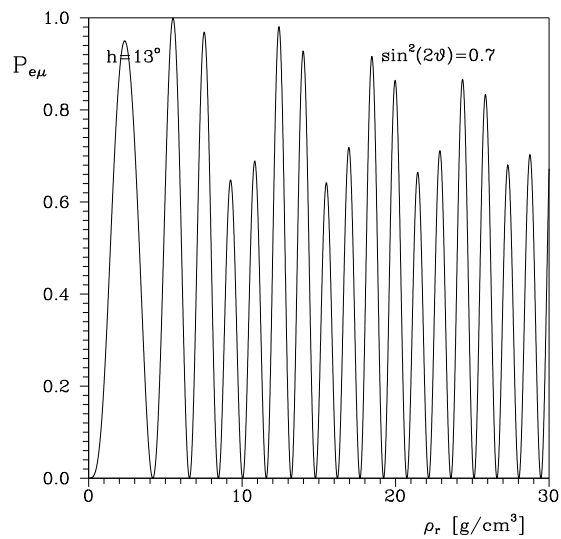
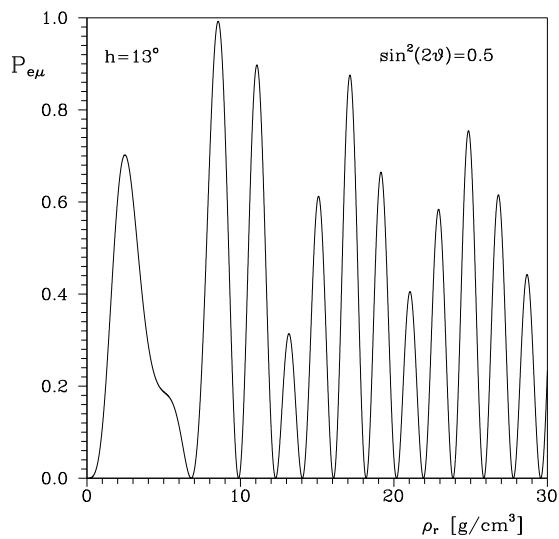
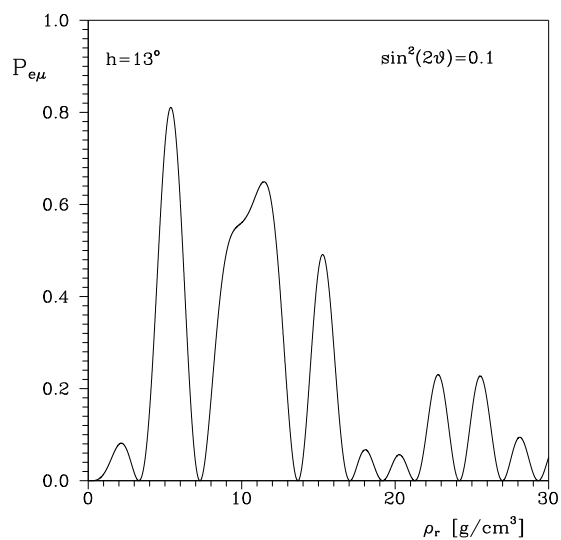
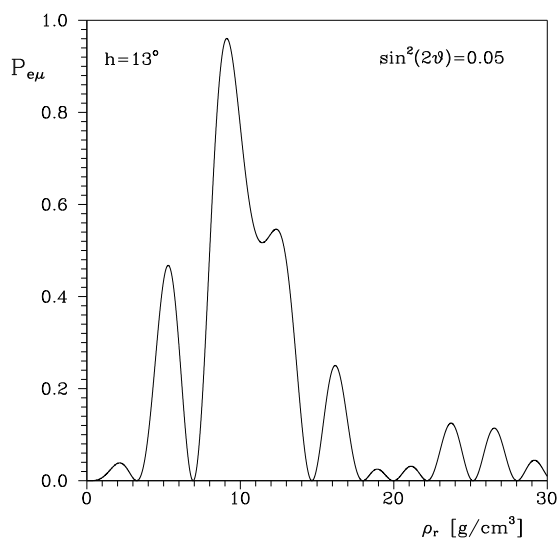
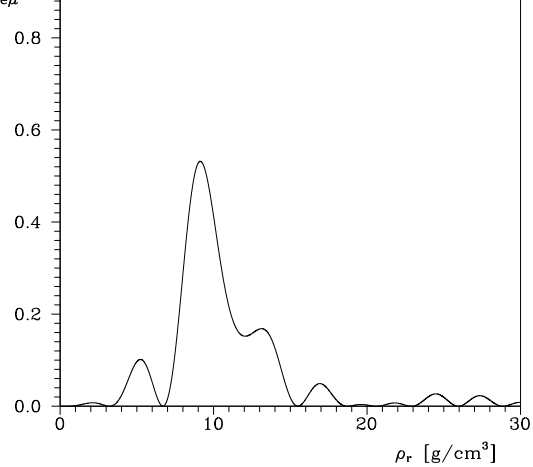
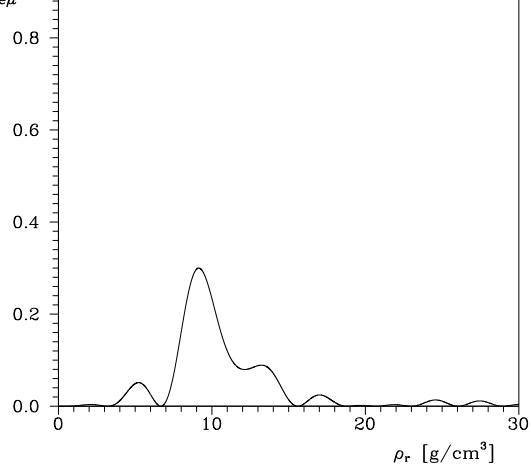
Active, SdTvS = 0.01, RhoR = 10 gr/cm3

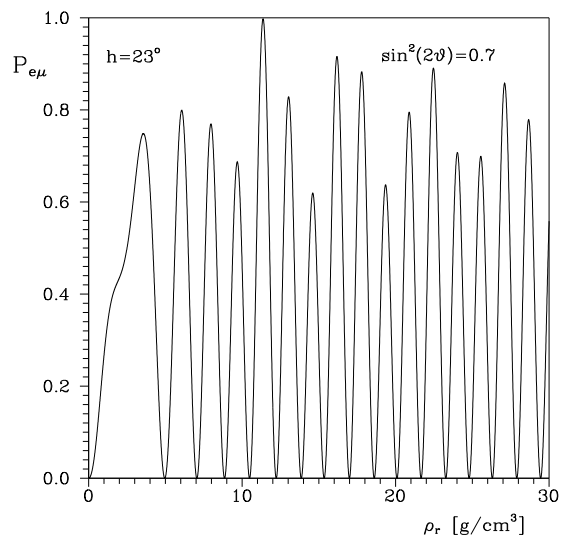
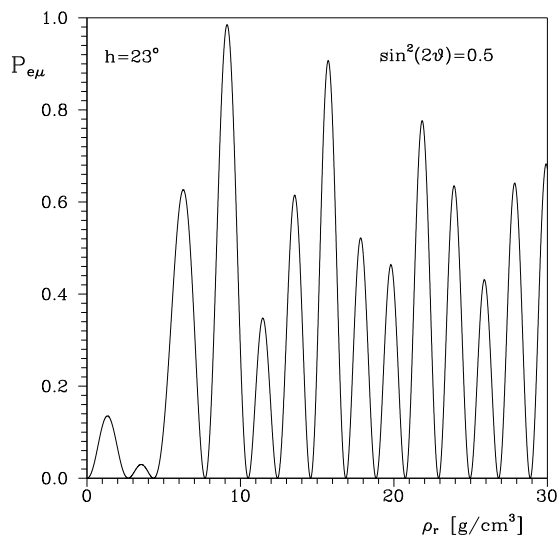
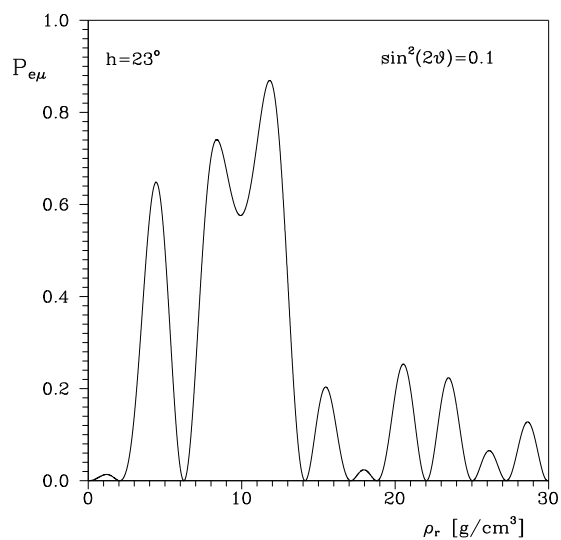
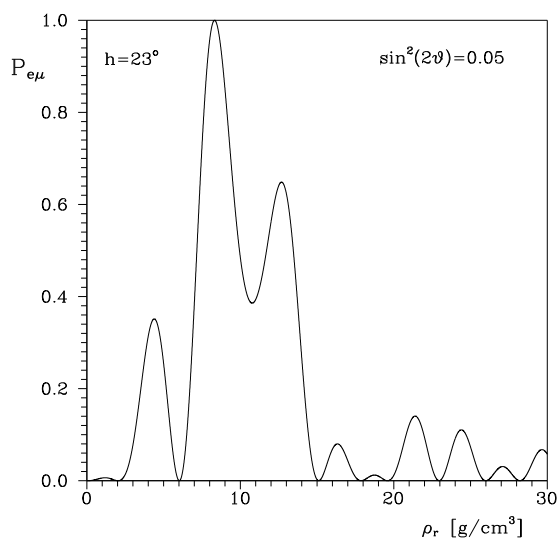
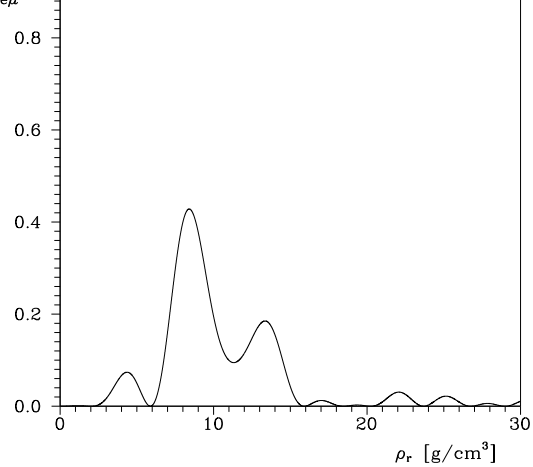
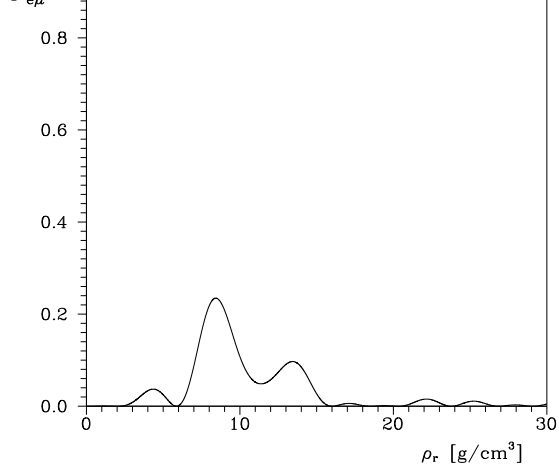


$$\sin^2 2\theta_\nu = 0.010$$

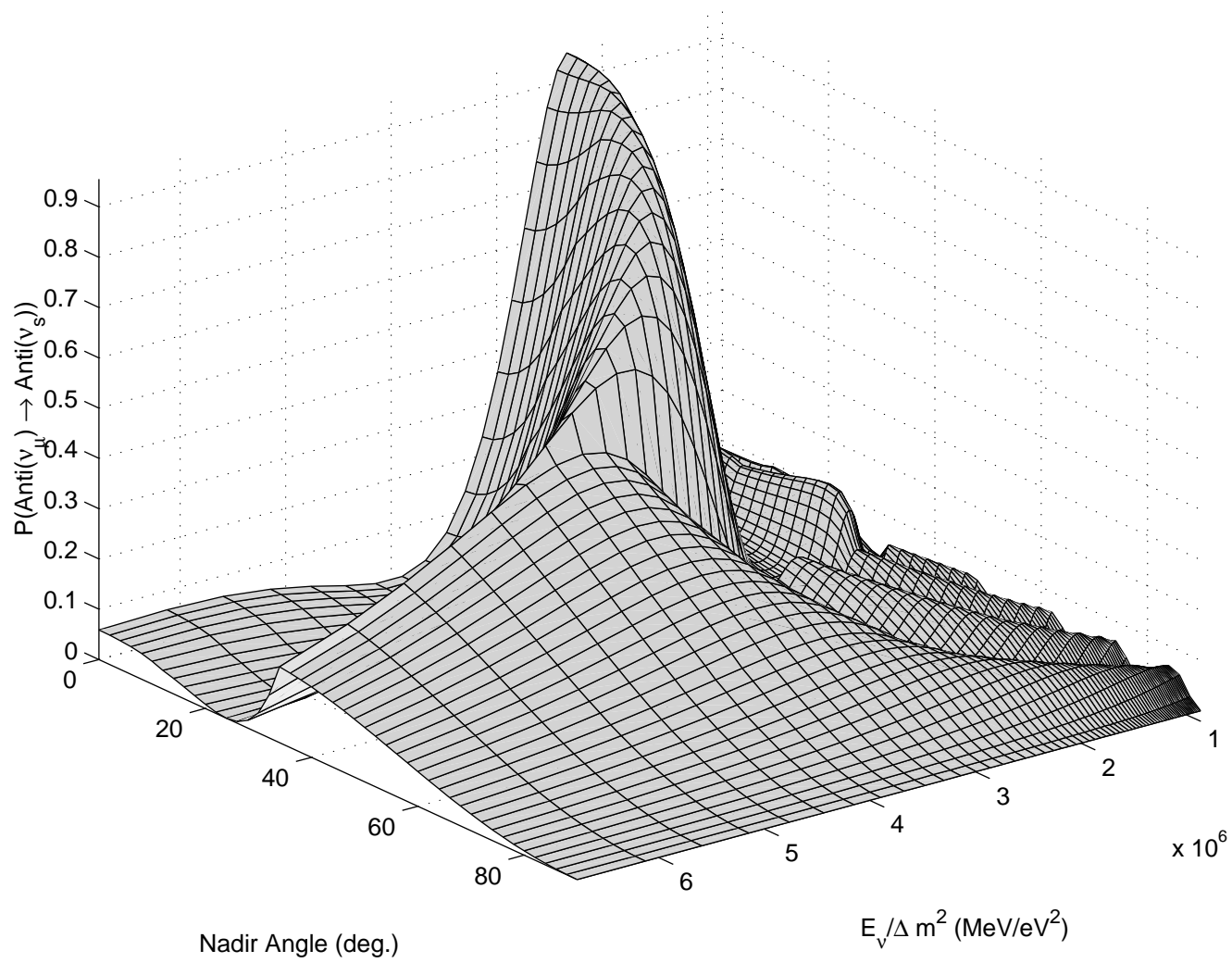




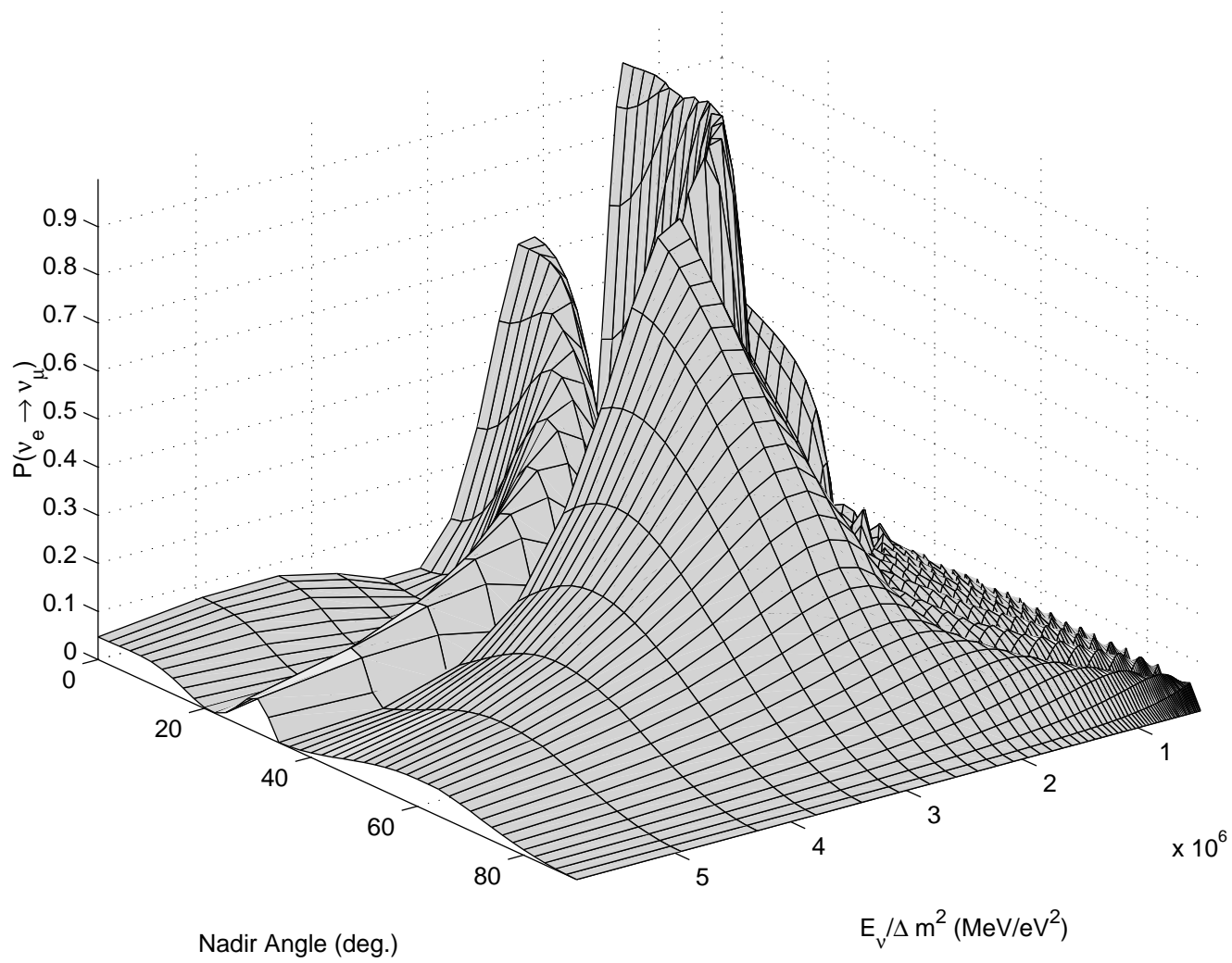




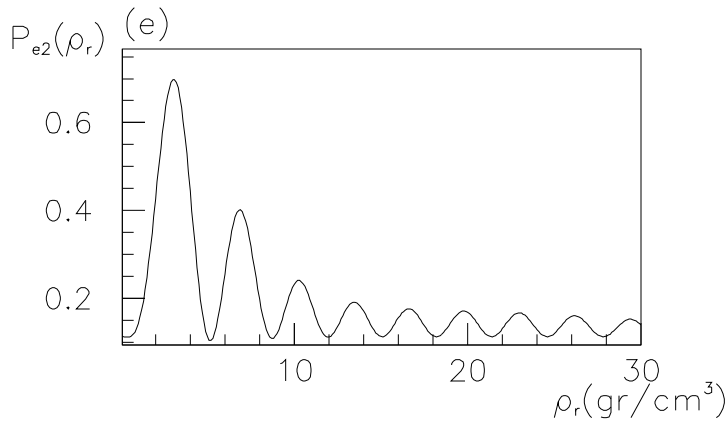
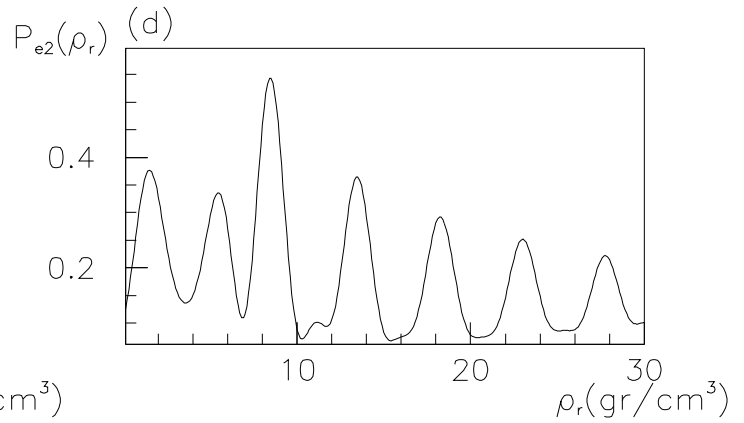
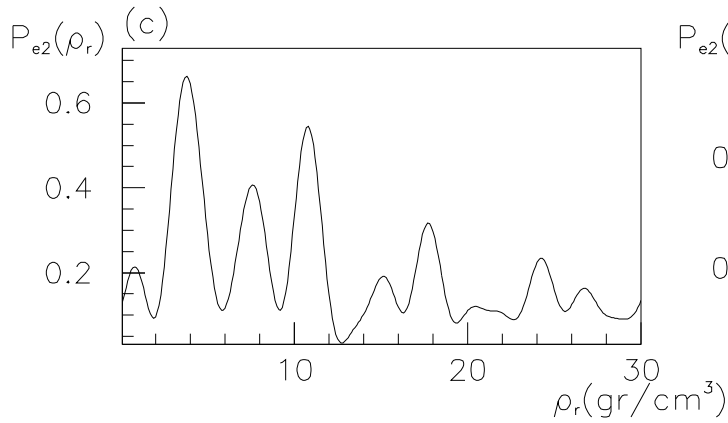
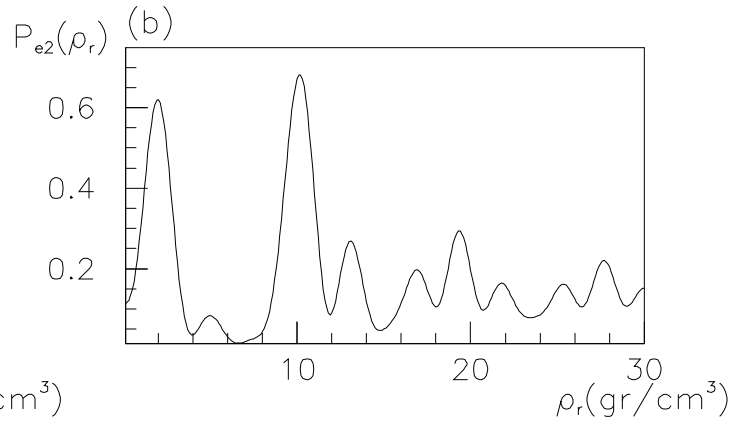
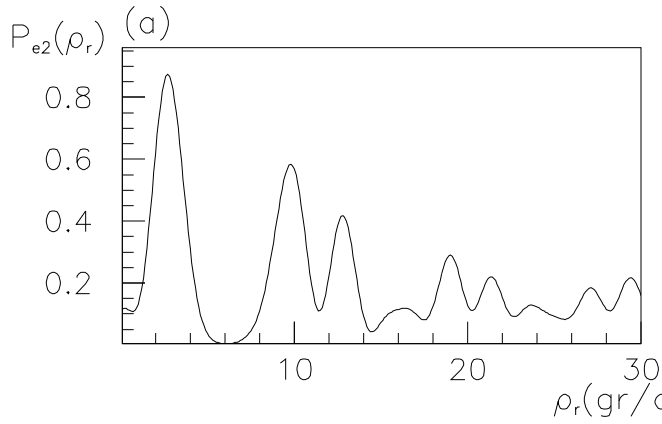
$$\sin^2 2\theta_\nu = 0.050$$



$$\sin^2 2\theta_\nu = 0.050$$



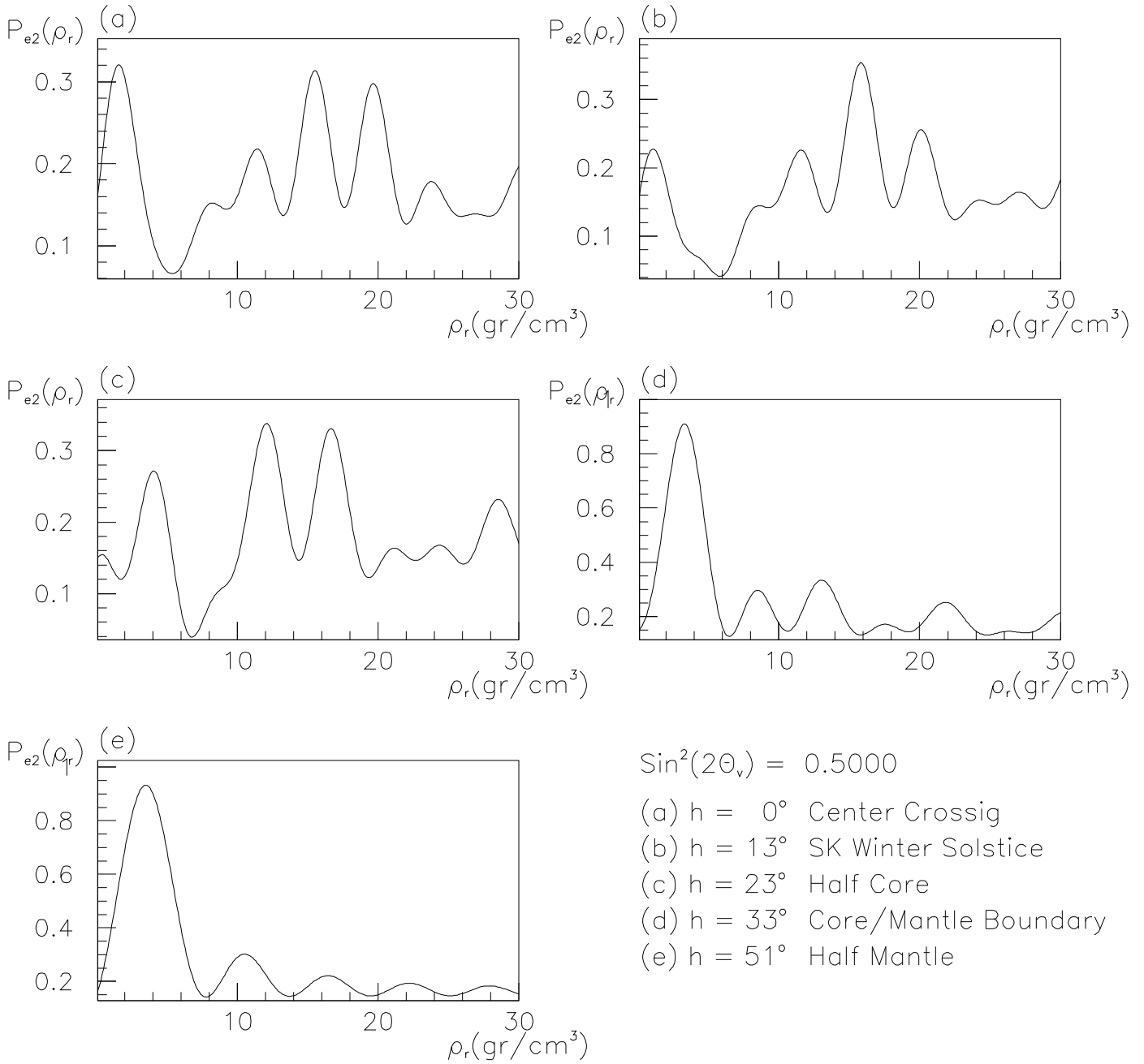
Active



$$\sin^2(2\theta_v) = 0.4000$$

- (a) $h = 0^\circ$ Center Crossig
- (b) $h = 13^\circ$ SK Winter Solstice
- (c) $h = 23^\circ$ Half Core
- (d) $h = 33^\circ$ Core/Mantle Boundary
- (e) $h = 51^\circ$ Half Mantle

Sterile



Active

